

# **OPTIMAL PLACEMENT OF MULTI ACTUATORS AND TARGET RESPONSE REDUCTION IN ACTIVE CONTROL OF BUILDING FRAMES**

**Ph.D. Thesis**

**RAJSHREE CHARAN  
2011RST7137**



**DEPARTMENT OF CIVIL ENGINEERING  
MALAVIYA NATIONAL INSTITUTE OF TECHNOLOGY JAIPUR**

**MARCH 2019**



## **DECLARATION**

I, **RAJSHREE CHARAN**, declare that this thesis titled, “**OPTIMAL PLACEMENT OF MULTI ACTUATORS AND TARGET RESPONSE REDUCTIONS IN ACTIVE CONTROL OF BUILDING FRAMES**” and the work presented in it are my own. I confirm that:

- This work was done wholly or mainly while in candidature for a research degree at this university.
- Where any part of this thesis has previously been submitted for a degree or any other qualification at this university or any other institution, this has been clearly stated.
- Where I have consulted the published work of others, this is always clearly attributed.
- Where I have quoted from the work of others, the source is always given. With the exception of such quotations, this thesis is entirely my own work.
- I have acknowledged all main sources of help.
- Where the thesis is based on work done by myself, jointly with others, I have made clear exactly what was done by others and what I have contributed myself.

Date: 01-03-2019

Rajshree Charan  
(2011RST7137)

## CERTIFICATE

This is to certify that the thesis entitled, “**Optimal Placement of Multi Actuators and Target Response Reductions in Active Control of Building Frames**”, being submitted by **Ms Rajshree Charan (2011RST7137)** is a bonafide research work carried out under my supervision and guidance in fulfillment of the requirement for the award of the degree of **Doctor of Philosophy** in the Civil Engineering Department, Malaviya National Institute of Technology, Jaipur, India. The matter embodied in this thesis is original and has not been submitted to any other University or Institute for the award of any other degree.

Place: Jaipur

(S. D. Bharti)

(M. K. Shrimali)

Date: 01-03-2019:

Professor (Structural Engg.)

Professor (Structural Engg.)

MNIT Jaipur

MNIT Jaipur

## ACKNOWLEDGEMENT

The work presented in this thesis would not have been possible without my close association with many people. I take this opportunity to extend my sincere gratitude and appreciation to all those who made this Ph.D. thesis possible.

I shall begin with God the almighty: without His will, I would have never found the right path. His mercy was with me throughout my life and ever more in this study

I would like to extend my sincere gratitude to my research guide Professor M.K. Shrimali and Dr. S.D Bharti for their dedicated help, advice, inspiration, encouragement and continuous support, throughout my Ph.D. Their enthusiasm, integral view on research and mission of providing high-quality work, has made a deep impression on me. During our course of interaction during the past years, I have learnt extensively from them. I owe them lots of gratitude for having me shown this way of research. I am really glad to be associated with a person like Dr. M.K. Shrimali and Dr. S.D Bharti in my life.

My special words of thanks should also go to Dr. T.K. Datta for his continuous support, guidance, cooperation, encouragement. His constant motivation and support have always kept me going ahead. I owe a lot of gratitude to him for always being there for me and I feel privileged to be associated with a person like him during my life. This work was not possible without his constant support and scientific help

I express my sincere gratitude towards Mr. Vishist Bhaiya, who always remains available for technical discussions and guidance. I could always look back on him for any support during my course of Ph.D. I would also like to express sincere gratitude towards my teachers, friends, faculty members, and staff members, at MNIT Jaipur. Their unending encouragement has been a source of positive energy, which helped me to have a better outlook, not only in terms of technical matters, but also in interpersonal learning and growth. The peer group at MNIT Jaipur, especially, Mr. Arnav Anuj Kasar, Mr. Shashi Narayan, Mr. Mohit Bhandari, Mr. Vijay Sharma, Mr. Nishant Roy and Mrs. Sunita Tolani are acknowledged. I will always cherish the warmth shown by them. I must thank the office staff, Mr. Sanjay Tailor for his kind support.

My special regards to all my teachers because of whose teaching at different stages of education has made it possible for me to see this day. Because of their kindness I feel, was able to reach a stage where I could write this thesis.

My heartfelt regard goes to my father in law, mother in law, brother-in-law and sister-in-laws for their love and moral support. A special thanks to my sister Jaishree, brother in law Raghavender and my younger brother Prakhar for their love and affection. Their trust in me has been the primary driving force and support for this work.

I owe my deepest gratitude towards my better half for his eternal support and understanding of my goals and aspirations. His infallible love and support have always been my strength. His patience and sacrifice will remain my inspiration throughout my life. Without his help, I would not have been able to complete much of what I have done and become who I am. It would be ungrateful on my part if I thank Ashish in these few words. I am thankful to my daughter Aadhyashree who is the pride and joy of my life, for giving me happiness and continue motivation to do better in life.

I feel a deep sense of gratitude for my maa and daddy, who formed part of my vision and taught me good things that really matter in life. Their infallible love and support have always been my strength. Their patience and sacrifice will remain my inspiration throughout my life. I am very much grateful to them for their constant inspiration and encouragement. Almighty God, has showered grace on me, by giving an opportunity to pursue this enriching journey.

## ABSTRACT

The concept of structural control has emerged as a very attractive proposition for the control of seismic response and seismic disaster mitigation of civil engineering structures. Over the past few decades, an enormous amount of researches has taken place in this area leading to implementable control strategies in practice. The strategies include the use of active, passive, and semi-active devices, independently or in combination, to control the earthquake induced responses of structures. A vast number of control algorithms, developed for efficient control schemes, cover a wide spectrum of classical and modern methods, including Fuzzy logic, ANN, ANN cum Fuzzy logic and adaptive control. Practically, every aspect of structural control has been investigated in details, leaving limited scope of research in this area. Yet, researches are continuing in this area, especially in respect of practical implementations like, optimal placement of actuators, control schemes to target or specified control, predictive control of site specific random ground motion, adaptive structural features for response reduction etc.

The present study aims at a few of these topics. Three objectives are set for the study. They include:

- (i) Optimal placement of multi actuators in building frames for active control of responses.
- (ii) Development of an ANN based active control scheme for a predetermined reduction in response of building frames with single actuator placed at the top of the structure.
- (iii) Predictive active control of building frames using ANN for site-specific random ground motion specified by its power spectral density function.

For fulfilling the first objective, a practical case of actuator placement in a ten story-building frame is considered in which actuators can be placed only in a few floors for practical reasons. Thus, the analytical formulation of the optimization problem becomes involved. Consequently, a simple trial and search technique is used to find the reductions of two important response quantities, namely, top story displacement and base shear. The response reductions are investigated for different placements of one actuator, and combinations of two actuators and three actuators in the building frame. A LQR control algorithm is used for finding the controlled responses for a set of real earthquake records. Response reductions and the corresponding peak control forces are plotted against actuator positions/ different combinations of actuator positions. The plots clearly demonstrate the possible optimum positions of the actuators where they can be

placed from practical considerations. The results of the study reveal that the optimum positions for base shear hold inverse relationship with those of top floor displacement. Further, optimum positions of actuator differ with performance objectives, i.e, reduction of a response quantity considered alone, the reduction of a response quantity per unit peak control force and comparable reductions for both responses together.

The second study develops an ANN based control scheme for predetermined response reductions of the same building frame for unknown time histories of earthquakes. For this purpose, the same two response quantities are considered. Three ANNs are separately trained off-line. Two ANNs have two input nodes and one output node. Each has one hidden layer. The third ANN has three input nodes, one output node and a hidden layer. First two ANNs are trained for predetermined response reductions for top story displacement and base shear separately, while the third ANN is trained for predetermined reductions of both responses simultaneously. Training data sets are generated by finding reductions of the two response quantities of the frame for a number of real earthquake records scaled to different PGA levels. LQR algorithm is used for obtaining the time histories of control forces and the controlled responses. For the training of the ANN, one of the input nodes contains the ground motion time history; other input nodes contain response reductions. The output node contains time history of control force. After the ANN is trained, the output node provides the time history of control force for the desired reductions of the responses for the unknown time histories of the earthquake (which are not included in training). It is observed that all three ANNs are effectively trained to provide the desired time histories of the control force of the unknown problems, verified by comparing results of ANN control with LQR control. Results of a large number of unknown problems are graphically presented to show the efficiency of the control scheme.

The third study is similar to that of the second one . In this case, the data for training are synthetically generated from the site-specific power spectral density function of ground acceleration. Two types of ground motion are considered, namely, broadband and narrow band earthquakes. It is assumed that the power spectral density function of the control force has the same shape as that of the ground acceleration. With this assumption, the time histories of control forces are synthetically generated from their power spectral density functions. The peak values of the control forces are assumed to be fractions of the weight of the structure. Different combinations of PGA values and peak values of control forces are created for training the ANNs.



Response reductions for a given set of the time histories of ground acceleration and control force are obtained in the frame using SIMULINK tool box of MATLAB. The ANNs are tested for both known and unknown problems. The results of the ANN control are compared with those of LQR. Also, results are obtained in a number of real earthquake records which include some near field earthquakes. The results of the numerical study show that the predictive active control using ANNs is highly effective in providing the time histories of control forces for target response reductions of the building frame for site-specific earthquakes.

# TABLE OF CONTENTS

DECLARATION .....	i
CERTIFICATE.....	ii
ACKNOWLEDMENT.....	iii
ABSTRACT.....	v
TABLE OF CONTENT .....	viii-x
LIST OF FIGURE.....	xi-xviii
LIST OF TABLE.....	xix
NOMENCLATURE.....	xx
<b>CHAPTER-1 .....</b>	<b>01</b>
<b>INTRODUCTION.....</b>	<b>01</b>
1.1 General.....	01
1.2 Need for the Present Study.....	05
1.3 Scope and objectives of the work.....	07
1.4 Organization of thesis.....	07
<b>CHAPTER – 2 .....</b>	<b>10</b>
<b>LITERATURE REVIEW .....</b>	<b>10</b>
2.1 General.....	10
2.2 Brief review of active structural control.....	11
2.3 Algorithms used for active control of structures.....	13
2.4 Application of artificial neural network (ANN) in structures .....	17
2.5 Application of control of structures using (ANN) .....	19
2.6 Control using Fuzzy logic and Neuro-fuzzy technique.....	21
2.7 Concluding remarks .....	24
<b>CHAPTER -3.....</b>	<b>26</b>
<b>OPTIMUM PLACEMENT OF ACTUATORS IN ACTIVE CONTROL OF BUILDING FRAMES .....</b>	<b>26</b>
3.1 Introduction.....	26
3.2 Theory	

.....	26
3.2.1 State-space representation of MDOF system .....	27
3.2.2 Linear quadratic regulator (LQR) .....	28
3.3 Numerical examples and discussion of results.....	29
3.3.1 The optimum control with one actuator .....	32
3.3.2 The response reduction with two actuators .....	40
3.3.3 The response reduction with three actuators .....	47
3.4 Conclusion .....	56
<b>CHAPTER – 4 .....</b>	<b>58</b>
<b>PREDICTIVE ACTIVE CONTROL OF BUILDING FRAMES.....</b>	<b>58</b>
4.1 Introduction.....	58
4.2 Theory .....	59
4.2.1 Training of the neural network.....	59
4.2.2 Testing the neural network .....	61
4.3 Numerical examples.....	62
4.3.1 Testing the ANN for known problems .....	62
4.3.2 Testing for unknown problems.....	66
4.3.3 Testing of neural network for problems outside the range of training.....	76
4.4 Conclusion .....	79
<b>CHAPTER-5.....</b>	<b>82</b>
<b>PREDICTIVE ACTIVE CONTROL FOR SITE SPECIFIC GROUND MOTION.....</b>	<b>82</b>
5.1 Introduction.....	82
5.2 Theory .....	82
5.1.1 Training of the neural network.....	83
5.1.2 Testing neural network.....	84
5.3 Numerical examples.....	85
5.4 Discussions of results .....	92
5.4.1 Results of the hard soil.....	92
5.4.2 Testing the neural network for the soft soil condition .....	108
5.4.3 Testing of the neural network for the unknown problems outside the range of PGA used in training .....	113
5.4.4 Comparison between the linear quadratic regulator (LQR) and ANN control .....	114

5.5 Conclusions .....	116
<b>CHAPTER-6.....</b>	<b>119</b>
<b>CONCLUSIONS AND RECOMMENDATIONS FOR FUTURE WORK ..</b>	<b>119</b>
6.1 Conclusion .....	119
6.2 Recommendation for future work .....	121
<b>REFERENCES .....</b>	<b>122</b>

## LIST OF FIGURES

FIGURE NO.	CAPTION	PAGE NO.
3.1	LQR feedback model in Simulink	29
3.2	Model of a ten storey building frame with active tendon placed on the top floor	30
3.3	Variations of percentage reductions in response to actuator position (Bhuj earthquake).	33
3.4	Variations of percentage reductions in response to actuator position (Kobe earthquake)	33
3.5	Variations of percentage reductions in response to actuator position (Elcentro earthquake)	34
3.6	Variations of percentage reductions in response to actuator position (Spitak earthquake)	34
3.7	Variation of normalized peak control force with actuator position (Bhuj earthquake)	35
3.8	Variation of normalized peak control force with actuator position (Kobe earthquake)	35
3.9	Variation of normalized peak control force with actuator position (Elcentro earthquake)	36
3.10	Variation of normalized peak control force with actuator position (Spitak earthquake)	36
3.11	Variations of R values for maximum base shear, peak top floor displacement and maximum interstory drift with actuator position (Bhuj earthquake)	37
3.12	Variations of R values for maximum base shear, peak top floor displacement and maximum interstory drift with actuator position (Elcentro earthquake)	37
3.13	Variations of R values for maximum base shear, peak top floor displacement and maximum interstory drift with actuator position (Kobe earthquake)	38
3.14	Variations of R values for maximum base shear, peak top floor displacement and maximum interstory drift with actuator position (Spitak earthquake)	38
3.15	Variations of percentage reductions of response with two actuator position (Bhuj earthquake)	41

3.16	Variations of percentage reductions of response with two actuator position (Kobe earthquake)	42
3.17	Variations of percentage reductions of response with two actuator position (Elcentro earthquake)	42
3.18	Variations of percentage reductions in response with two actuator position (Spitak earthquake)	43
3.19	Variation of normalized peak control force with two actuator position (Bhuj earthquake)	43
3.20	Variation of normalized peak control force with two actuator position (Kobe earthquake)	44
3.21	Variation of normalized peak control force with two actuator position (Elcentro earthquake)	44
3.22	Variation of normalized peak control force with two actuator position (Spitak earthquake)	45
3.23	Variation of R values for maximum base shear, peak top floor displacement and maximum interstory drift with two actuator position (Bhuj earthquake)	45
3.24	Variation of R values for maximum base shear, peak top floor displacement and maximum interstory drift with two actuator position (Kobe earthquake)	46
3.25	Variation of R values for maximum base shear, peak top floor displacement and maximum interstory drift with two actuator position (Elcentro earthquake)	46
3.26	Variation of R values for maximum base shear, peak top floor displacement and maximum interstory drift with two actuator position (Spitak earthquake)	47
3.27	Variations of percentage reductions of response with three actuator position (Bhuj earthquake)	49
3.28	Variations of percentage reductions of response with three actuator position (Kobe earthquake)	49
3.29	Variations of percentage reductions of response with three actuator position (Elcentro earthquake)	50
3.30	Variations of percentage reductions of response with three actuator position (Spitak earthquake)	50
3.31	Variation of normalized peak control force with three actuator position (Bhuj earthquake)	51
3.32	Variation of normalized peak control force with three actuator position (Kobe earthquake)	51
3.33	Variation of normalized peak control force with three actuator position (Elcentro earthquake)	52

3.34	Variation of normalized peak control force with three actuator position (Spitak earthquake)	52
3.35	Variation of R values for maximum base shear, peak top floor displacement and maximum interstory drift with three actuator position (Bhuj earthquake)	53
3.36	Variation of R values for maximum base shear, peak top floor displacement and maximum interstory drift with three actuator position (Kobe earthquake)	53
3.37	Variation of R values for maximum base shear, peak top floor displacement and maximum interstory drift with three actuator position (Elcentro earthquake)	54
3.38	Variation of R values for maximum base shear, peak top floor displacement and maximum interstory drift with three actuator position (Spitak earthquake)	54
4.1	Block diagram representation of a three layered ANN (Network 1)	59
4.2	Block diagram representation of a three layered ANN (Network 2)	60
4.3	Block diagram representation of a three layered ANN (Network 3)	60
4.4	Comparison between target and actual percentage reduction in top storey displacement for Kobe earthquake (Network 1)	63
4.5	Comparison between target and actual percentage reduction in top storey displacement for Spitak earthquake (Network 1)	63
4.6	Comparison between target and actual percentage reduction in base shear for Kobe earthquake (Network 2)	64
4.7	Comparison between target and actual percentage reduction in base shear for Spitak earthquake (Network 2)	64
4.8	Comparisons between target and actual percentage reduction in base shear and top storey displacement for Kobe earthquake (Network-3)	65
4.9	Comparisons between target and actual percentage reduction in base shear and top storey displacement for Spitak earthquake (Network 3)	65
4.10	Comparison between target and actual percentage reduction in top floor displacement for Bhuj earthquake (Network1).	67
4.11	Comparison between target and actual percentage reduction in top floor displacement for Elcentro earthquake (Network1)	67

4.12	Comparison between target and actual percentage reduction in top floor displacement for Eliamo earthquake (Network1)	68
4.13	Comparison between target and actual percentage reduction in top floor displacement for Lomapieta earthquake (Network 1)	68
4.14	Comparison between target and actual percentage reduction in top floor displacement for Northridge earthquake (Network 1)	69
4.15	Comparison between target and actual percentage reduction in top floor displacement for Victoria earthquake (Network 1)	69
4.16	Comparison between target and actual percentage reduction in base shear for Bhuj earthquake (Network 2)	70
4.17	Comparison between target and actual percentage reduction in base shear for Elcentro earthquake (Network 2)	70
4.18	Comparison between target and actual percentage reduction in base shear for Eliamo earthquake (Network 2)	71
4.19	Comparison between target and actual percentage reduction in base shear for Lomapieta earthquake (Network 2)	71
4.20	Comparison between target and actual percentage reduction in base shear for Northridge earthquake (Network 2)	72
4.21	Comparison between target and actual percentage reduction in base shear for Victoria earthquake (Network 2)	72
4.22	Comparisons between target and actual percentage reduction in base shear and top storey displacement for Victoria earthquake (Network 3)	73
4.23	Comparisons between target and actual percentage reduction in base shear and top storey displacement for Elcentro earthquake (Network 3)	73
4.24	Comparisons between target and actual percentage reduction in base shear and top storey displacement for Bhuj earthquake (Network 3)	74
4.25	Comparisons between target and actual percentage reduction in base shear and top storey displacement for Eliamo earthquake (Network 3)	74
4.26	Comparisons between target and actual percentage reduction in base shear and top storey displacement for Northridge earthquake (Network 3)	75
4.27	Comparisons between target and actual percentage reduction in base shear and top storey displacement for Lomapieta earthquake (Network 3)	75
4.28	Normalized time history of simulated narrowband earthquake (PSDF as Clough and Penzien double filter PSDF)	77



4.29	Normalized near field time history of earthquake with fling step effect (Chi- Chi earthquake,1999)	77
5.1	A block diagram representation of a three layered ANN	84
5.2	Normalized PSDF of Ground Acceleration	86
5.3	The architecture of ANN used for training and testing	87
5.4	Typical simulated time history of ground acceleration (PGA=0.1g) for hard soil condition	88
5.5	Typical time histories of simulated control force (peak= 0.2W) for hard soil	88
5.6	Typical simulated time history of ground acceleration (PGA=0.3g) for hard soil condition	89
5.7	Typical time histories of simulated control force (peak= 0.4W) for hard soil	89
5.8	Typical simulated time history of ground acceleration (PGA=0.3g) for soft soil condition	90
5.9	Typical time histories of simulated control force (peak= 0.15W) for soft soil	90
5.10	Typical simulated time history of ground acceleration (PGA=0.1g) for soft soil condition	91
5.11	Typical time histories of simulated control force (peak= 0.3W) for soft soil	91
5.12	Comparison between target and actual percentage of reductions in base shear and top floor displacement (target value remains the same for both) for PGA 0.35g.(known problem)	92
5.13	Comparison between target and actual percentage reductions in base shear and top floor displacement for (20% fixed target reduction in Base shear) for PGA=0.35g(known problem)	93
5.14	Comparison between target and actual percentage reductions in base shear and top floor displacement for PGA 0.05g	94
5.15	Comparison between target and actual percentage reductions in base shear and top floor displacement for PGA 0.10g	94
5.16	Comparison between target and actual percentage reductions in base shear and top floor displacement for PGA 0.15g	95

5.17	Comparison between target and actual percentage reductions in base shear and top floor displacement for PGA 0.2g	95
5.18	Comparison between target and actual percentage reductions in base shear and top floor displacement for PGA 0.25g	96
5.19	Comparison between target and actual percentage reductions in base shear and top floor displacement for PGA 0.30g	96
5.20	Comparison between target and actual percentage reductions in base shear and top floor displacement for PGA 0.35g	97
5.21	Comparison between target and actual percentage reductions in base shear and top floor displacement for PGA 0.40g	97
5.22	Comparison between target and actual percentage reductions in base shear and top floor displacement (for fixed 20% target reduction in base shear) for PGA=0.1g	98
5.23	Comparison between target and actual percentage reductions in base shear and top floor displacement (for fixed 30% target reduction in base shear) for PGA=0.1g	98
5.24	Comparison between target and actual percentage reductions in base shear and top floor displacement (for fixed 40% target reduction in base shear) for PGA=0.1g	99
5.25	Comparison between target and actual percentage reductions in base shear and top floor displacement (for fixed 50% target reduction in base shear) for PGA=0.1g	99
5.26	Comparison between target and actual percentage reductions in base shear and top floor displacement (for fixed 60% target reduction in base shear) for PGA=0.1g	100
5.27	Comparison between target and actual percentage reductions in base shear and top floor displacement (for fixed 70% target reduction in base shear) for PGA=0.1g	100
5.28	Comparison between target and actual percentage reductions in base shear and top floor displacement (for fixed 20% target reduction in base shear) for PGA=0.2g	101
5.29	Comparison between target and actual percentage reductions in base shear and top floor displacement (for fixed 30% target reduction in base shear) for PGA=0.2g	101
5.30	Comparison between target and actual percentage reductions in base shear and top floor displacement (for fixed 40% target reduction in base shear) for PGA=0.2g	102
5.31	Comparison between target and actual percentage reductions in base shear and top floor displacement (for fixed 50% target reduction in base shear) for PGA=0.2g	102

5.32	Comparison between target and actual percentage reductions in base shear and top floor displacement (for fixed 60% target reduction in base shear) for PGA=0.2g	103
5.33	Comparison between target and actual percentage reductions in base shear and top floor displacement (for fixed 70% target reduction in base shear) for PGA=0.2g	103
5.34	Comparison between target and actual percentage reductions in base shear and top floor displacement (for fixed 20% target reduction in base shear) for PGA=0.4g	104
5.35	Comparison between target and actual percentage reductions in base shear and top floor displacement (for fixed 30% target reduction in base shear) for PGA=0.4g	104
5.36	Comparison between target and actual percentage reductions in base shear and top floor displacement (for fixed 40% target reduction in base shear) for PGA=0.4g	105
5.37	Comparison between target and actual percentage reductions in base shear and top floor displacement (for fixed 50% target reduction in base shear) for PGA=0.4g	105
5.38	Comparison between target and actual percentage reductions in base shear and top floor displacement (for fixed 60% target reduction in base shear) for PGA=0.4g	106
5.39	Comparison between target and actual percentage reductions in base shear and top floor displacement (for fixed 70% target reduction in base shear) for PGA=0.4g	106
5.40	Variation of peak control force with PGA for the same percentage reduction of both responses (hard soil)	107
5.41	Comparison between the target and actual percentage of reduction in base shear and top floor displacement (target value remains same for both) for PGA 0.05g	108
5.42	Comparison between the target and actual percentage of reduction in base shear and top floor displacement (target value remains same for both) for PGA 0.10g	109
5.43	Comparison between the target and actual percentage of reduction in base shear and top floor displacement (target value remains same for both) for PGA 0.15g	109
5.44	Comparison between the target and actual percentage of reduction in base shear and top floor displacement (target value remains same for both) for PGA 0.20g	110
5.45	Comparison between the target and actual percentage of reduction in base shear and top floor displacement (target value remains same for both) for PGA 0.25g	110

5.46	Comparison between the target and actual percentage of reduction in base shear and top floor displacement (target value remains same for both) for PGA 0.30g	111
5.47	Comparison between the target and actual percentage of reduction in base shear and top floor displacement (target value remains same for both) for PGA 0.35g	111
5.48	Comparison between the target and actual percentage of reduction in base shear and top floor displacement (target value remains same for both) for PGA 0.4g	112
5.49	Variation of peak control force with PGA for the same percentage reductions of both responses (soft soil)	112
5.50	Comparison between target and actual percentage reductions in base shear and top floor displacement for PGA 0.5g	113
5.51	Comparison between target and actual percentage reductions in base shear and top floor displacement for PGA 0.6g	114
5.52	Comparison between target and LQR percentage reductions in base shear and top floor displacement for PGA= 0.1g	115
5.53	Comparison between target and LQR percentage reductions in base shear and top floor displacement for PGA= 0.2g	115
5.54	Comparison between target and LQR percentage reductions in base shear and top floor displacement for PGA= 0.4g	116

## LIST OF TABLES

Table No.	Caption	Page No.
3.1	Summary of earthquake time histories used	31
3.2	Optimal position of actuator based on percentage reductions of responses	39
3.3	Optimal position of actuator based on R values	39
3.4	Combinations of two actuators placed in the frame	40
3.5	Optimal position of two actuators based on percentage reductions of responses	40
3.6	Optimal position of two actuators based on R value for the case of two actuators	47
3.7	Combinations of three actuators placed in the frame	48
3.8	Optimal position of three actuators based on percentage reduction of responses	55
3.9	Optimal position of three actuators based on R value for the case of three actuators	55
3.10	Maximum control force required	55
4.1	Summary of earthquake time histories used	62
4.2	Summary of Earthquake Time Histories	66
4.3	Results for Narrowband Earthquake	78
4.4	Results for Near field time history with Fling step effect	78
4.5	Results for Narrowband Earthquake	78
4.6	Results for Near field time history with Fling step effect	78
4.7	Results for Narrowband Earthquake	79
4.8	Results for Near field time history with Fling step effect	79
5.1	Combinations of PGA and peak control force used in the training data	86

## NOMENCLATURE

Notation	Expansion
[M]	Mass matrix
[C]	Damping matrix
[K]	Stiffness matrix
[X]	Dimensional displacement vector
$\ddot{x}_g$	Earthquake ground acceleration
[I]	Influence coefficient matrix of size $n \times 1$
[D]	A controller location matrix of size $n \times m$
[U]	Vector of control force of size $m$
[Z]	State vector
[A]	Linear system matrix
[B]	Control location matrix
[E]	Excitation influence matrix
[I]	Identity matrix
[D]	Damper location matrix
[Q]	Weighing matrix multiplied by a state vector in LQR function
[R]	Weighing matrix multiplied by control force in LQR function
$\alpha$ And $\beta$	Proportional coefficient
$\omega_i$ And $\omega_j$	Structural model frequencies
$\zeta$	Structural damping ratios
$\zeta_g, w_g$ And $\zeta_s, w_s$	Double Filter coefficients
So	Ordinate of the PSDF of white noise
Ss	Output of first filter
[J]	Performance index
[P]	Transformation matrix

# CHAPTER-1

## INTRODUCTION

### 1.1 General

The vibrations induced by the earthquakes can cause serious damages to the buildings and the equipments installed in them. Reduction in such damages can be achieved through several methods, including code compliant design, additional stiffening, installing damping devices and providing structural control systems. Structural control is now recognized as an effective way to mitigate damages or distress caused by the earthquake or the wind forces in the structure. For the earthquake, the structural control is considered as seismic design philosophy to alleviate structure's strength to resist the earthquake. The structural control refers to those techniques which are used to reduce or control the undesirable responses in the structures due to external forces acting on it. For this purpose, additional energy dissipation devices with or without appropriate control systems or external power are installed in the structure to reduce the effect of the environmental loadings. Therefore, the structural control is usually classified by its method or the types of devices used to impart the control force. Generally, three classes of structural control devices are employed, which include passive, active and semi-active, corresponding to passive, active and semi-active control respectively.

Stiffening of structures shifts the resonant frequency of the structure beyond the frequency band of excitation. Damping devices reduce the resonance peaks of the responses by dissipating the vibration energy. Additional damping can be added passively by using the fluid dampers, the elastomeric elements or the hysteretic elements or by transferring energy to the dynamic vibration absorbers. Another kind of the passive control device, which has found wide application, is the base isolation device. This device combines damping with the lateral flexibility of the system to reduce the seismic effect on structures. Although, the passive control strategies are the most well accepted strategies for the structural vibration reduction, they are not the most efficient control technique as they cannot adapt to different loading events and structural vibrations. On the other hand, the active control systems are more adaptive and

efficient in vibration reduction as they can sense the external vibrations and can react accordingly.

Yao (1972) first attempted to give the concept of the active control to the civil engineering structures. The concept of the active control had been started in early 1970's and the full-scale application was performed in 1989. An active control system can be defined as a system that typically requires a large power source for the operation of electro hydraulic or electromechanical (servo-motor) actuator, which increases the structural damping or stiffness or both. The active control system uses sensors for measuring both the excitation and the structural responses for controlling the unwanted vibrations (Rahmat et. al.,2010). The working principle of the active control system is that, based on the measured structural response, the control algorithm generates control signal required to attenuate the vibration. Based on this control signal, the actuators placed in desired locations of the structure generate a secondary vibration response, which reduces the overall structure response (Roy et al., 2003). Depending on the size of the building structure, the power requirements of these actuators vary from kilowatts to several megawatts (Fan et.al, 2011). Hence, an actuator capable of generating the required control force should be used. As the active devices can work with a number of vibration modes, it is a perfect choice for the multi degree of freedom (MDOF) structures.

In structural applications, the control force can be applied in several ways such as, (i) Active tuned mass damper, usually placed on the top of the building, in which, the reaction force provided by a tuned mass damper to its support can be augmented appropriately by an external force applied to the mass of the damper; (ii) Active tendon control mechanism is another control mechanism, which generally consists of a set of prestressed diagonal tendon connected to the structure; (iii) Gas pulse generator which produces pulsed force by the release of air jet. A majority of researchers in the field of the active control to civil engineering structures have been focusing on building structures subjected to wind or earthquake forces [Sae-Ung and Yao (1978), Pantelides (1990)].

For effective control of structures, a number of active control strategies have been investigated. They include both linear and nonlinear feedback and feed forward-feedback control strategies. These control strategies attempt to minimize a performance index of the structures in



order to arrive at a control law which dictates the external force to be applied to the structure. The control force depends upon the level of responses and the excitations of the structure. Apart from these strategies, other control strategies have also been attempted, such as pulse control, instantaneous control, predictive control, control by aerodynamic appendages and sliding mode control. In pulse control, a train of force pulse is generated and in order to conserve energy, the control is activated only when some pre-specified threshold has been reached. In the instantaneous control, a time dependent performance index is minimized at every time instant to derive the optimal control law. The external excitation term is considered at each time step, which is not considered in classical optimal control strategy. In predictive control, the control signal makes the predicted process output equal to a desired process output. Predictive control theory is formulated in discrete time to be applied in digital control loops. The theory of sliding mode control is to design controllers to drive the response trajectory into the sliding surface and maintain it there. The motion on the sliding surface is always stable. A number of reviews on the active structural control were presented (Chhabra et al., 2016). Housner et al. (1997) provided a comprehensive state of the art review on the structural control. Spencer et al.(2003) provided a state-of-the-art review on the structural control comparing the passive, active and semi-active control.

Active control of building frames using the Artificial Neural Network (ANN) has been a subject of intensive research in the past. Numerous applications of the ANN for structural control are reported in the literature. The development of the neural network started 50 years ago (Sivanandam, S, et. al.,2006). An ANN consists of many nodes, i.e. processing units analogous to neurons in the brain. An ANN is gross simplification of real (biological) networks of neurons. Each node possesses a node function associated with it which, along with a set of local parameters, determines the output of nodes, given an input. Modification in the local parameters may alter the node function. An ANN thus is an information - processing system. Researchers in recent years have also used the theories of the neural network extensively in the field of the structural control. The primary advantages of this “intelligent” controller are that it obviates the need for the development of any control strategy analytically. This control strategy is used in the active and semi active control of structures.

In the active control of structure using ANN, the control force is generated with the help of an ANN, which would reduce the response of the structure when subjected to unknown future earthquakes.

For a given structural system under specified dynamic excitation, the neural net provides the signal for the control force to reduce the response of the structure. Active control of a three-storey frame structure subjected to ground excitations was illustrated by introducing the neural network based control algorithm [Ghaboussi and Jaghataie (1995)]. Bani-Hani and Ghaboussi (1998) employed neurocontroller method for nonlinear structural control. Rao and Datta (1998) presented a methodology to employ the artificial neural network for the active control of structures under seismic excitation for a target percentage reduction of response.

Various types of neuron-controllers have been reported in the literature (Ghaboussi and Joghataei, 1995; Chen et.al, 1995; Bani-Hani and Ghaboussi, 1998; Rao and Dutta,1998; Madan, 2006). A Neuro-controller is trained with and without the help of a trained emulator network. The purpose of the emulator network is to aid the learning of the Neuro-controller in establishing the desired relation between the immediate past history of the response of the structure and the adjusted control signal of the actuator.

Some of the limitations of the active control of structures are well recognized. For example, control strategies are derived for idealized models (discrete system). However, actual structures are distributed parameter systems. As a result, simulated control schemes may not be truly effective on the actual system. Further, in treating ideal systems, the assumption is made that all operations in the control loop can be performed instantaneously. In reality, however, time has to be consumed in processing information, measured in performing on-line computation, and in executing the control forces as required. Thus, the time delay causes unsynchronized application of the control forces and this non-synchronization not only can render the control ineffective, but may also cause instability in the system. This limitation led to a number of researches on the time delay compensation in the structural control.

Another severe limitation of the effective use of the structural control is that output feedback algorithms need number of inputs from sensors. But, practical considerations preclude the availability of such complete set of information. Implementable control schemes require as

few controllers as possible to be used. Thus, optimization of the number and locations of the sensors and controllers is important in structural control from the standpoint of economy and external energy savings. An optimization of structure and control system design has attracted significant attention over the years. While several different approaches have been proposed for simultaneous structural and control system optimization, most of the proposed methods essentially solve a single objective optimization problem. Placement of actuators in the structure is an important aspect of structural control optimization. The determination of the number and the location of actuators in active vibration control of structures is an important design aspect. Misplaced actuators lead to controllability and observability problems; therefore, to get an optimum control performance with the minimum control cost, the actuators should be placed at optimum locations. Different objective functions have been used by researchers to find the optimal locations of the actuators. For example, minimizing the control energy by maximizing the controllability or maximizing the control forces transmitted by the actuators to the structure is one strategy. Mirza and Van Niekerk (1999) proposed a method to determine the optimal location of actuators based on the disturbance sensitivity grammar matrix. Striou (2000) considered is minimizing the optimal value of the controller performance index to find the optimum locations of actuators and sensors. Li et al. (2004) proposed a three level optimal design problem for finding the optimum number and locations of actuators using a two-level genetic algorithm. For the determination of optimum locations of actuators many such optimization techniques are available, but they are complex in nature.

## **1.2 Need for the Present Study**

From the review of literature presented in detail in the subsequent Chapter, it is evident that large numbers of studies have been carried out on the ANN control. Considerable research has been done for the development of control algorithms using ANN, Fuzzy logic controller and a combination of these two controllers namely, adaptive neuro-fuzzy inference system (ANFIS) control algorithms. The advantages and appeal of the ANN control are its online applications. ANNs are trained either offline or online to replace the computer based algorithm. However, it has the limitation that generalized control of responses for structural systems is difficult to obtain. More is the number of data sets available for training, better is the learning of the ANN

and its prediction. It is also observed that ANN acquire some extra intelligence to control systems outside the domain of the training.

With the vast literature available on ANN, it is difficult to find gap areas for conducting research on the application of the ANN for structural control. In the present study, a few simple applications of the ANN for structural control under earthquake excitation have been attempted, which are not widely reported in the literature. These applications are centered on the predictive active control of structures. It is an inverse problem which can be ideally tackled by an ANN. Predictive control using an ANN consists of an offline training of the ANN and use the trained ANN for online application. Two problems of predictive control are attempted, namely, i) Prediction of the time history of the control force for the target percentage reduction of a few selected response quantities of the structure for non-specific earthquakes and ii) Prediction of the time history of the control force for site specific earthquakes for the target percentage reduction of the same response quantities as above. The former generates the training data from the controlled responses of structures under a set of real earthquakes; the controlled responses are obtained with the help of the control force derived from a standard algorithm. The latter assumes a pattern of variation of control force with frequency, which is consistent with the site-specific power spectral density function (PSDF) of ground motion. The time history of the control force is synthetically generated from the PSDF of the control force and is used to obtain the controlled responses of the structure. The training data consists of the time history of responses and the time history of the control force.

Another study attempted in the present work deals with the investigation of optimal placement of actuators in active control of building frames. Although there exist sophisticated optimization algorithms developed for optimal placement of actuators for achieving best response reductions like genetic algorithm, steepest gradient optimization technique, etc., they suffer from the following two drawbacks:

- i) These algorithms are complicated, time consuming and lack robustness.
- ii) There are many floors where actuators cannot be placed because of practical limitations. These floors vary from problem to problem, therefore, cannot be generalized in a form of a specified constraint in the optimization problem.

### **1.3 Scope and objectives of the work**

The objective of the present study deals with the two problem areas mentioned above. For the formulation of the problem and for generating the data sets for training the neural networks, the most widely used and well established control algorithms namely, linear quadratic regulator (LQR) are used. The problems are formulated and solved for fully observed state. However, the problems can be easily extended for partially observed states. The precise objectives of the study are:

- 1) To investigate the characteristics of the reduction of two important response parameters, i.e. the top floor displacement and base shear for different positions of actuators placed on a ten storied building frame. Three separate studies are conducted, namely, i) placement of one actuator on different floors, ii) placement of two actuators on different floors, and iii) placement of three actuators on different floors.
- 2) Prediction of the desired time history of control forces for target percentage reduction of responses to real earthquake ground motions using ANN and compare the actual reduction of responses obtained by the predicted control force with the target reduction of responses.
- 3) Prediction of the time history of desired control force of the target percentage reduction of responses for site specific ground motion treated as a stationary random process represented by its power spectral density function (PSDF) and carry out the same comparison as stated above.
- 4) Discussions on the effectiveness of the control schemes and the optimal placement of actuators for best response reduction.

### **1.4 Organization of thesis**

To fulfill the above objectives, the work presented in the thesis has been divided into six Chapters.

**Chapter 1** provides a general background of the research undertaken, brief literature review, the need of the present study, scope and objective of the work.

**Chapter 2** provides an extensive literature review to highlight the importance of the work done on the thesis. For the convenience of presentation, the literature review has been carried out in four subheadings. The first part covers a brief review of active structural control, including acceleration feedback control strategy and time delay compensation technique. The second part of literature survey is related to the structural application of ANN bringing out the theoretical basis and its silent features. The third part gives a brief review of the application of control of structures using ANN. At the end, a brief review of the available literature on the control algorithms, like fuzzy logic control algorithm and ANFIS is presented.

**Chapter 3** deals with actuator placement which has a significant impact on the dynamic response of actively controlled structures. Misplaced actuators and sensors often lead to controllability and observability related problems. Three types of placements of actuators are considered in the study, namely, i) single actuator placed at different floors, ii) specific combinations of two actuators placed on different floors, and iii) specific combinations of three actuators placed on different floors.

A computational procedure based on the control algorithm in MATLAB is developed. Control responses are obtained using LQR (linear, quadratic regulator) algorithm for four real earthquakes. The percentage reduction of peak top floor displacement and maximum base shear are investigated for different positions of the actuators placed on the building frame for finding the optimum location of the actuators. Results are discussed using three parameters, namely, R factor, defined as a percentage reduction in response per unit control force, the peak control force and the percentage reduction in response quantities of interest. Further, the results are discussed with respect to the peak ground acceleration (PGA) and the peak control force. A ten story building frame is analyzed under different earthquakes.

**Chapter-4** describes the predictive active control using ANN for achieving target percentage reduction of response quantities of interest for specified real earthquake ground motions. Three types of neural networks are trained and tested for achieving the desired objective. The response quantities of interest are considered as peak top floor displacement and maximum base shear. The three neural network architectures consist of input nodes, hidden layers, and an output node. For two neural networks, the input nodes are provided with the time history of ground acceleration, and the percentage reduction in peak top floor displacement in one and in the other, percentage reduction of maximum base shear. In third neural network, both

percentage reduction in peak top floor displacement and maximum base shear are considered along with the time history of ground motion in the input modes. The output node of all neural networks provides the desired time history of control force required to obtain the target percentage reduction of responses. Training data sets are obtained by finding the controlled responses of building frames for a number of ground motions scaled to cater to different PGA values considered in the study and the time histories of control forces. For this purpose, the LQR control algorithm is employed. Neural networks are tested for both known and unknown data sets. The unknown data set includes time histories of ground motion for earthquakes, which are not included in the training set. Further, the neural networks are tested for narrowband and near field earthquakes at levels of PGA, which were outside the domain of training data. The numerical study is conducted on a ten-storied building frame.

**Chapter-5** deals with the predictive control using ANN for site-specific earthquakes. Records of ground acceleration for earthquakes are synthetically generated from their PSDFs. Two types of ground motions are considered, namely, broad band and narrow band for generating the training data. For obtaining the time history of control force, it is assumed that the desired control force and the earthquake excitations have similar frequency contents. Therefore, the control force may be represented by the same nature of the PSDF as that of the excitation. Thus, the time histories of control force are simulated from the PSDF of ground motion suitably normalized. In this manner, different pairs of simulated time histories of ground motion and control force are generated. For each pair, the controlled responses are obtained using SIMULINK tool box of MATLAB. In the input nodes, the percentage reductions of responses and the time history of ground motion are provided. The corresponding time history of control force is provided in the output node for training the ANNs. Three types of ANNs are considered as discussed in Chapter 4. The ANNs are tested for both known and unknown problems. The neural networks are also tested for different percentage reductions of responses and different ground motions with PGA values not involved in the training set. The same ten-storied building frame as used in Chapter -4 is taken as the illustrative problem for the numerical study.

**Chapter-6** summarizes the work done on the thesis, provides the important conclusions drawn from the studies and outlines the future work to be carried out in the area of the research carried out in the thesis.

## CHAPTER – 2

### LITERATURE REVIEW

#### 2.1 General

The development of control theory for the protection of structures against natural hazards like wind and earthquakes has always been a major concern, and in the past few decades, researchers have paid considerable attention in this field. However, its application to civil engineering structures is unique in many ways. Civil engineering structures are typically massive and distributed systems having large degrees of freedom and are exposed to various loads having high amount of uncertainties which creates a need for higher control force and power.

Depending upon the amount of energy required, a structural control system could be categorized into four types, namely active, semi active, hybrid and passive control system. Until the past few decades, the passive control systems like base isolation were commonly employed. Due to the advancement in technology, active control systems and hybrid control systems are being used in the buildings nowadays. An active control system is fully adaptive. Smart structures using active control systems employ external power to generate the control force, which is directly applied to the structure to reduce its response. Since building structures are usually large, huge force-generating equipment and large external power supplies are required for active seismic response control..

Song (1987) has contributed a lot in the area of active structural control. According to Soong (1987), the earliest attempts in active control to reduce structural motion were made in the 1960's using pre-stressing tendons as control devices to stabilize tall structures and it was also mentioned that an initial systematic study in active structural control was given by Yao (1972). Many state of the art reviews on the structural control exists in the literature. Housner et al. (1997) provided a comprehensive state of the art review on the structural control. Spencer et al. (2003) presented a contemporary review of the structural control comparing the passive, active and semi-active control. Datta (2003) explored the difficulties in practical implementation of structural control systems.

For convenience, the literature survey is broadly divided into four parts. The first part of literature survey lays out a brief review of the active structural control. The second part of



literature survey deals with the comparison of different control algorithms used in active control of structures. The third part of literature survey gives insight into the structural application of ANN. The fourth part offers an overview of the application of control of structures using ANN. The last part provides a review of the structural control using fuzzy logic and neuro-fuzzy technique (ANFIS)

## **2.2 Brief review of active structural control**

The structural vibration control produced by wind and earthquake can be done by various means such as modifying rigidities, masses, damping, or shape, and by providing passive or active counter forces. An active control system is one in which an external power source is used to apply force to the structure in a prescribed manner. These forces can be used to both add and dissipate energy in the structure.

Some of the earlier works on the application of control theory in structural control provide a great foundation for the theory of active control of structures. For active control of buildings, active mass damper (AMD) [Chang and Soong (1980); Kobori et al. (1991a,b); Chang and Yang (1995); Ankireddi and Yang (1996)], active tendon systems [Abdel-Rohman and Leipholz (1979, 1983); Yang and Akbarpour (1987)] and active bracing system have been deployed. The active control forces are regulated by the measured information from sensors attached to the structure as well as by the particular control algorithm used. The structural characteristics are modified by active control forces, leading to a reduction of the structural vibration. For all control strategies, an optimization procedure is used to compute the control law or control forces. Among the various linear control strategies, feedback control strategy has been the most widely used. Soong et.al. (1991) provided an overview of different active control systems. Discussions were made on several experimental studies conducted in this area, including active tendon or brace system, active mass damper and active mass driver system, variable stiffness systems and other control systems. Full scale implementation and testing of active control devices along with the challenges faced in the real time applications are discussed. Spencer et al. (1993) used the H2 frequency domain control method, coupled with acceleration feedback, to design an acceleration feedback strategy for a building subjected to earthquake excitation. A controller is designed to stabilize the closed loop feedback system which minimizes

the norm of the transfer function matrix. The performance of this control strategy developed for seismically excited three-storey single bay scale model building (hydraulic actuator installed between the ground and the first floor) was also experimentally verified. Sarbjeet and Datta (1998) suggested a control strategy based on the combination of feed forward and feedback gain controls wherein an open closed loop is presented for reduction of the displacement response of the shear frame model of tall buildings to random ground motion. This is represented by double-filtered white noise.

Gang et al. (2001) suggested a general formulation of the model predictive control (MPC) scheme for real time controlling the response of structures under earthquakes. The MPC scheme was based on an explicit use of a prediction model of the system response to obtain the control actions by minimizing an objective function. Optimization objectives in MPC include minimization of the difference between the predicted and desired response trajectories, and the control effort subjected to certain constraints. In this study, the prediction model was formulated using both feed forward (FF) and feedback (FB) components to increase the effectiveness of the MPC scheme.

Shooshtari et al. (2004) presented a method for the extension of control process in the inelastic range of deformations for active control of reinforced concrete (R/C) structures against seismic excitations. Computer software was developed for dynamic inelastic analysis of reinforced concrete structures, including the effects of control forces, illustrating the significance of active control analytically. The effects of instantaneous optimal control algorithms were investigated on structural response. Numerical examples were solved to illustrate the process of active structural control for R/C frame structures. The significance of the arrangement of control forces is presented. The results showed that the seismic response of reinforced concrete structures can be reduced significantly with active control. A 1/3<sup>rd</sup> to 2/3<sup>rd</sup> reduction in inter-storey drift is obtained.

Vural Aksakalli and Daniel Ursu (2006) widely used classical linear controllers in the control of nonlinear stochastic systems and thus there was concern about the ability of the controller to adequately regulate the system. An alternative approach to cope with such systems was to avoid the need to build the traditional “open-loop” model for the system.

Sinan Korkmaz (2011) provided advances in theory and practice of active control technology. It also provided an overview of advances enabling feasible applications of active structures. Computing challenges which are important to the creation of the next generation of active structures are identified.

Fiasco and Adeli (2011) presented a state-of-the-art review of research performed in the area of smart structures. Active control of structures using a variety of systems, including active tuned mass dampers, distributed actuators, active tendon systems and active coupled building systems and semi-active control systems, including magneto rheological (MR) fluid dampers, semi-active stiffness dampers, semi-active tuned liquid column dampers, and piezoelectric dampers are discussed in the paper. The paper suggested that there is a need for a control algorithm that will determine the magnitude of control forces at any given time and place of actuators within the structure, strategy, which will apply the required forces to compensate for the forces of nature and minimize the vibrations of the structure containing three physical components namely, sensors, actuators and a computer.

### **2.3 Algorithms used for active control of structures**

Many control algorithms were developed for the active control of structures. Doyle et.al (1989) derived state space solutions to  $H_2$  and  $H_\infty$  control problems. Output feedback solutions for full information, full control, disturbance feed-forward and output estimation were described. Chang et.al. (1988) conducted an experimental study of the application of active control of structures under earthquake excitation. A SDOF model structure with linear optimal feedback control algorithm was used which were controlled using the pre-stressing tendons connected to a servo-hydraulic actuator. Spencer et.al. (1994) discussed frequency domain optimal control using both  $H_2$  and  $H_\infty$  control methods, for active control of structures under seismic loading. The results showed the efficiency of the frequency domain control methods which can be used to optimally control a structure using output feedback of acceleration measurements and to selectively shape the output structural response in a desirable manner.

Alavinasab et.al. (2006) presented a new energy-based technique to eliminate trial and error way of finding appropriate gain matrices in linear quadratic regulator (LQR) controllers used in active control of structures. A three-storey building with active tendons were analyzed

using real earthquake records. Control forces were calculated based on the minimization of the total energy of the structure in each time step. The results showed that the proposed method was more efficient than the other proposed weighting matrices used in LQR for reducing structural vibration due to the energy concept and self-tuning.

Guclu (2006) studied the active response control of a multi degree freedom system (MDOF) system using Sliding Mode Controller (SMC) and Proportional-Integral-Derivative (PID) controller separately. Against the real earthquake excitation, the simulated results showed a better control performance for SMC than a PID controller.

Shafieezadeh et al. (2007) used fractional order filters to improve the performance of LQR controllers. A two-storey building equipped with actuators placed on each storey was considered in the study. Simulations were performed on the system subjected to both artificial and real ground motion records. The results showed that the inclusion of fractional order filters improved the response, reduction performance of the LQR controller. Also, it was concluded that the use of single fractional order of all the state variables to give better result than assigning distinct fractional orders for difference state variables.

K-Karamodin and H. H-Kazemi (2008) proposed a semi-active control method in which seismically excited nonlinear benchmark building equipped with a magnetorheological (MR) damper was presented and evaluated. Linear, quadratic Gaussian (LQG) was used to estimate the control force. The required voltage for the MR damper to produce the control force estimated by LQG controller was calculated by a neural network predictive control algorithm (NNPC). To control the structure, the LQG controller and the NNPC were linked. The coupled LQG and NNPC systems were then used to train a semi-active Neuro-controller designated as SANC, which produced the necessary control voltage that actuated the MR damper. The effectiveness of the NNPC and SANC was illustrated and verified using the simulated response of a 3-story full-scale, nonlinear, seismically excited, benchmark building excited by several historical earthquake records. The semi-active system using the NNPC algorithm was compared with the performances of passive as well as active and clipped optimal control (COC) systems, which were based on the same nominal controller as was used in the NNPC algorithm. The results demonstrated that the SANC algorithm was quite effective in the seismic response, reduction for

a wide range of motions from moderate to severe seismic events, compared with the passive systems and performed superior to the active and COC systems.

Boujari et.al.(2012) investigated the effectiveness of classical PID and 2DOF PID control algorithms for active vibration control of structures. A three story building model excited under four ground motion records, namely El Centro 1940, Hachinohe 1968, Northridge 1994, and Kobe 1995 were considered in the study. Simulations were performed in MATLAB environment and the results of these two methods obtained and compared to each other. The results showed that 2DOF PID exhibited more effective in reducing system's response compared to a classical PID control algorithm.

Etedali et.al.(2013) studied the seismic control of a benchmark isolated building equipped with piezoelectric friction dampers (PFD) using PD/PID controllers. The controllers were optimized using genetic algorithms. Considering seven pairs of earthquakes and nine performance indices, the performance of the closed-loop system was evaluated. Then, the results were compared with those given by the maximum passive operation of piezoelectric friction dampers and LQG controllers. The simulation results showed that the proposed controllers performed better in terms of simultaneous reduction of floor acceleration and maximum displacement of the isolator. The simulation results showed that the Optimal PID has a performance similar to that provided by the Optimal PD. In comparison with the maximum passive operation and LQG methods, an advantage of the proposed method was that it provided a simple strategy to estimate the controller forces.

Ghaffarzadeh et.al. (2014) proposed an analytical method based on block-pulse functions which does not require the Riccati Equation for calculating the control force. Seismic motions with various PGAs were used to verify the effectiveness of the proposed method. Controlled and uncontrolled top floor displacement responses based on proposed method and LQR method were compared. The comparison disclosed that the outcome of the proposed method is as satisfactory as the results of the LQR method. The salient advantage of this method lies in its ability to obtain reasonable results with less computational expenses.

Amir (2014) investigated the advantage of using a non-linear passive damping system in vibration control of two adjacent structures under the El Centro earthquake. Using the optimum

LQR algorithm, the non-linear damping coefficient was determined and the response of the structure was obtained. It is concluded that the control system is found to be very effective in mitigating the dynamic responses of the adjacent structures and there was an optimum damping coefficient of damper for minimum responses. A relation between control force and velocity of the stroke was estimated. This estimation provides the nonlinear parameter of a damping system which could control the response of the structure similar to an active control system performance.

Thenozhi et.al.(2014) conducted an experimental study on a two storey building model with AMD, using PD and PID controllers. Both the linear and nonlinear cases for structural stiffness were considered in the analysis. By using Lyapunov theory, conditions of stability were derived to tune the PD/PID gains. The results demonstrate that the PID controller performed better than the PD controller. The results showed that even though the chosen gains were not optimal, the controllers guaranteed stable control performances.

Kaveh Hassani and Won-Sook Lee (2014) presented that Linear Quadratic Regulator (LQR) was an optimal multivariable feedback control approach that minimizes the excursion in state trajectories of a system while requiring minimum controller effort. The behavior of an LQR controller was determined by two parameters, namely state and control weighting matrices. These two matrices were main design parameters to be selected by the designer and greatly influence the success of the LQR controller synthesis. However, it was not a trivial task to decide these two matrices. The classic approaches such as trial-and-error, Bryson's method, and pole placement are labor-intensive, time consuming and do not guarantee the expected performance.

Djedoui et.al (2016) investigated an active hybrid control system combining base isolation and active tuned mass damper (AMD) installed on the lowest floor of a base-isolated frame building. Simulation was carried out on a six degree of freedom base-isolated frame structure using MATLAB. PID controller was used to find the control force and the performances of the proposed active hybrid control system are tested under El Centro, Northridge, and Loma-Prieta earthquakes. The results showed that the active hybrid control system is more efficient. A reduction of 70% in base displacement, velocity and 15% in base acceleration is obtained.

## 2.4 Application of artificial neural network (ANN) in structures

ANN has been widely used in the field of structural engineering applications, namely material behavior, damage detection, initial design choices, system identification and structural dynamics. Narendra and Parthasarathy (1990) demonstrated the capabilities of the neural networks in the identification and control of nonlinear dynamical systems. They studied the concepts and definitions relating to i) characterization and identification of systems, ii) input-state-output representation of systems, iii) identification and control, iv) multi-layer and recurrent networks and v) back propagation in static and dynamic systems.

Ghaboussi et al. (1991) modeled the behaviors of concrete with a fully connected back propagation neural network, in the state of plane stress under monotonic biaxial loading and compressive uniaxial cyclic loading. For concrete in the biaxial stress state, both stress-controlled and strain-controlled models were developed. Neural networks were trained with the experimental/published data and tested with a set of new data.

Gleb Beliakov and Ajith Abraham (2002) proposed that selection of the topology of a neural network and correct parameters for the learning algorithm was a tedious task for designing an optimal artificial neural network which was smaller, faster and with a better performance. Neural networks were initially trained using the cutting angle method and later the learning was fine-tuned (meta-learning) using conventional gradient descent or other optimization techniques. Experiments were carried out on three time series benchmarks and a comparison was done using evolutionary neural networks.

Yingmin et. al.(2004) presented a method for the simulation of structural seismic responses based on neural networks. Modeling of linear and nonlinear systems, measures to improve generalization precision of neural networks, involving collection of samples, selection of object function, determination of the number of neural cells and choice of training method and construction of topology had been discussed through several examples.

Gunaydm and Dogan (2004) gave a neural network approach for early cost estimation of structural systems of buildings. His paper investigated the utility of neural network methodology to overcome cost estimation problems in early phases of building design processes. Cost and design data from thirty projects were used for training and testing neural network methodology with eight design parameters utilized in estimating the square meter cost of reinforced concrete structural systems of 4–8 storey residential buildings in Turkey, an average cost estimation

accuracy of 93% was achieved. Performance of neural network model depends on the quality and the quantity of examples. His model established a methodology that provided an economical and rapid means of cost estimating for the structural system of future building design processes.

Salajegheh and Gholizadeh (2005) suggested some improved genetic algorithms for the fast optimum design of structures by using neural networks. To reduce the computational cost of the standard genetic algorithm (GA), two different strategies were used. The first strategy was by modifying the standard GA, called virtual sub-population method (VSP). The second one was by using artificial neural networks for approximating the structural analysis. In the study, radial basis function (RBF), counter propagation (CP) and generalized regression (GR) neural networks were used. These methods had some similarity with different nature. Numerical results indicated that the ability of RBF was more than CP and GR performs better than the other two methods.

Gholizadeh et al. (2009) introduced an efficient method to predict the time history responses of structures subject to earthquakes employing neural network techniques. A new intelligent neural system (INS) was designed by combining competitive and radial basis function (RBF) neural networks. The input space was classified by a competitive neural network (CNN) based on the natural frequencies of the structures. Later an RBF network was assigned to each class and was trained by using the data located in the class. Results demonstrated high performance and computational advantages of INS comparing with the single RBF network.

Adeli and Panakkat (2009) presented a probabilistic neural network (PNN) for predicting the magnitude of the largest earthquake in a pre-defined future time period in a seismic region using eight mathematically computed parameters known as seismicity indicators. Prediction accuracies of the model were evaluated using three different statistical measures: the probability of detection, the false alarm ratio, and the true skill score or R score. The PNN model was trained and tested using data for the Southern California region. Good prediction accuracies for earthquakes of magnitude between 4.5 and 6.0 were achieved.

Arjun and Kumar (2011) developed a neural network model, using a combination of average values of four geophysical properties of the site (Standard Penetration Test (SPT) blow count, primary wave velocity, shear wave velocity, and density of soil) including hypo central distance of less than 50 km and magnitudes more than 5.0 from Japanese ground motion records,



to estimate duration of strong ground motion. An attempt was made to train the neural network with magnitude, hypo central distance and average shear wave velocity as three input variables. Results showed that the duration of strong motion was mostly dependent on average shear wave velocity rather than other geophysical properties of site

Chen-Wu Chen et.al. (2013) studied the non-linear structures' stability analysis when genetic algorithm based adaptive neural network was used. The initial values of the consequent parameter vector utilized a genetic algorithm. Next, a modified adaptive neural network controller was proposed to simultaneously stabilize and control the system. A stability criterion was also derived from the Lyapunov's direct method to ensure the stability of the nonlinear system.

## **2.5 Application of control of structures using ANN**

The first applications of neural networks to control can be found in the early 1960s [Widrow and Lehr (1990)], where a simple neurocontroller was used to control an inverted pendulum. In some of the earlier works, a book by Rumelhart and McClelland (1986), contributed to the renewed interest in neural network research.

Bani-Hani and Ghaboussi (1998) employed neurocontroller method for nonlinear (material inelasticity and damage) structural control. The non-linear state space Equation had been solved numerically by using fourth order Runge-Kutte method. Rao and Datta (1998) presented a methodology to employ the artificial neural network for active control of structures, under seismic excitation for a target percentage reduction of response. The methodology is illustrated with the help of active control of a single degree freedom system subjected to base excitation. The efficiency of the ANNs is tested for Treasure Island earthquake data.

Li et al. (2000) employed a time series analysis method (TSA) to obtain the relationship between damping and vibration amplitude. Kim and Jung (2000) proposed an optimal control algorithm using artificial neural networks in which linear structures as well as the nonlinear structures could be controlled by the proposed neurocontroller

Madan Alok (2005) concluded from past researches that ANN is effective and efficient computational processors for performing a variety of tasks including pattern recognition,

classification, associative recall, combinatorial problem solving, adaptive control, multi-sensor data fusion, noise filtering and data compression, modelling and forecasting. The paper presented a potentially feasible approach for training ANN in active control of earthquake-induced vibrations in building structures without the aid of teacher signals i.e. target control forces. Simulated case studies were presented to demonstrate the feasibility of implementing the unsupervised learning approach in ANN for effective vibration control of structures under the influence of earthquake ground motions.

Chang and DookieKim (2005) proposed active control of building structures using lattice probabilistic neural network (LPNN). With the lattice pattern of the state vector used as the training data, LPNN calculated the control force using only the adjacent information of input; thus, response was greatly faster. Three story building under El Centro earthquake was used to train the LPNN. Northridge earthquake was used to verify the proposed method. In the numerical simulation of the building structure control, the control results of the LPNN were compared to the uncontrolled results.

Datta and Bhardwaj (2006) presented an active control scheme using ANN for seismic control of building frames for future earthquakes. The ANN control scheme requires feedback responses (displacement, velocity and acceleration), ground excitation and a target percentage reduction as inputs to the ANN. The output of the ANN was the time history of control force. A ten-story building frame was taken as an illustrative example. Feedback responses were taken from 1st, 5th and 10th stories of the frame. The control was affected by a single control force applied at the top of the building frame with AMD. The results of the study showed that (1) the control scheme was very effective in controlling the response of the building frame for excitations under El Centro earthquake taken as an unknown problem (2) The peak control force required to obtain a significant percentage reduction in response was not very large and (3) Time delay.

Cheng et al. (2008) proposed new neural-network-based control algorithm in the computer simulation of active control of a three-story frame structure subjected to ground excitations. First, an emulator neural network was trained to forecast the future response of the structure from the immediate history of the system's response which consisted of the structure plus an actuator. The trained emulator was used in predicting the future responses and in

evaluating the sensitivities of the control signal with respect to those responses. At each time step of the simulation, the control signal was adjusted to induce the required control force in the actuator based control criterion. A controller neural network was trained to learn the relation between the immediate history of the response of the structure and actuator, and the adjusted control signals. The trained neurocontroller was used in controlling the structure for different dynamic loading conditions. The results of three numerical examples involving both structural and non-structural problems indicated that the proposed method provided accurate and computationally efficient estimates of the probability of failure.

Deepak et al.(2016) presented information in which a multi objective optimization procedure was proposed to deal with the optimal number and locations of collocated/no collocated sensors and actuators and determination of LQR controller gain simultaneously using hybrid multi objective genetic algorithm artificial neural network (GA-ANN). The multi objective optimization problem was formulated using trade-off objective functions, ensuring good observability/controllability of the structure while minimizing the spill over effect and maximizing closed loop average damping ratio. ANNs were used to train the input as varying numbers and placements of sensors and actuators and the outputs were taken as the three objective function i.e., controllability, observability, and closed loop average damping ratio, thus forming three ANN models. The trained mathematical models of ANN were fed into the multi objective. GA

## **2.6 Control using Fuzzy logic and Neuro-fuzzy technique**

For intelligent control, two main methodologies have been developed independently of each other: (1) artificial neural network and (2) fuzzy logic. Fuzzy logic was introduced by Zadeh (1965) as a means of processing imprecise and vague linguistic information. The fuzzy logic technique was not affected by the selection of the structural model, hence it was considered to be intrinsically robust and simple. Fuzzy logic uses inexact data and “soft” computing techniques to reason and derive control actions. The fundamental concept is that of “partial membership” to a set; partial membership is defined in terms of the membership functions, which are the basis for the “if-then” rules of the fuzzy control. Fuzzy logic uses generalizations of the conventional logic, Boolean operators handle partial memberships and fuzzy rules.

Antsaklis and Passino (1992) compiled several significant contributions to the field. Nerves et.al. (1995) discussed various control strategies, including proportional control, optimal LQR control, variable-structure control, neural network control, and adaptive fuzzy control and their effectiveness, efficiency, and implement ability were compared. The results showed that the proportional controller was able to reduce the response for wind excitation, but it is ineffective for earthquake excitation. The LQR controller gave satisfactory damping for both wind and earthquake excitations. It was widely used in the structural control of building frames, namely, in active control (Battaini et. al., 1998; Al-Dawod et. al., 2003), semiactive control (Yalla et. al., 2001 Faravelli and Rossi, 2002; Bharadwaj and Dutta, 2006) and hybrid control (Ahlawat and Ramaswamy, 2002).

Scorer and Roschke (2001) proposed Neuro-fuzzy technique, namely, ANFIS (Adaptive-Network- based Fuzzy Inference System) for the structural control. An ANFIS model was used to create a fuzzy controller for creating a target controller, integrating the controller as a voltage producer during representative disturbance and for collecting the time histories of the building acceleration. It collected the training data set and replaced it with a target controller with the newly developed fuzzy controller.

Li et. al. (2004) proposed a three level optimal design problem for finding the optimum number and locations of actuators using a two-level genetic algorithm. A scheme based on the H2 norm of transfer function was presented for the determination of optimum locations of actuators.

Lin (2005) proposed a novel development of piezoelectric actuators as elements of smart structures. The vibrations of smart structures were controlled by using a decomposed parallel fuzzy control approach. The study demonstrated the general methodology by decomposing a large scale system into smaller subsystems in a parallel structure so that the proposed fuzzy control methodology can be applied for studying a complex system. New control structures were created for new application possibilities of fuzzy control, which enabled one to minimize the completeness of the problem solved and utilized the capacity of computational technologies in full range.

Kim et. al. (2006) developed a neuro-fuzzy model in order to represent the behavior of damper to control displacement, velocity and voltage, which were obtained from a series of laboratory evaluation tests. Acceleration and relative displacement were considered as input and

command voltage was considered as output for the semi- active fuzzy controller. To define the fuzzy control, fuzzy rule base was used. Numerical modeling of friction pendulum system bearings and magneto rheological damper was done by Neuro-fuzzy models. This model was used to control the responses of a single degree of freedom mass that was equipped with the hybrid base isolation system.

Seung-yung et. al. (2007) designed a semi active fuzzy controller for the purpose of enhancing the seismic performance of cable stayed bridge. The current status of the structure was identified by the fuzzy logic controller. It continuously quantified the input current of the magneto-rheological (MR) damper which led to the optimal damping force. The response of the MR damper was taken as input information and the input voltage to MR damper was taken as output information by a fuzzy logic controller. The rule base proposed was that the output variable is proportional to the scale of each given input.

Pourzeynal et.al. (2007) optimized an active tuned mass damper (ATMD) control systems for using genetic algorithms and fuzzy logic control (GFLC). The design and optimization of different parameters of the ATMD control scheme were studied for getting the best results in the reduction of the building response under earthquake excitations. The proposed method had the advantage of both the fuzzy logic controller (FLC) and genetic algorithms (GAs) to handle the uncertain as well as the nonlinear phenomena. The building was modeled as a shear frame and the problem was solved in state space. The proposed method was applied to an 11-storey realistic building, located in the city of Rasht, Islamic Republic of Iran. The results obtained from the proposed control scheme (GFLC) were then compared with those obtained from the TMD, and linear quadratic regulator (LQR) control methods. It was found that integration of the GAs and FLC was highly effective in the reduction of the responses of the seismically excited example building.

Xu and Guo (2008) used a neuro-fuzzy control strategy to solve time-delay problem and fuzzy controller was used to determine the control current in MR dampers. The fuzzy controller was used to determine the control current quickly by taking earthquake acceleration excitation and predicted displacement of first floor as input and control current as the output. The basic idea of the fuzzy rules was that the control current increases with the increase in displacement response and earthquake acceleration. Trapezoidal and triangular combination functions were used as the membership function of earthquake acceleration and the first floor displacement

response of the structure. The neural network comprised of one input layer, two hidden layer and one output layer.

Guclu and Yazici (2008) designed fuzzy logic and PD controllers for a multi-degree-of freedom structure with active tuned mass damper (ATMD) to suppress earthquake-induced vibrations. Fuzzy logic controller (FLC) was preferred because of its robust character, superior performance and heuristic knowledge used effectively and easily in active control. For two types of actuators, fifteen degree of freedom structural system was modeled. These actuators were installed on the first storey and fifteenth storey which has ATMD. Linear motors were used as the active isolators for the structural control. The time histories of the storey displacements and accelerations, ATMD displacements, control voltages, frequency responses of both uncontrolled and controlled structures were presented in the study. Performance of the designed fuzzy logic controller was shown for different loads and disturbances. The results of the simulations showed a good performance by the FLC for different loads and earthquakes

Fan Yuan et. al. (2011) discussed fuzzy neural network controller based on the character of fuzzy logic and neural network theory. For the nonlinear system characteristics of uncertainty, the paper used fuzzy neural network technology to control nonlinear system, thereby improving the control quality. Considering the single inverted pendulum as an example, the paper constructed nonlinear mathematical model and realized the control with the method of the adaptive fuzzy neural network. It was then compared with the control method of liner quadratic regulato. The results indicated that the method of adaptive fuzzy neural network realized the stabilization of control better without the linear model of the system and had much higher robustness.

## **2.7 Concluding remarks**

From the review of literature, it is evident that a large number of studies have been carried out on the ANN control. A lot of research has been done for the development of control algorithms for ANN, FLC and the combination of the 2 controllers namely, adaptive Neuro-fuzzy inference system (ANFIS) control algorithm. The advantages and appeal of ANN control are its online applications. ANNs are trained either offline or online to replace the computer based algorithms. However, it has the limitation that generalized control of responses for

structural systems is difficult to obtain. More the number of data sets available for training, better is the learning of the ANNs and its prediction. It is also observed that the ANN has acquired some extra intelligence to control systems outside the domain of the training.

In the present study, a few simple applications of the ANN for structural control under earthquake excitation have been attempted, which are not widely reported in the literature. The present study centers on predictive active control of structures. It is an inverse problem which can be ideally tackled by the ANN. Predictive control using the ANN constitutes an offline training of the ANN and use the trained neural network for online application. Two problems of predictive control are attempted, namely, i) Prediction of the time history of control force for the target percentage reduction in selected response quantities for non-specific earthquakes and ii) Prediction of the time history of control force for the site specific earthquakes for target percentage reduction in response quantities of interest.

The former generates the training data from the controlled responses of the structure under the set of real earthquakes using some standard algorithms. The latter assumes a pattern of variations of control force with frequency, consistent with the site-specific power spectral density function (PSDF) of ground motion. Synthetic generation of data sets is used for the problem.

Apart from the predictive active control, the problem of optimal placement of actuators using simple trial and error method was incorporated in the thesis keeping in view the complexity of the optimization algorithms developed for the problem in the past like, genetic algorithm, steepest gradient optimization technique, etc. The algorithms are not only complicated and time consuming but also lacks robustness. Further, such algorithms require imposition of non- specified constraints, which are difficult to incorporate analytically such as, actuators cannot be placed on any floors because of practical reasons.

Arising out of the review of literature and gap areas cited as above, the scope and objective of the present study is formulated and stated at the end of the introduction Chapter.

## CHAPTER -3

# OPTIMUM PLACEMENT OF ACTUATORS IN ACTIVE CONTROL OF BUILDING FRAMES

### 3.1 Introduction

As mentioned in the previous chapter, the optimal placement of the actuator for obtaining the best possible reduction in responses was a topic of interest for researchers. Many optimization techniques were used for obtaining the optimal reduction in responses. Placement of more than three actuators in building frame in practice is difficult and cumbersome. As a result, number of actuators to be placed in the frame is generally restricted as three. For optimization problem, involving three actuators, many computational problems are involved, namely, numerical stability, convergence of the solution, possibility of dynamic instability and in some cases, amplification of some response quantities. The above problems are generally encountered in many standard optimization techniques which are used for optimization. Further, some constraints may have to be imposed in the algorithm for floors where actuators cannot be placed for practical reasons. Under such circumstances, optimal placement of actuator is best achieved using the trial or iterative method.

In this chapter, optimal placements of actuators in a ten storey building frame for a maximum number of three actuators are presented using the method of trail. Three cases of actuator placement are considered, namely, one actuator, two actuators and three actuators. The response quantities of interest are the top floor displacement, the maximum inter storey drift and the maximum base shear. The optimal reduction in responses for these quantities is obtained for four real earthquakes, namely, Kobe, Spitak, Elcentro and Bhuj. LQR algorithm is used to obtain the controlled responses.

### 3.2 Theory

The classical control theory is based on the frequency domain analysis employing transfer function approaches. A major limitation of the theory was the use of single-input single-output methods. Modern control theory is based on time domain analysis expressed by first order



differential Equations utilizing state space representation. The Equation of motion of a  $n$  degree-of-freedom system, subjected to ground excitations and control forces, can be written as

$$M\ddot{X}(t) + C\dot{X}(t) + KX(t) = -MI\ddot{x}_g + Du \quad (3.1)$$

$M$ ,  $C$ , and  $K$  are  $n \times n$  mass, damping, and stiffness matrices, respectively;  $X$  is the  $n$  dimensional displacement vector;  $\ddot{x}_g$  is the ground acceleration;  $I$  is the influence coefficient matrix of size  $n \times 1$ ;  $D$  is the controller location matrix of size  $n \times m$ ;  $u$  is a vector of control force of size  $m$ .

When open-closed loop configuration is used, it is assumed that the control force vector  $u(t)$  is linearly proportional to the responses  $x(t)$  and  $\dot{x}(t)$  and the excitations  $\ddot{x}_g(t)$ . Then,  $u$  may be written as:

$$u(t) = K_1X(t) + C_1\dot{x}(t) + E\ddot{x}_g(t) \quad (3.2)$$

In which  $K_1$ ,  $C_1$ , and  $E$  are time independent matrices of size  $m \times n$  and  $m \times 1$ , respectively.

Substituting Equation (3.2) into Equation (3.1) results in

$$M\ddot{x} + (C - DC_1)\dot{x} + (K - DK_1)x = (DE - MI)\ddot{x}_g \quad (3.3)$$

Hence, the application of control force may be viewed as modifying the structural parameters, i.e. stiffness and damping so that it can respond more favorably to the external excitation. Equation (3.2) can be written as matrix Equation and the resulting matrix is commonly known as gain matrix in the control literature. Further, when information on the state of the system and the excitation are required to find the control force in the Equation (3.2), the control scheme is popularly termed as open-close loop feedback control.

### 3.2.1 State-space representation of MDOF system

Equation (3.1) represents the second-order differential Equation of motion of the MDOF system subjected to the support motion and the control force. The concept of the state of a dynamic system refers to a minimum set of variables, known as state variables which fully describe the system and its response to any given set of inputs.

The controlled Equations of motion in Equation (3.1), are written in state-space form as:

$$\dot{Z} = AZ + Bu + E\ddot{x}_g ; Z = [x \ \dot{x}]^T \quad (3.4)$$

Where,  $Z$  is a  $2n \times 1$  state vector;  $A$  is a  $2n \times 2n$  linear system matrix;  $B$  is a  $2n \times m$  control location matrix; and  $E$  is a  $2n \times 1$  excitation influence matrix given as

$$A = \begin{bmatrix} 0 & I \\ -M^{-1}C & -M^{-1}K \end{bmatrix}; \quad B = \begin{bmatrix} 0 \\ M^{-1}D \end{bmatrix}; \quad E = \begin{bmatrix} 0 \\ -I \end{bmatrix}$$

Where,  $I$  is an identity matrix of appropriate size and  $D$  is the damper location matrix; the other matrices have already been defined.

### 3.2.2 Linear quadratic regulator (LQR)

In classical linear optimal control, the control force is assumed to be a linear function of the state vector and the control of the responses is obtained by minimizing a quadratic performance function. Therefore, it is popularly known as a linear quadratic regulator (LQR) control. Assuming the state vector to be zero at time  $t = 0$ , the performance index is defined as

$$J = \int_0^{t_f} [x^T Q x + u^T R u] dt \quad (3.5)$$

In which,  $t_f$  is the duration of the earthquake excitation;  $Q$  is a  $2n \times 2n$  semi-definite matrix and  $R$  is a  $n \times m$  positive definite matrices. The matrices  $Q$  and  $R$  are termed weighting matrices. The relative values of the elements of the matrices are selected according to the importance attached to the different parameters of control. For example, large values of the elements of  $Q$  compared with those of  $R$  denote that reduction of response is given more weightage at the cost of control force. The opposite is indicated when the elements of  $R$  are relatively large. Similarly, in the  $Q$  matrix, relatively large values of the diagonal elements corresponding to the displacement response denote that the velocity response is penalized in the minimization procedure.

The LQR estimates the control force by minimizing the quadratic cost function. For a continuous-time linear system defined on  $t \in [t_0, t_1]$ , the Equation of motion written in state space form is

$$\dot{X} = AX + Bu \quad (3.6)$$

With a quadratic cost function defined as

$$J = x^T(t_1)F(t_1)x(t_1) + \int_{t_0}^{t_1} [x^T(t)Qx(t) + u^T(t)Ru(t)] dt \quad (3.7)$$

The feedback control law that minimizes the value of the cost is

$$u = -Kx \quad (3.8)$$

Where,  $K$  is given by

$$K = R^{-1}(B^T P(t) ) \quad (3.9)$$

And  $P$  is found by solving the continuous time Riccati differential Equation

$$-\dot{P}(t) = A^T P(t) + P(t)A - P(t)B^T R^{-1} B^T P(t) + Q \quad (3.10)$$

From Equation (3.6), it is clear that the time histories of controlled response and the control force are such that they provide a minimum value for the performance index  $J$ . Furthermore, the Equation (3.7) shows that the performance index  $J$  is in a way equivalent to the total energy of the system, including that of the external force over the entire duration of the excitation. Thus, the control algorithm in some sense obtains the control force by minimizing the total energy of the system over the duration of the excitation. This algorithm is known as a linear quadratic regulator (LQR) algorithm as the control force is a linear function of the state vector and the performance function is a quadratic function of the state variable and the control force. Figure 3.1 shows the Simulink block diagram for LQR.

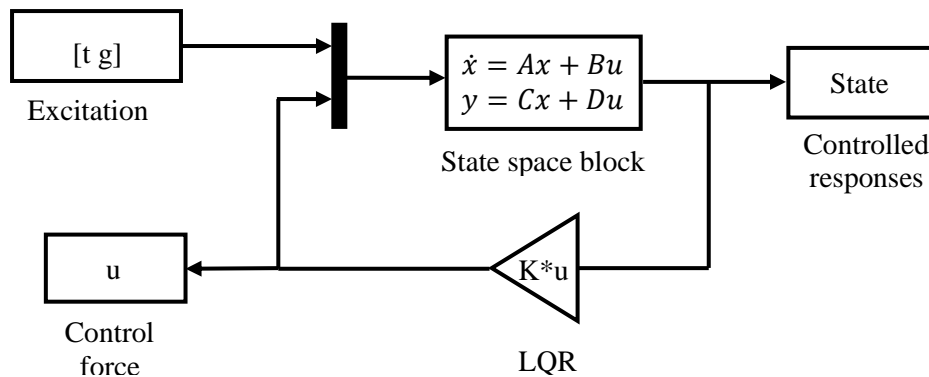


Figure3.1. LQR feedback model in Simulink

### 3.3 Numerical examples and discussion of results

The optimum control force is determined by placing actuators at different locations using a linear quadratic regulation algorithm (LQR). The ten storey building frame shown in Figure 3.2 is used for the numerical study. The actuator in a floor is effected by using the active tendon

system as shown in Figure 3.2. Mass, damping, and stiffness are assumed to be the same for each floor. The properties of the structure are given as mentioned below:

The mass of each floor ( $M$ ) = 20 tonnes; Stiffness ( $K$ ) = 25000 kN/m; Damping ratio = 5%

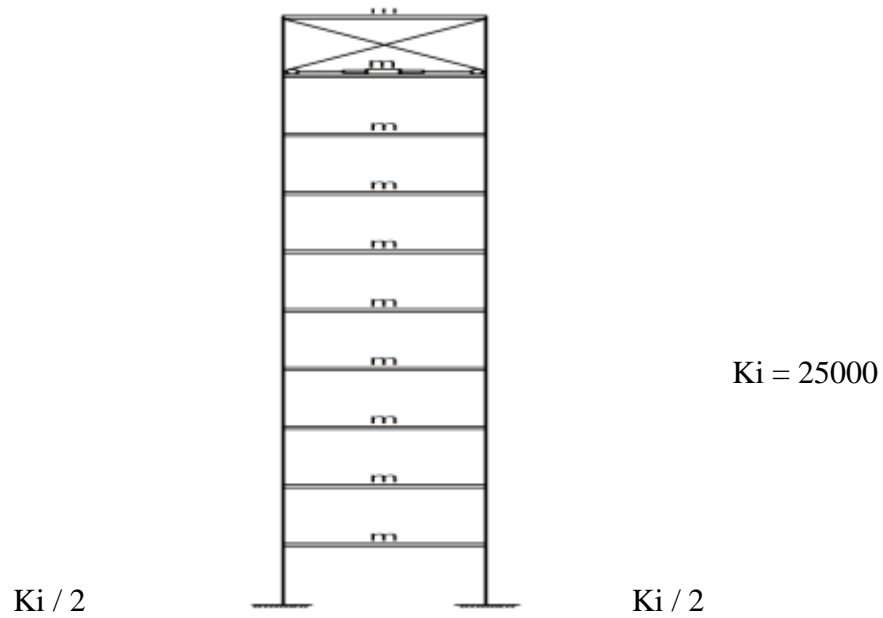


Figure 3.2 Model of a ten storey building frame with active tendon placed on the top floor

Resulting mass and stiffness matrices are

$$M = \begin{bmatrix} 20 & 0 & 0 & 0 & 0 & 0 & 0 \\ 0 & 20 & 0 & 0 & 0 & 0 & 0 \\ 0 & 0 & 20 & 0 & 0 & 0 & 0 \\ 0 & 0 & 0 & 20 & 0 & 0 & 0 \\ 0 & 0 & 0 & 0 & 20 & 0 & 0 \\ 0 & 0 & 0 & 0 & 0 & 20 & 0 \\ 0 & 0 & 0 & 0 & 0 & 0 & 20 \end{bmatrix} \text{Tonnes}$$

$$K = \begin{bmatrix} 50000 & -25000 & 0 & 0 & 0 & 0 & 0 \\ -25000 & 50000 & -25000 & 0 & 0 & 0 & 0 \\ 0 & -25000 & 50000 & -25000 & 0 & 0 & 0 \\ 0 & 0 & -25000 & 50000 & -25000 & 0 & 0 \\ 0 & 0 & 0 & -25000 & 50000 & -25000 & 0 \\ 0 & 0 & 0 & 0 & -25000 & 50000 & -25000 \\ 0 & 0 & 0 & 0 & 0 & -25000 & 25000 \end{bmatrix} \text{ KN/m}$$

The Rayleigh damping matrix [C] is constructed using  $[C] = \alpha M + \beta K$  where  $\alpha = \zeta \frac{2\omega_i \times \omega_j}{\omega_i + \omega_j}$

and  $\beta = \zeta \frac{2}{\omega_i + \omega_j}$  in which  $\alpha$  and  $\beta$  are the proportional coefficient,  $\omega_i$  and  $\omega_j$  are the structural model frequencies, and  $\zeta$  is the structural damping ratios. In the present example, the value of  $\omega_i = 19.06$ ;  $\omega_j = 31.24$ .

The damping matrix, thus obtained is

$$C = \begin{bmatrix} 182.03 & -85.49 & 0 & 0 & 0 & 0 & 0 \\ -85.49 & 182.03 & -85.49 & 0 & 0 & 0 & 0 \\ 0 & -85.49 & 182.03 & -85.49 & 0 & 0 & 0 \\ 0 & 0 & -85.49 & 182.03 & -85.49 & 0 & 0 \\ 0 & 0 & 0 & -85.49 & 182.03 & -85.49 & 0 \\ 0 & 0 & 0 & 0 & -85.49 & 182.03 & -85.49 \\ 0 & 0 & 0 & 0 & 0 & -85.49 & 96.53 \end{bmatrix} \text{ KNs/m}$$

To investigate the effectiveness of the control system for different excitations, four time histories of ground motion are selected for numerical simulations, namely, Bhuj, Elcentro, Spitak and Kobe.

Table3.1 Summary of earthquake time histories used

Sr. No	YEAR	EARTHQUAKE	RECORDING STATION	PGA (m/s <sup>2</sup> )
1	1940	El cento (California)	Imperial valley	3.1276
2	1988	Spitak (Armenia)	Gukasian	1.9521
3	1995	Kobe (Japan)	Nishi – Akashi	4.9320
4	2001	Bhuj	Ahmedabad	1.0382

The control and uncontrolled responses of the frame are obtained for each earthquake. The peak control force required for obtaining the optimal response is recorded and shown along with the percentage reduction of responses. The method of trial consists of placing the actuator at different floors and plotting the percentage reduction in each case.

### **3.3.1 The optimum control with one actuator**

The percentage reduction in the maximum base shear (B.S.), the peak top floor displacement (TFD) and the maximum interstory drift (DRIFT) for different placements of the actuator are observed. The results are presented in the form of three types of plots, namely, (i) the variation of the percentage of reduction in the response quantities of interest with the position of the actuator; (ii) the variation of R factor with the position of the actuator and (iii) the variation of normalized maximum control force with the position of the actuator. 'R' is defined as the ratio of the percentage reduction in the response quantity of interest per unit peak control force, expressed as a percentage of the total building weight. The variations are shown for four different earthquakes, i.e. Bhuj, Elcentro, Kobe and Spitak.

Variation of percentage reduction of response quantities of interest with the actuator position is shown in Figure 3.3 to 3.6. It is seen from the figures that the variation of the percentage reductions in the peak top storey displacement and the maximum interstory drift increase as the actuator is placed on higher floors. The maximum percentage reductions for the two responses are 57% and 50% for Bhuj earthquake; 48% and 41% for Kobe earthquake; 73% and 66% for Elcentro earthquake and 63% and 55% for Spitak earthquake.

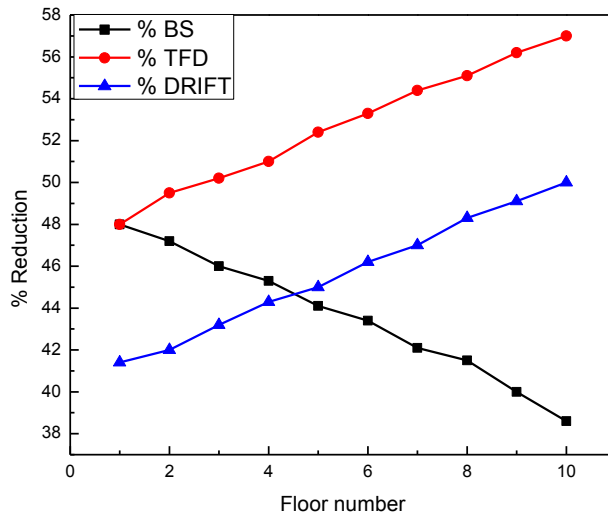


Figure 3.3 Variations of percentage reductions in response to actuator position (Bhuj earthquake).

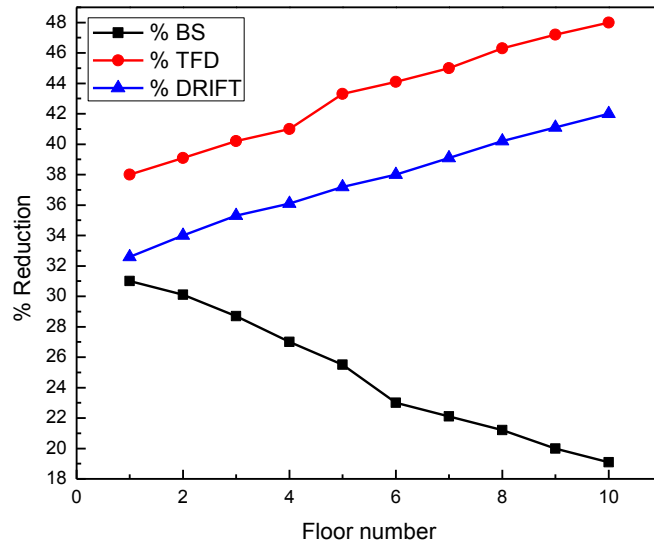


Figure 3.4 Variations of percentage reductions in response to actuator position (Kobe earthquake)

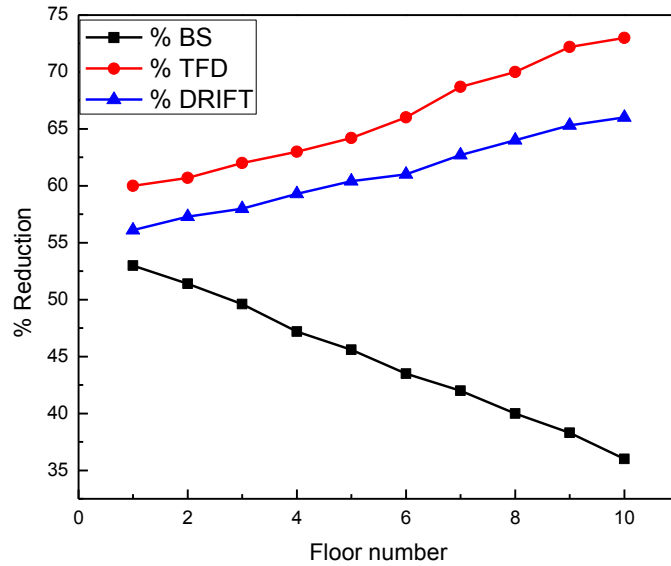


Figure 3.5 Variations of percentage reductions in response to actuator position (Elcentro earthquake).

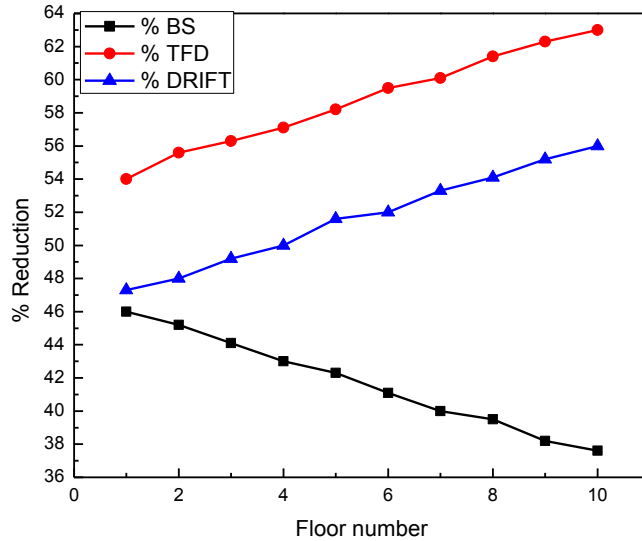


Figure 3.6 Variations of percentage reductions in response to actuator position (Spitak earthquake).

For base shear, a reverse trend, i.e. the percentage reduction in base shear is maximum when the actuator is at the first floor level and minimum when it is at the top floor level. The values of the maximum and the minimum percentage of reductions are 48% and 38% for Bhuj



earthquake; 31% and 19% for Kobe earthquake; 53% and 36% for Elcentro earthquake; and 46% and 37% for Spitak earthquake. Corresponding maximum and minimum values of normalized peak control force are 0.052 and 0.03 for the Bhuj earthquake as shown in the Figure 3.7. Note that the nature of variation of peak control force with the position of the actuator is opposite to those of the peak top floor displacement and the maximum interstory drift (Figures. 3.7 to 3.10)

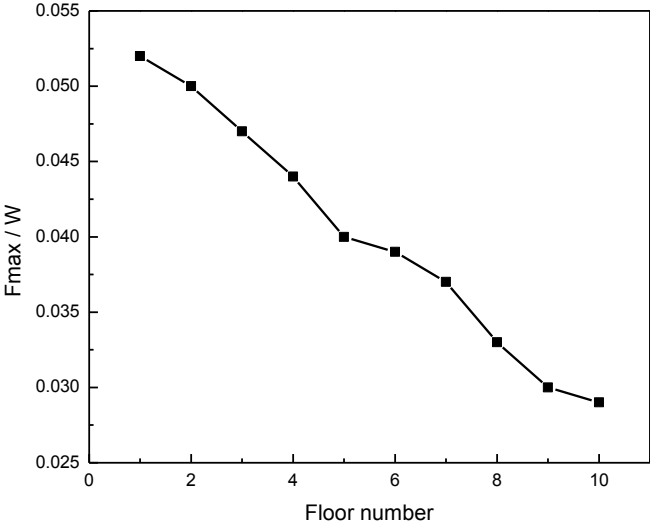


Figure 3.7 Variation of normalized peak control force with actuator position (Bhuj earthquake).

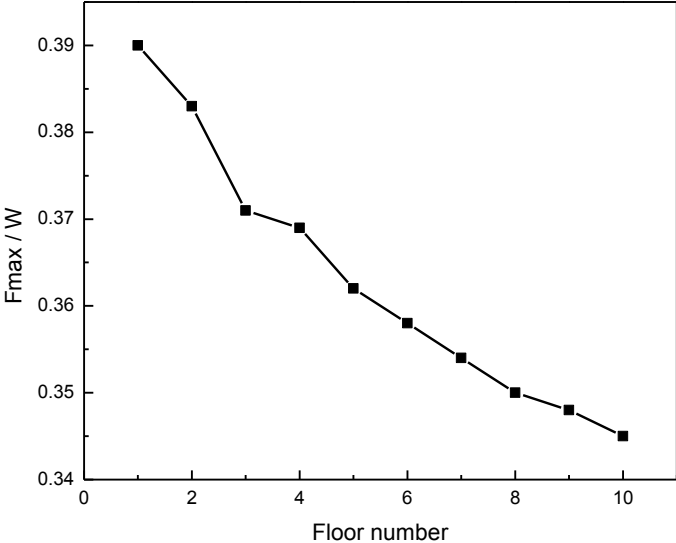


Figure 3.8 Variation of normalized peak control force with actuator position (Kobe earthquake).

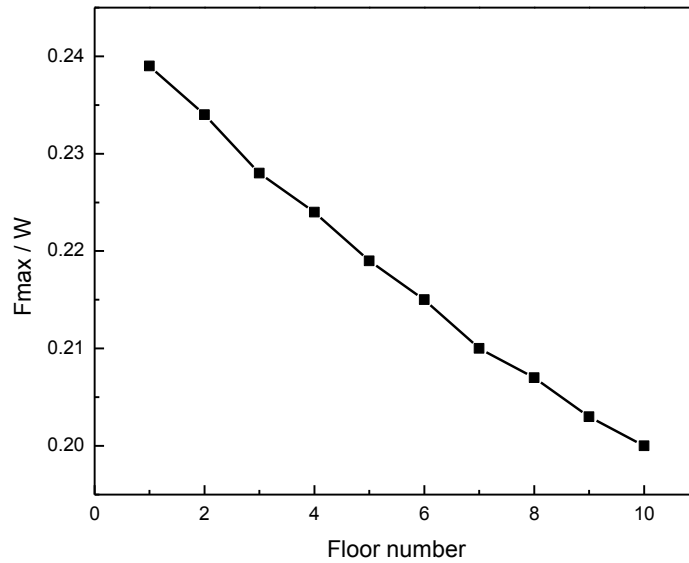


Figure 3.9 Variation of normalized peak control force with actuator position (Elcentro earthquake).

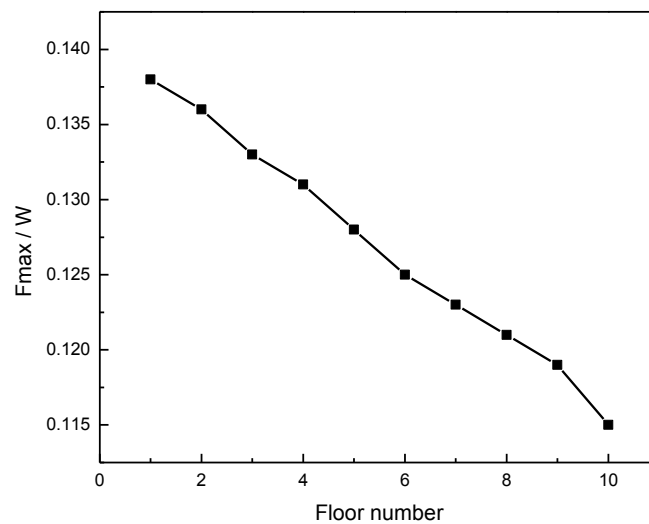


Figure 3.10 Variation of normalized peak control force with actuator position (Spitak earthquake).

Because of the natures of variations of the percentage reduction in responses and the maximum control force with the actuator position as discussed in the preceding paragraphs, the variation of the factor R for the responses to actuator position follows the pattern as shown in

Figures 3.11 to 3.14. The variations of the factor R for top storey displacement and drift remain the same as those of percentage reductions in top floor displacement and drift. So far as the base shear is concerned, it is seen that both the variations of percentage reduction in base shear and peak control force with the actuator position have the same nature. As a consequence, the nature of variation of the factor R for base shear with actuator position varies differently for different earthquakes. The variation depends upon the relative values of percentage reduction in base shear and normalized peak control force.

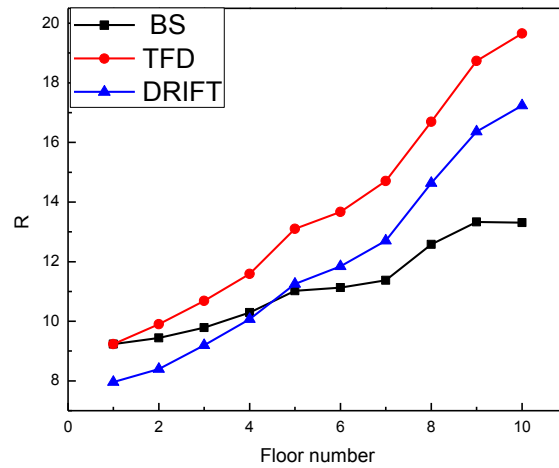


Figure 3.11 Variations of R values for maximum base shear, peak top floor displacement and maximum interstorey drift with actuator position (Bhuj earthquake).

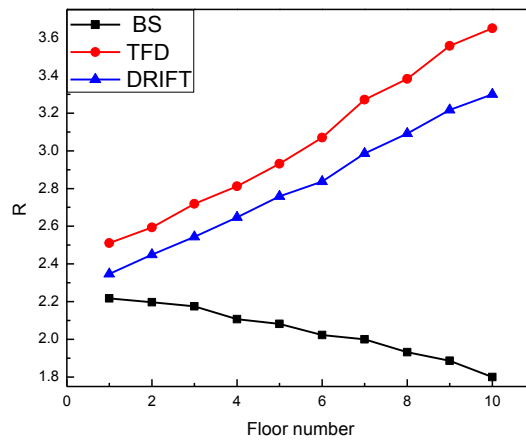


Figure 3.12 Variations of R values for maximum base shear, peak top floor displacement and maximum interstorey drift with actuator position (Elcentro earthquake).

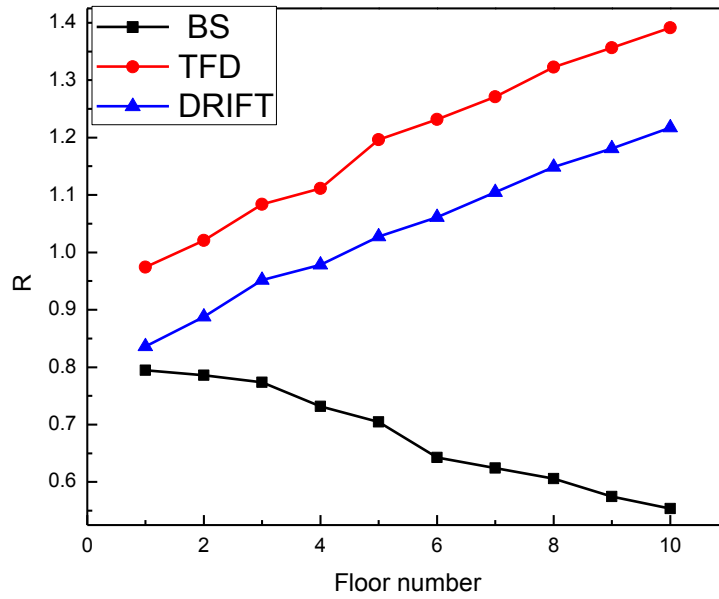


Figure 3.13 Variations of R values for maximum base shear, peak top floor displacement and maximum interstory drift with actuator position (Kobe earthquake).

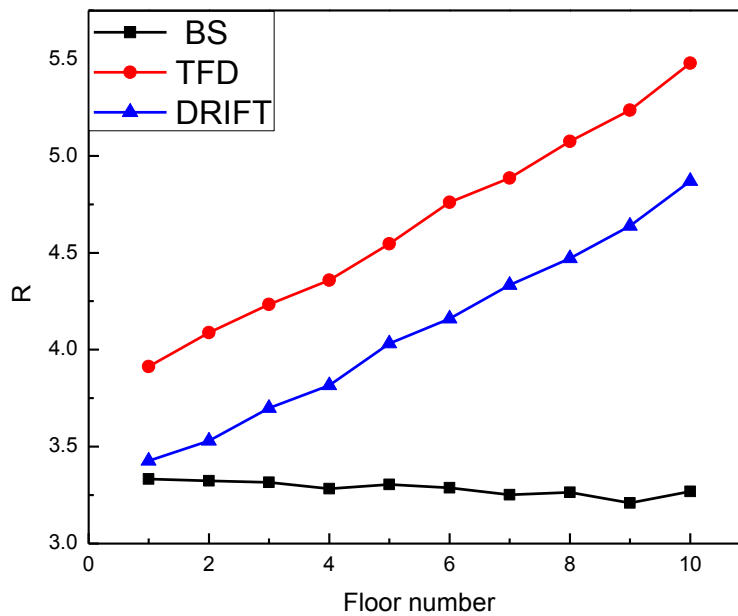


Figure 3.14 Variations of R values for maximum base shear, peak top floor displacement and maximum interstory drift with actuator position (Spitak earthquake).

Table 3.2 Optimum position of the actuator based on percentage reductions of responses

Sr. No.	Earthquake	Floor number		
		Base shear	Top floor displacement	Drift
1	Kobe(PGA = 0.4g)	1 (31%)	10 (48%)	10 (44%)
2	Elcentro (PGA = 0.32g)	1 (53%)	10(73%)	10 (66%)
3	Spitak (PGA = 0.2g)	1 (46%)	10 (63%)	10 (55%)
4	Bhuj (PGA = 0.106g)	1(48%)	10 (57%)	10 (52%)

Tables 3.2 and 3.3 show the optimal positions of actuator based on a percentage reduction of responses and based on R values.

Table 3.3 Optimum position of the actuator based on R values

Sr No.	Earthquake	Actuator position (floor number)		
		Base shear	Top floor displacement	Drift
1	Kobe(PGA=0.4g)	1 (0.79)	10 (1.39)	10 (1.21)
2	Elcentro(PGA=0.32g)	1 (2.21)	10(3.65)	10 (3.3)
3	Spitak (PGA=0.2g)	1 (3.33)	10 (5.47.)	10 (4.82)
4	Bhuj (PGA=0.106g)	10(13.31)	10 (19.65)	10 (17.2)

In the Tables, the quantity in the bracket refers to the maximum percentage reduction achieved or the maximum value of R. It is observed that the optimum position of the actuator may differ with the two different considerations, maximum percentage of reductions in responses only and the value of R. For example, the optimum position of the actuator for base shear is different from Bhuj earthquake for the two cases. Therefore, the optimum position of actuators should be decided based on the specified criterion like percentage reduction in response only, percentage reduction in response per unit control force (R) and specified peak control force that can be applied.

Thus, it is observed that if both R values and the percentage reduction in response, without considering the magnitude of peak control force are considered, then the optimum positions of the actuator for obtaining the best reduction in peak top floor displacement and maximum interstory drift in the top floor for all earthquakes remain the same for the example problem. If reduction of base shear alone is considered, then the optimum position of the actuator

is at first storey level for all earthquakes. However, if reductions in response per unit control force (i.e. R factor) is considered the optimal position of actuator turns out to be 10. Since peak control force depends upon the PGA, the optimal position of the actuator may also depend upon the PGA level of earthquake if R factor is considered as the basis of deciding the optimal position of the actuator.

### 3.3.2 The response reduction with two actuators

In the case of optimal control with two actuators, different combinations of placement of actuators are attempted. The combinations are shown in Table 3.4

Table 3.4 Combinations of two actuators placed in the frame

SR NO	LOCATION (Floor wise)
1	1—2
2	1-3
3	1-7
4	2-8
5	2-9
6	1-10
7	3-5
8	3-8
9	4-9
10	6-10

The results are presented in the form of figures and Tables as in the case of single actuator.

Table 3.5 Optimal position of two actuators based on percentage reductions of responses

Sr. No	Earthquake	Actuator positions (floor number)		
		Base shear	Top floor displacement	Drift
1	Kobe(PGA=0.4g)	1 -2(46%)	6-10 (69%)	6-10 (62%)
2	Elcentro (PGA=0.32g)	1-2(66%)	6-10(83%)	6-10(79%)
3	Spitak (PGA=0.2g)	1-2(58%)	6-10 (75%)	6-10 (72%)
4	Bhuj (PGA=0.106g)	1-2(62%)	6-10 (69%)	6-10 (65%)

It is seen from the Figures 3.15 to 3.18 that the pattern of variations of response reductions with actuator positions remain the same as observed in the case of single actuator. However, the percentage reductions are increased for all responses as it would be expected. Note that there are two peak control forces shown in the Figures 3.19 to 3.22. The two control forces correspond to actuators, one and two, where actuator one refers to the first number shown in Table 3.4. While determining the values of R, the maximum value of the peak control forces of the two actuators is considered. The variations of R with actuator positions are shown in Figures 3.23 to 3.26. In this case also, the variation of R is opposite to that found in the percentage reduction of base shear for Bhuj earthquake. The reason for this is explained in the case of single actuator. Tables 3.5 and 3.6 show the optimal positions of actuators based on a percentage reduction of responses and R values.

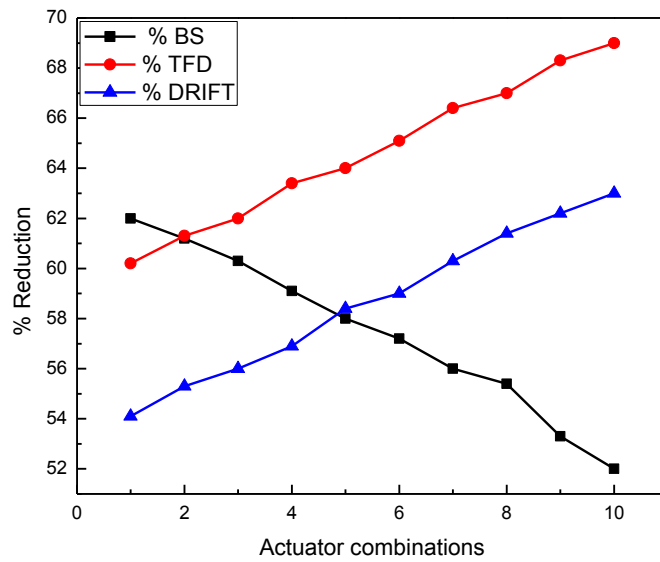


Figure 3.15 Variations of percentage reductions in response with two actuator position (Bhuj earthquake).

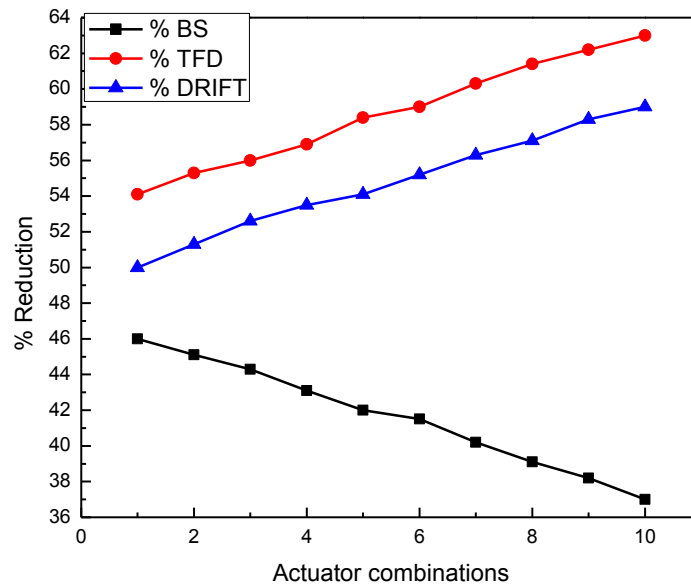


Figure 3.16 Variations of percentage reductions in response with two actuator position (Kobe earthquake).

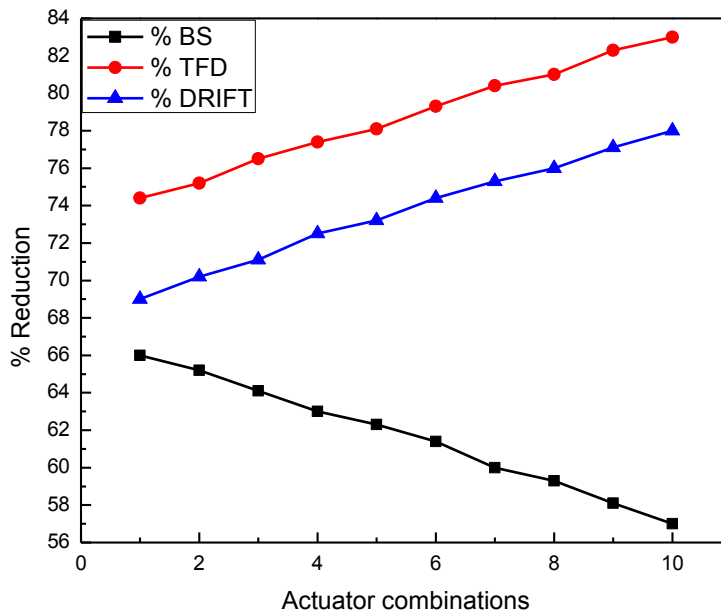


Figure 3.17 Variations of percentage reductions in response with two actuator position (Elcentro earthquake).



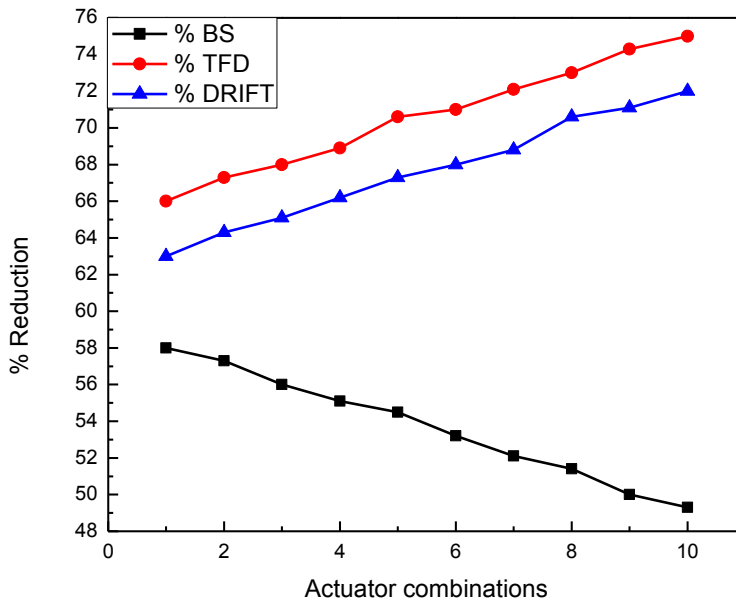


Figure 3.18 Variations of percentage reductions in response with two actuator position (Spitak earthquake).

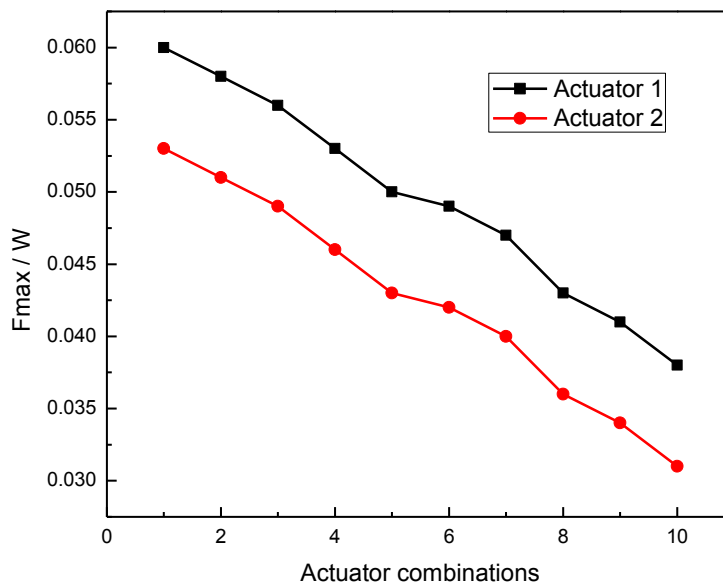


Figure 3.19 Variation of normalized peak control force with two actuator position (Bhuj earthquake).

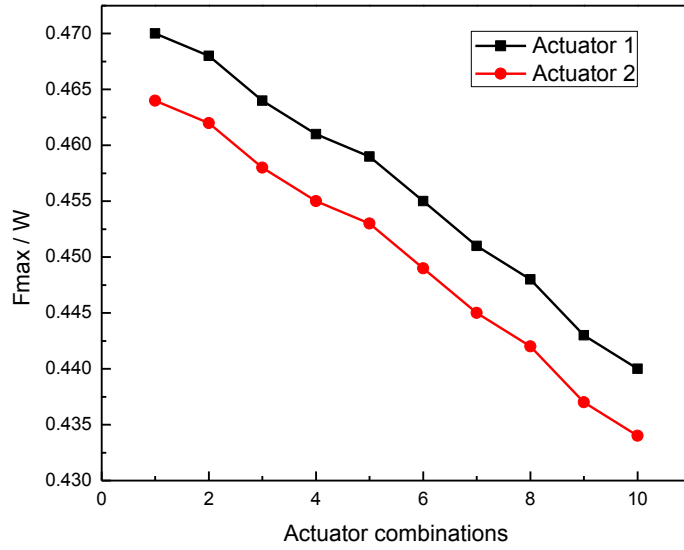


Figure 3.20 Variation of normalized peak control force with two actuator position (Kobe earthquake).

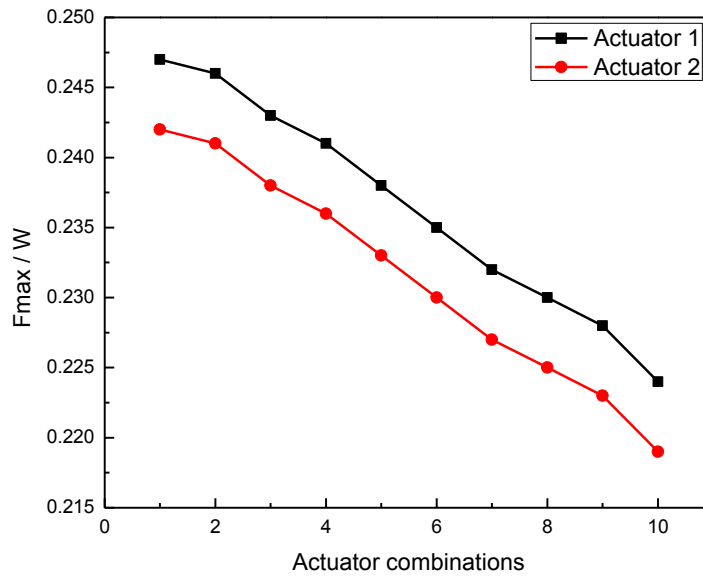


Figure 3.21 Variation of normalized peak control force with two actuator position (Elcentro earthquake).

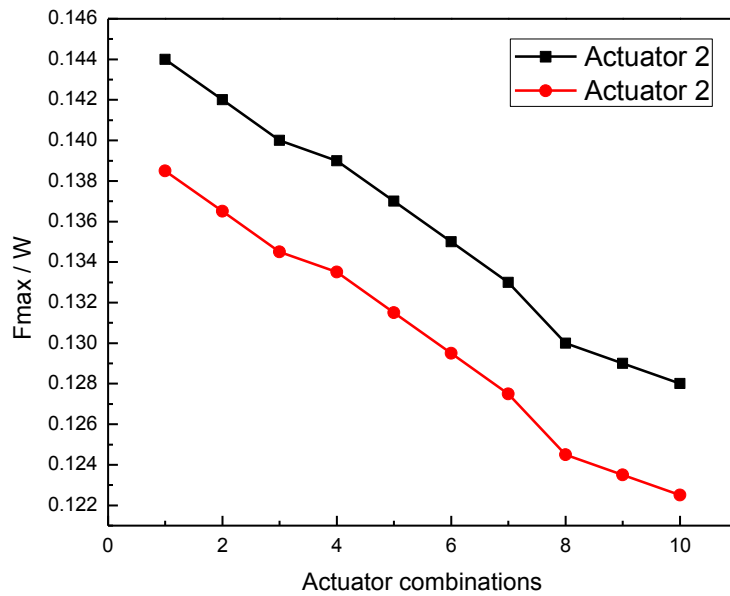


Figure 3.22 Variation of normalized peak control force with two actuator position (Spitak earthquake).

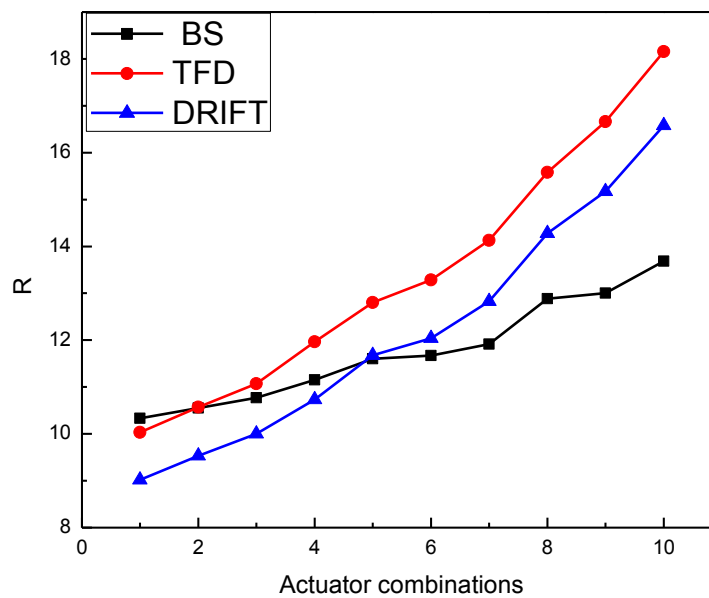


Figure 3.23 Variation of R values for maximum base shear, peak top floor displacement and maximum interstory drift with two actuator position (Bhuj earthquake).

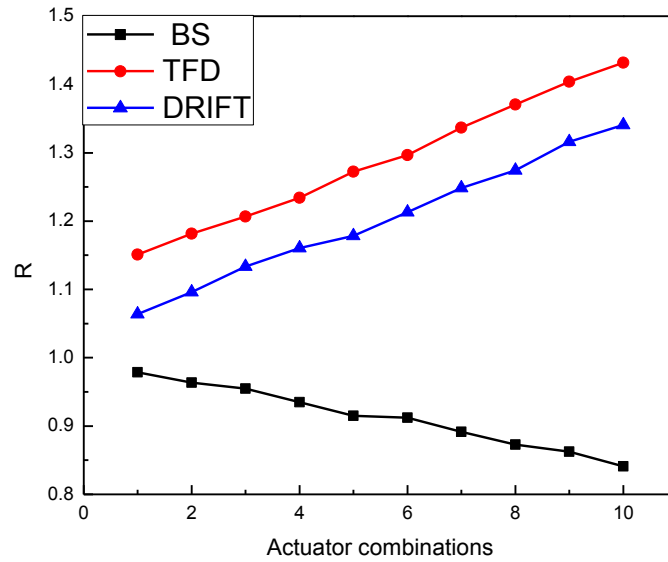


Figure 3.24 Variation of R values for maximum base shear, peak top floor displacement and maximum interstory drift with two actuator position (Kobe earthquake).

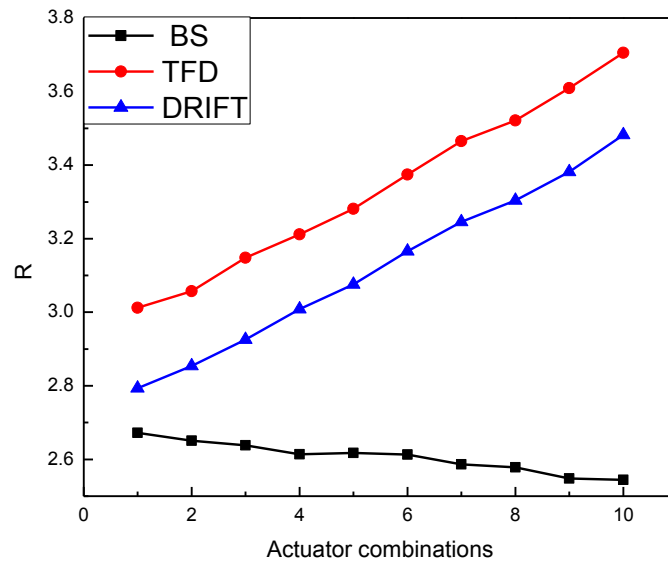


Figure 3.25 Variation of R values for maximum base shear, peak top floor displacement and maximum interstory drift with two actuator position (Elcentro earthquake).

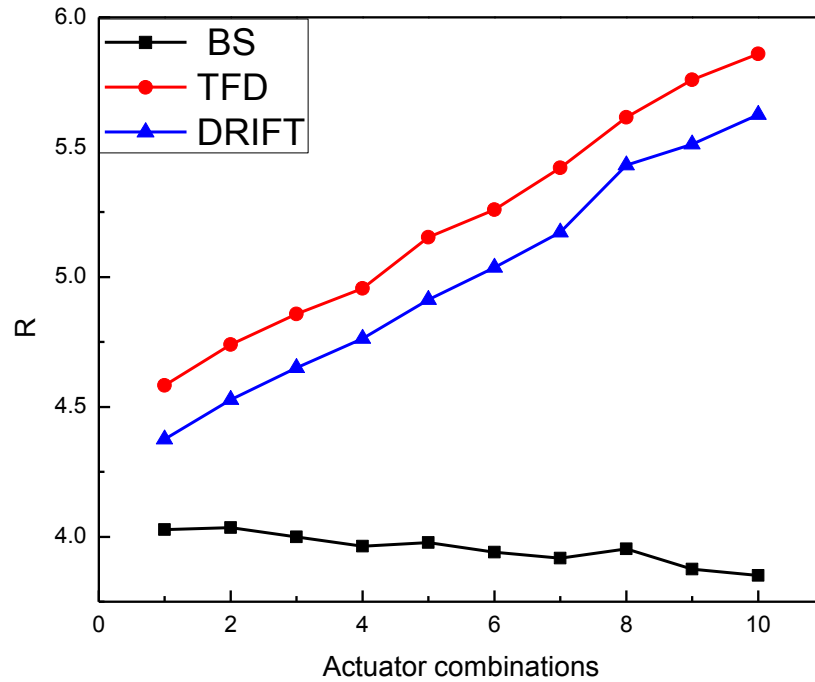


Figure 3.26 Variation of R values for maximum base shear, peak top floor displacement and maximum interstory drift with two actuator position (Spitak earthquake).

Table 3.6 Optimal position of two actuators based on R value for the case of two actuators

Sr. No.	Earthquake	Actuator position/ (floor number)		
		Base shear	Top floor displacement	Drift
1	Kobe(PGA=0.4g)	1 (0.79)	10 (1.39)	10 (1.21)
2	Elcentro (PGA=0.32g)	1 (2.21)	10(3.65)	10 (3.3)
3	Spitak (PGA=0.2g)	1 (3.33)	10 (5.47.)	10 (4.82)
4	Bhuj (PGA=0.106g)	10(13.1)	10 (18.13)	10 (16.5)

### 3.3.3 The response reduction with three actuators

In the case of optimal control with three actuators, different combinations for placement of actuators are attempted. The combinations are shown in Table 3.7.

Table 3.7 Combinations of three actuators placed in the frame:

<b>SR NO</b>	<b>LOCATION (Floor wise)</b>
1	1--2--10
2	1--3--10
3	1--4--10
4	1--5--10
5	1--6--10
6	1--7--10
7	1--8--10
8	1--9--10

Eight combinations are attempted for investigating the optimum percentage reduction in response expressed as a factor R i.e. percentage reduction per unit control force. The variation in the value of R with the different combinations of three actuator position shows a similar trend as that of a single actuator and two actuators for the combinations considered in the study of the different earthquakes. However, when the variation of the percentage reduction in response quantities with different combinations of actuator placement is plotted separately, without any consideration to the peak control force, the variations are different than the variation of R factor with the actuator combination as can be seen from the following figures

It is seen from the Figures 3.27 to 3.30 that the pattern of variations of response reduction with actuator position remains the same as those observed in the case of single actuator and two actuators. Note that there are three peak control forces shown in the Figures 3.31 to 3.34. There are control forces corresponding to the actuator one, two and three; the positions of the three actuators are indicated in the sequence as shown in the Table 3.7. For determining the values of R, the maximum value of the peak control forces of the three actuators is considered. The variation of R with actuator positions is shown in Figure 3.35 to 3.38. In this case also, the variation of R is opposite to that found in the percentage reduction of base shear for Bhuj earthquake. The reason for this is explained in the case of single actuator. Table 3.8 and 3.9 shows the optimum positions of actuators based on a percentage reduction of responses and based on R values respectively.

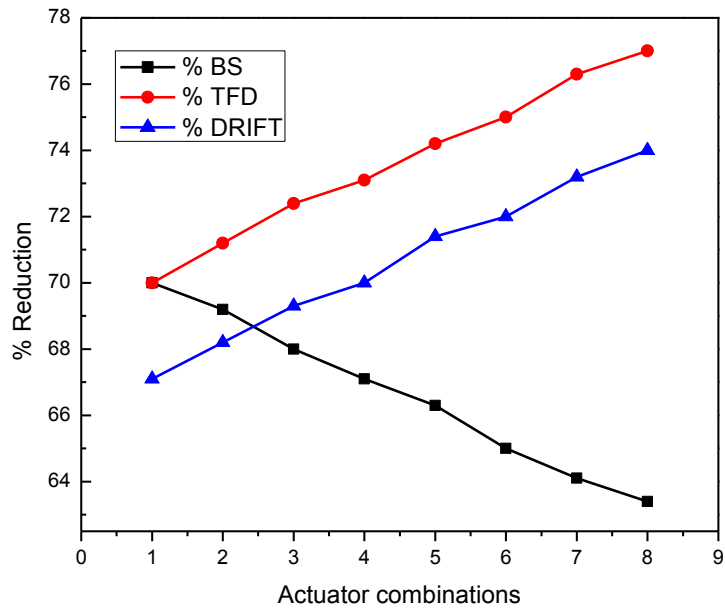


Figure 3.27 Variations of percentage reductions in response with three actuator position (Bhuj earthquake).

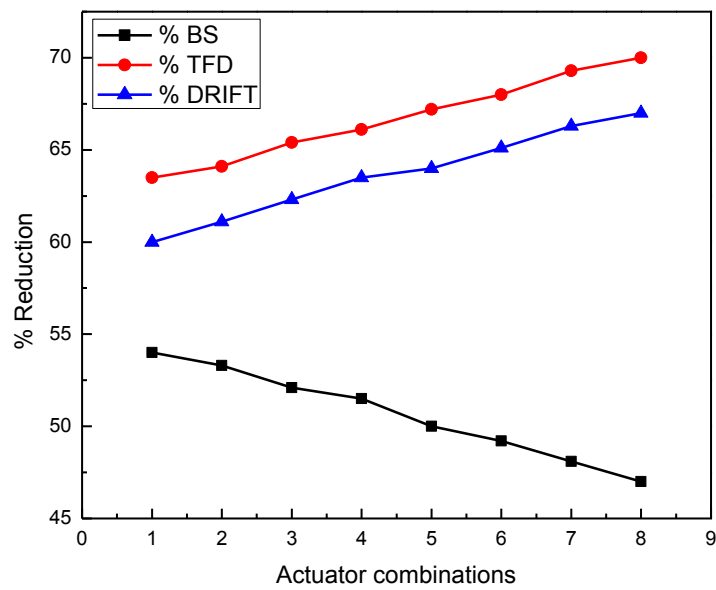


Figure 3.28 Variations of percentage reductions in response with three actuator position (Kobe earthquake)

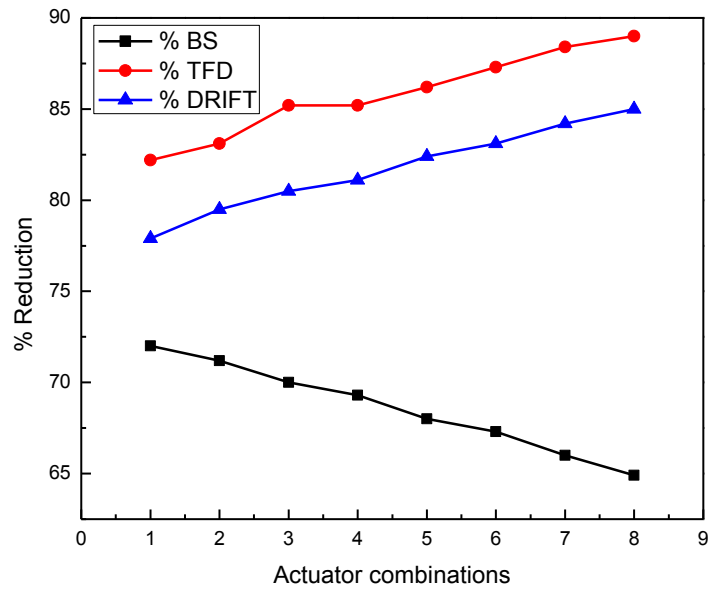


Figure 3.29 Variations of percentage reductions in response with three actuator position (Elcentro earthquake).

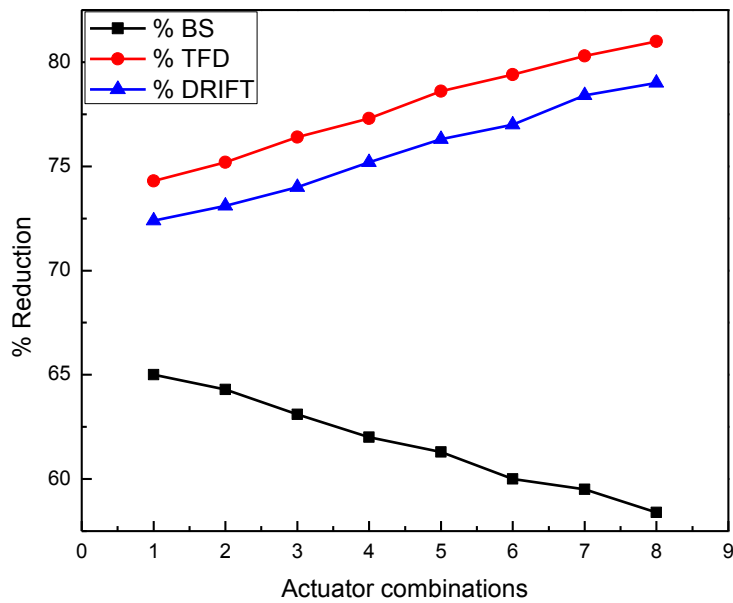


Figure 3.30 Variations of percentage reductions in response with three actuator position (Spitak earthquake)



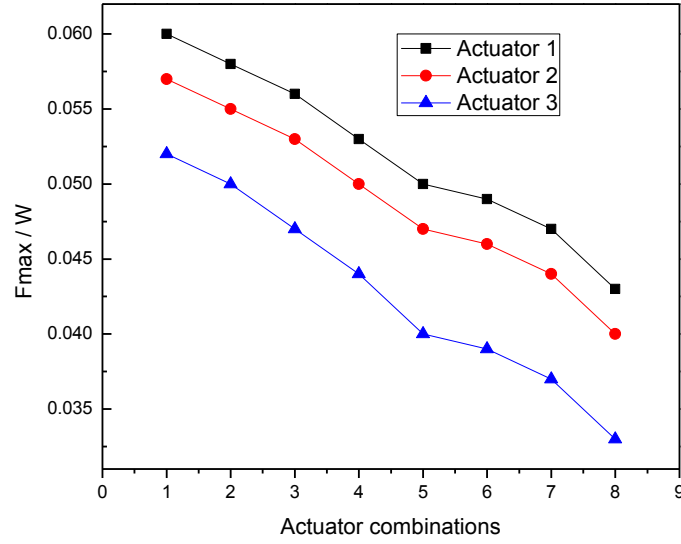


Figure 3.31 Variation of normalized peak control force with three actuator position (Bhuj earthquake).

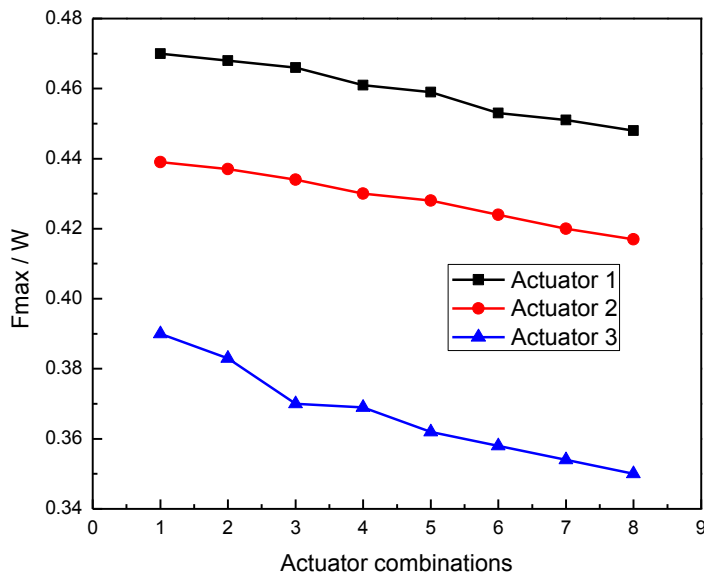


Figure 3.32 Variation of normalized peak control force with three actuator position (Kobe earthquake).

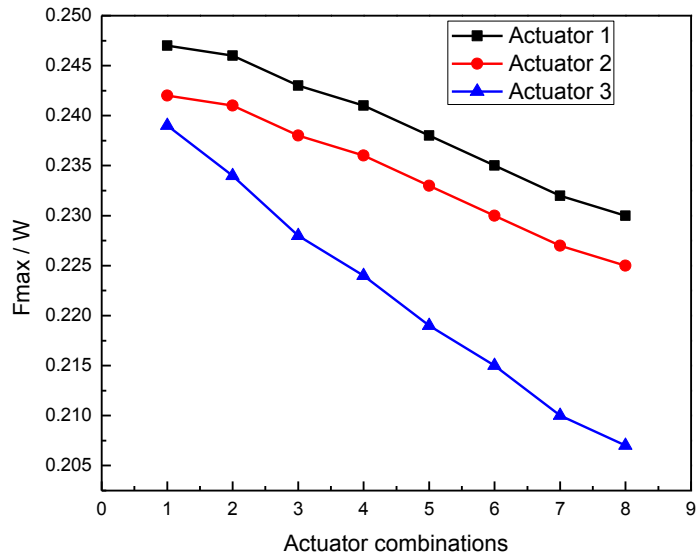


Figure 3.33 Variation of normalized peak control force with three actuator position (Elcentro earthquake).

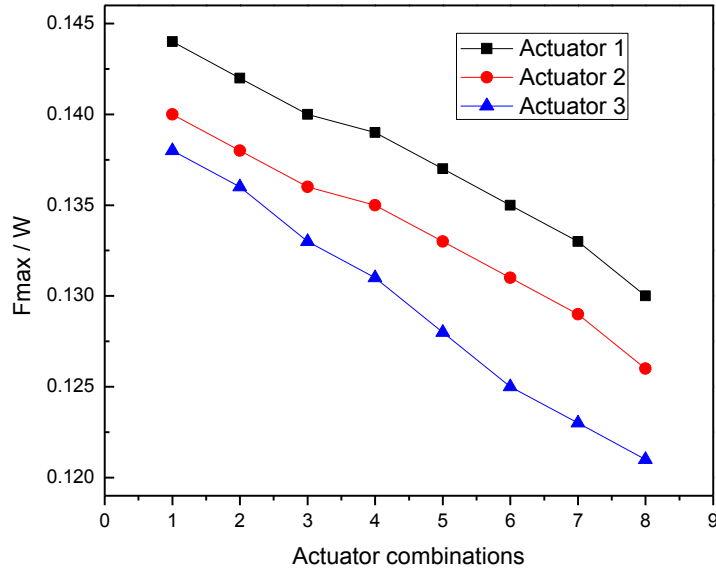


Figure 3.34 Variation of normalized peak control force with three actuator position (Spitak earthquake).

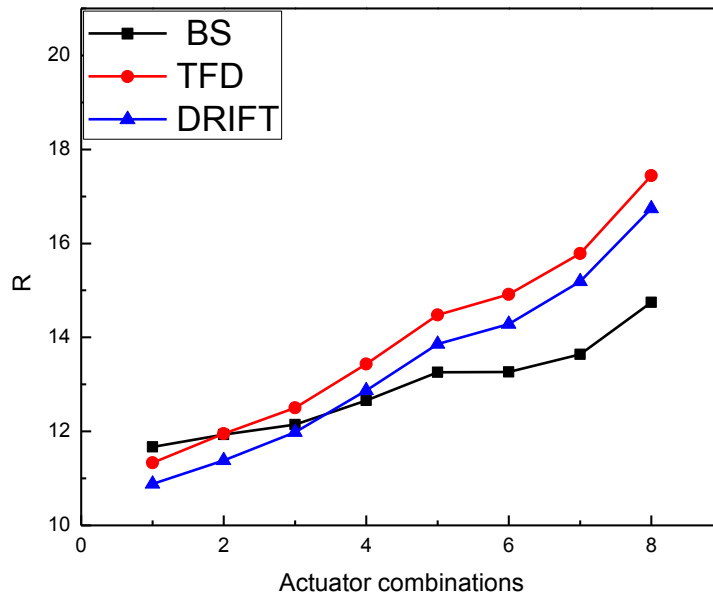


Figure 3.35 Variation of R values for maximum base shear, peak top floor displacement and maximum interstory drift with three actuator position (Bhuj earthquake).

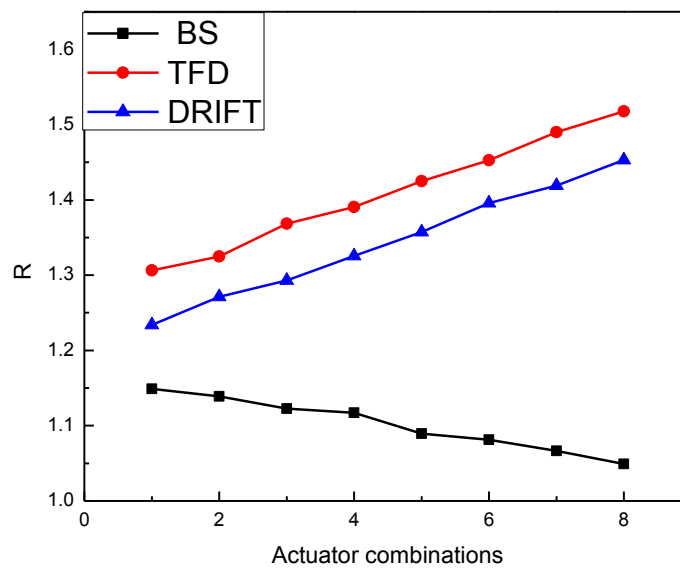


Figure 3.36 Variation of R values for maximum base shear, peak top floor displacement and maximum interstory drift with three actuator position (Kobe earthquake).

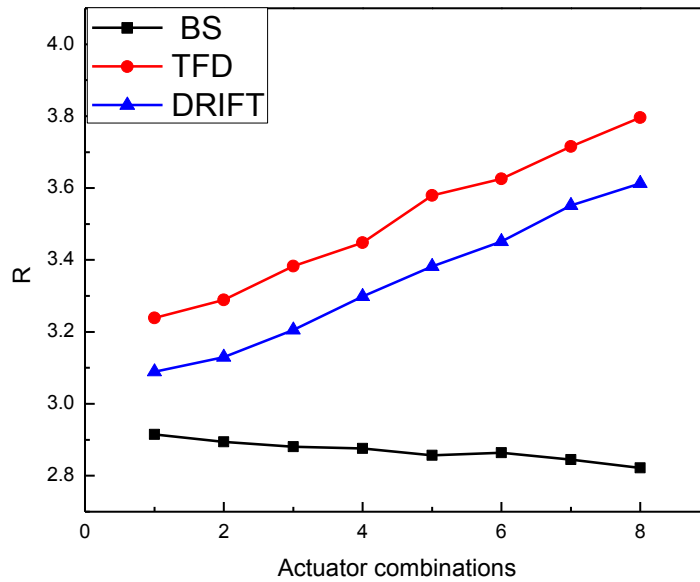


Figure 3.37 Variation of R values for maximum base shear, peak top floor displacement and maximum interstory drift with three actuator position (Elcentro earthquake).

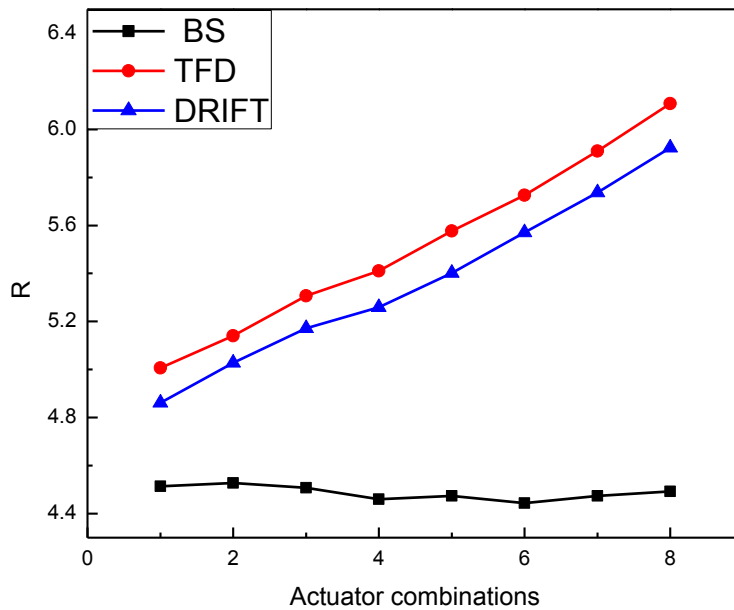


Figure 3.38 Variation of R values for maximum base shear, peak top floor displacement and maximum interstory drift with three actuator position (Spitak earthquake).

Table 3.8 Optimal position of three actuators based on a percentage reduction of responses

Sr. No.	Earthquake	Actuator position(floor number)		
		Base shear	Top floor displacement	Drift
1	Kobe(PGA = 0.4g)	1 -2-10(54%)	1-9-10 (70%)	1-9-10 (67%)
2	Elcentro(PGA= 0.32g)	1-2-10(72%)	1-9-10(89%)	1-9-10(85%)
3	Spitak (PGA = 0.2g)	1-2-10(65%)	1-9-10 (81%)	1-9-10 (79%)
4	Bhuj (PGA = 0.106g)	1-2-10(70%)	1-9-10 (77%)	1-9-10 (74%)

Table 3.9 Optimal position of three actuators based on R value for the case of three actuators

Sr. No.	Earthquake	Actuator placement (floor number)		
		Base shear	Top floor displacement	Drift
1	Kobe(PGA=0.4g)	1 (1.14)	10 (1.51)	10 (1.45)
2	Elcentro(PGA=0.32g)	1 (2.91)	10(3.65)	10 (3.61)
3	Spitak (PGA=0.2g)	1 (4.51)	10 (6.1.)	10 (5.92)
4	Bhuj (PGA=0.106g)	10(14.74)	10 (17.44)	10 (16.74)

The peak control forces required for three cases of actuator placement, one actuator, two actuators and three actuators are shown in Table 3.10.

Table 3.10 Maximum control force required

Sr. No.	Earthquake	One actuator	Two actuators	Three actuators
	Kobe(PGA = 0.4g)	0.39	0.439	0.47
1	Elcentro(PGA = 0.32g)	0.239	0.242	0.247
2	Spitak (PGA = 0.2g)	0.138	0.14	0.144
3	Bhuj (PGA = 0.106g)	0.052	0.057	0.06

It is seen from the Table that peak control force requirement does not significantly differ with the number of actuators used. However, there is a significant change in percentage reduction of responses (See Tables 3.5 to 3.9). Further, it may be noted that peak control force increases with the increase in peak ground acceleration of an earthquake, as expected.

### 3.4 Conclusion

Optimal placement of actuators in 10 storey building frame is investigated using a trial approach for 4 real earthquakes having different peak ground acceleration values. 3 cases are studied, namely, i) placement of only one actuator ii) a combination of two actuators placed at two different floors and iii) a combination of three actuators placed on three different floors. The optimal placements are selected based on the percentage reduction of three response quantities, namely, peak top floor displacement, maximum inter-storey drift and maximum base shear. Control responses are obtained using LQR algorithm. Optimal positions are investigated by considering i) percentage reduction in response alone ii) percentage reduction / unit peak control force, R factor and iii) by specifying an upper limit for the peak control force that can be accommodated in actuator.

The numerical study leads to the following conclusions:

- 1) For the single actuator, peak top floor displacement and max inter storey drift increase as the actuator is placed at higher floor. The max reductions are achieved when the actuator is placed on the 10th floor.
- 2) For the base shear, the pattern of variation is opposite to those of max top floor displacement and max inters storey drift.
- 3) The variation of peak control force has the same trend as that of percentage reduction in base shear.
- 4) The variation of the R factor (percentage reduction/unit control force.) is of the same nature as that of percentage reduction in responses for peak top floor displacement and max base shear. However, this variation of base shear is different from the percentage reduction of responses, in the case of Bhuj earthquake.
- 5) Therefore, it shows that optimal positions of the actuator may be different for different criteria used. Here, they are decided based on a percentage reduction of response alone and percentage reduction per unit control force.
- 6) In the case of two actuators and three actuators placed in the frame, the trend of results remains the same as that of single actuator.

- 7) Higher percentage reduction in responses can be achieved by increasing the number of actuators to control, as expected. However, considerable reduction in response can be achieved with single actuator also.
- 8) The max control force required to control the responses increases with increase in PGA level of the earthquake. The max control force does not change significantly with the number of actuators used. However, percentage reduction in responses changes significantly with the number of actuators used.

## CHAPTER – 4

### PREDICTIVE ACTIVE CONTROL OF BUILDING FRAMES

#### 4.1 Introduction

Considerable research has been carried out on the ANN control algorithms developed for active control of building frames with actuators. Both online and offline ANN control schemes are reported in the literature, which is reviewed in Chapter-2.

As found in the literature, the online ANN control scheme is complex, but their adaptability is more and therefore, they are versatile. However, they lack robustness because online training and testing are faced with different kinds of disturbance which are very difficult to incorporate in training schemes. Likewise, testing of neural network can be performed for variety of unknown cases. In spite of the development of offline trained neural network, the literature on the predictive active control using ANN is scanty. In this Chapter a simple predictive ANN control is presented. The training and testing of the neural network are performed offline. The control scheme is developed for controlling two important response quantities, namely, peak top storey displacement and maximum base shear. Three neural network architectures are considered in the study namely,

- i. For percentage reduction in target maximum top storey displacement only
- ii. For percentage reduction in target maximum base shear only
- iii. For percentage reductions of both target maximum top storey displacement and maximum base shear

In the last scheme, different combinations of percentage reduction in peak top storey displacement and maximum base shear are considered including the case of equal percentage reduction. For generating the training data, the percentage reduction in response quantities of interest is analytically obtained using LQR algorithm. The efficiency of the proposed scheme is investigated with the help of a set of unknown problems which involves earthquakes having characteristics same as those used for training and those which are different from the training set.



## 4.2 Theory

For each earthquake record, ten storey building frame is analyzed with its properties mentioned in Chapter 3. An actuator controller is placed at the top of building floor in the form of active tendon. Control force from the output node of the trained neural network is utilized to activate the trail for three different architectures of neural network for training and testing are used as shown in Figures 4.1 to 4.3.

### 4.2.1 Training of the neural network

For training the neural network, the ANN is trained with the generated data set, using three hidden layers with feed forward neural network architecture with three different cases. In the first case, Figure 4.1, time history of ground excitation and top floor displacement is considered as input and time history of peak control force per unit weight of building frame is considered as output node. In the second case, Figure 4.2, time history of ground excitation and base shear is considered as input and time history of peak control force per unit weight of building frame is considered as output node. In the third case, Figure 4.3, time history of ground excitation, base shear and top floor displacement is considered as input and time history of peak control force per unit weight of building frame is considered as output node.

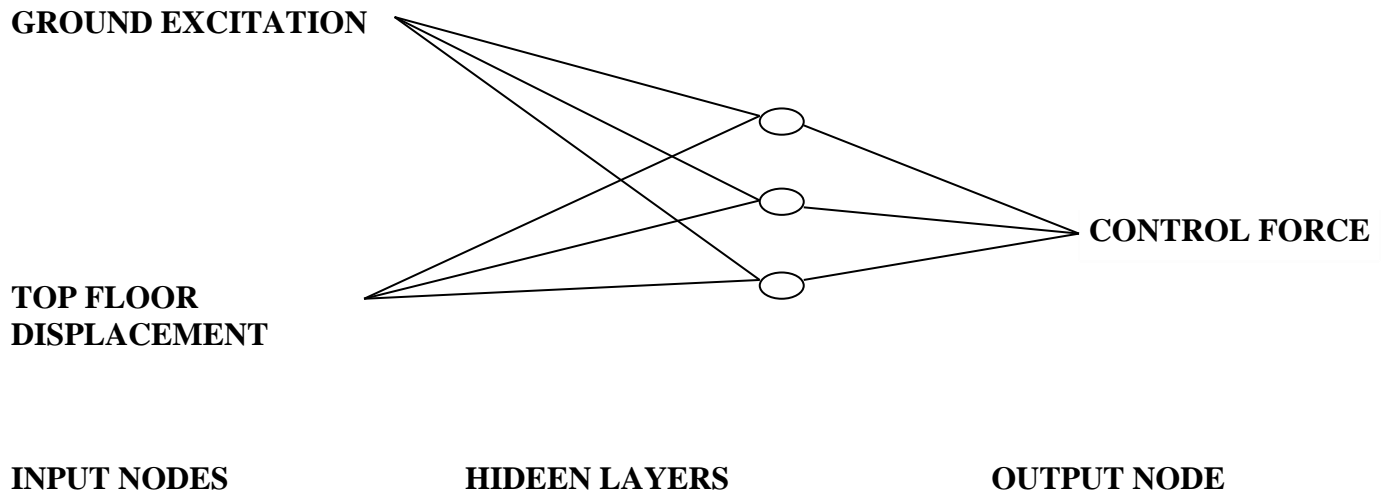


Fig 4.1 Block diagram representation of a three layered ANN (Network 1)

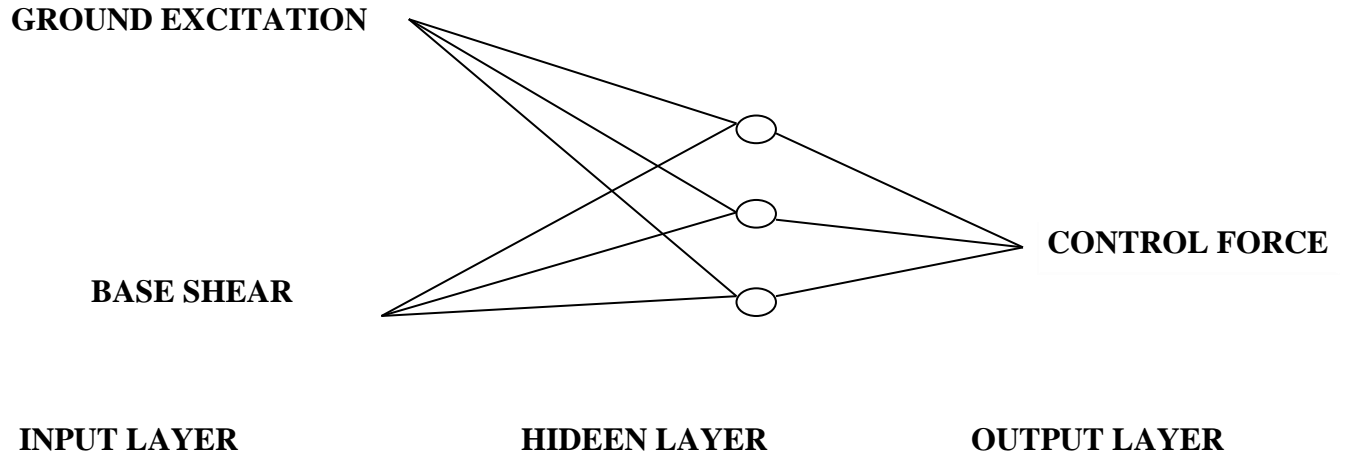


Figure 4.2 Block diagram representation of a three layered ANN (Network 2)

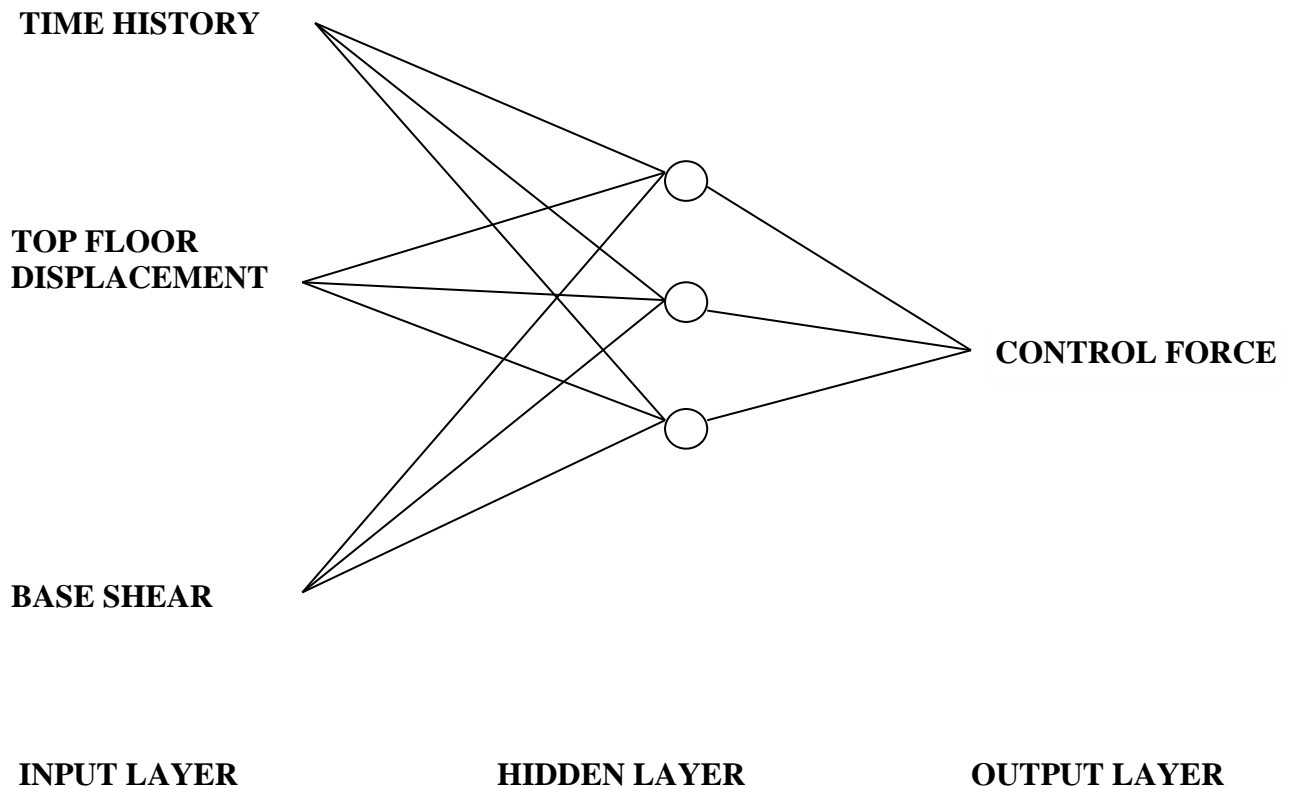


Figure 4.3 Block diagram representation of a three layered ANN (Network 3)

Nine neurons are considered in each hidden layer. The number of nodes considered in the hidden layer is obtained using trail runs to achieve the best possible reduction for a given set of the time histories of the ground acceleration and control force. The transfer function for the nodes consists of tensing. Classical feed forward, back propagation algorithm is used for training for this purpose. ANN tool box of MATLAB is utilized for this purpose. The number of data sets

for training is selected based on the mean square error up to the tolerance limit. For each data set, numbers of epoch for achieving the required tolerance limit are fixed from different trails. Training function is Trainlm, adaption learning function is Learngdm and performance function is MSE. While training the neural network, mean square error tolerance is obtained as 0.0035 for 1000 numbers of epochs.

Data sets are generated by finding the response reductions in peak top storey displacement and maximum base shear using LQR. Q and R values of LQR are adjusted for each earthquake to get the best results. Data set for training the neural networks are then generated by arranging the data in the form of input and output of the neural networks. For each case the time history of control force is applied to the output node.

#### **4.2.2 Testing the neural network**

For testing the neural network, both known and unknown problems consist of selected pairs of data sets generated for training the ANN. The inputs to the trained ANN are the percentage reduction of responses and the time history of ground motion. The output of the ANN provides the time history of control force. This time history of control force wouldn't be the same as the one which was used as the training pair during the training of the ANN. With this time history of control force and the time history of ground motion, the percentage reductions of responses are obtained analytically. These percentages of reductions are called actual percentage reductions. The target ones are percentage reductions provided in the input nodes of trained ANN to find the time history of control force. A comparison of the actual and target percentage of reductions is the test of the ANN.

For the unknown problem, any time history of ground motion (within the range of PGA values for which ANN was trained) is applied to the input node of the ANN. Any assumed target percentage reductions of responses are also provided to the input nodes. With the time history of control force obtained from the output node, the responses are obtained analytically. The target and the actual percentage reductions are compared to find the efficiency of ANN. In this process of testing, it is assumed that in the real time application, there is no time delay between the applications of ground motion and the control force obtained from ANN.

### 4.3 Numerical examples

Ten earthquakes which are considered for training the neural network are shown in the Table 4.1. Each earthquake is scaled to obtain peak ground acceleration values ranging from 0.05g to 0.4g at an interval of 0.05g as mentioned before. They are randomly shuffled to create the data set. A total of 80 earthquake records are used for training the ANN.

Table 4.1 Summary of earthquake time histories used

S. NO	YEAR	EARTHQUAKE	RECORDING STATION	PGA (g. m/s <sup>2</sup> )
1	1935	Helena, Montana	Helena Montana Carroll College	0.143
2	1988	Spitak	Gukasian	0.2
3	1995	Kobe	Nishi - Akashi	0.493
4	1968	Borrego Mountain	El Centro Site Imperial Valley Irrig District	0.127
5	1954	Eureka	Eureka Federal Bldg	0.252
6	1952	Kern County, CA	Taft Lincoln School Tunnel	0.176
7	1955	San Jose	San Jose Bank of America Basement	0.105
8	1957	San Francisco	San Francisco Golden Gate Park	0.102
9	1954	Wheeler Ridge, California	Taft Lincoln School Tunnel	0.063
10	1984	Morgan Hill	Halls Valley	0.305

#### 4.3.1 Testing the ANN for known problems

Two known problems are considered for testing the ANN, i.e. the time history of earthquake for Kobe (PGA=0.4g) and Spitak (PGA=0.2g). The variations of the peak control force with percentage reduction in top storey displacement for the two earthquakes are shown in Figures 4.4 and 4.5. For different target percentage reductions in response, the actual percentage of reductions using the time histories of control forces were obtained from ANN. The plot of peak control force to target and actual percentage reduction is shown in the figures.

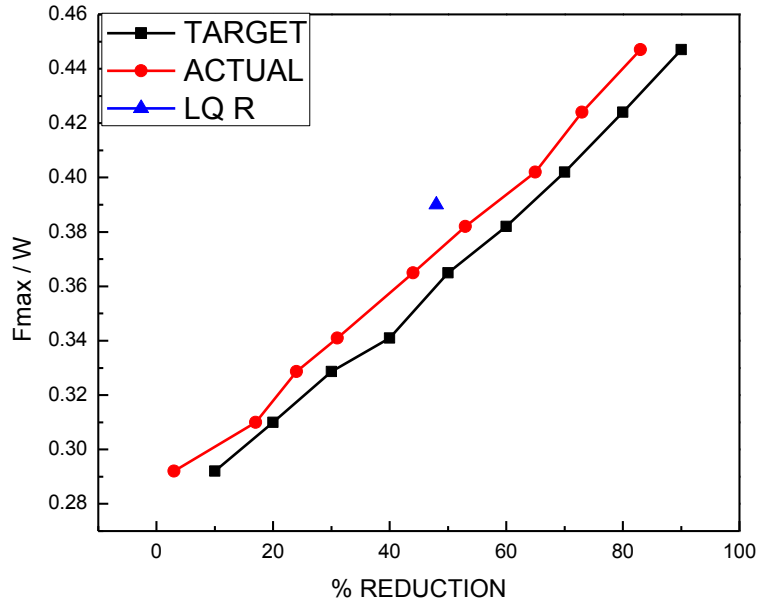


Figure 4.4 Comparison between target and actual percentage reduction in top storey displacement for Kobe earthquake (Network 1).

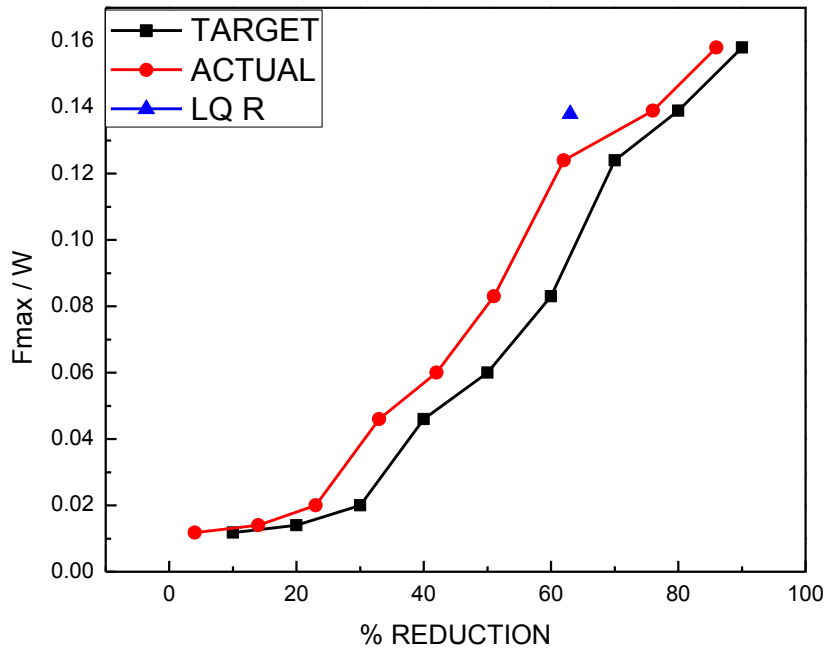


Fig 4.5 Comparison between target and actual percentage reduction in top storey displacement for Spitak earthquake (Network 1).

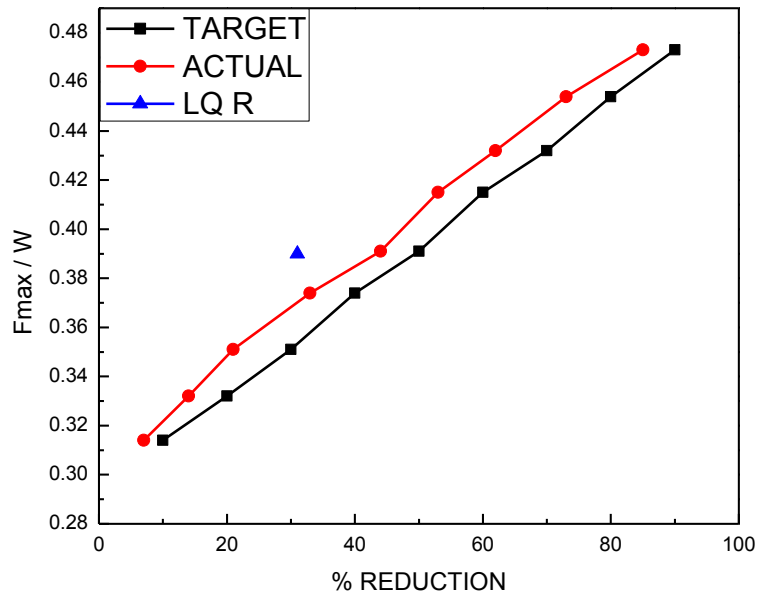


Figure 4.6 Comparison between target and actual percentage reduction in base shear for Kobe earthquake (Network 2).

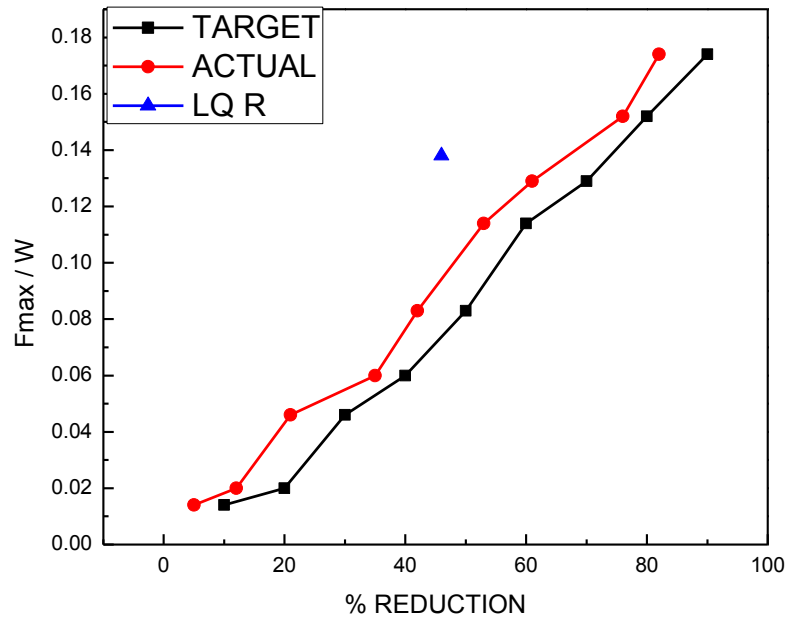


Figure 4.7 Comparison between target and actual percentage reduction in base shear for Spitak earthquake (Network 2).

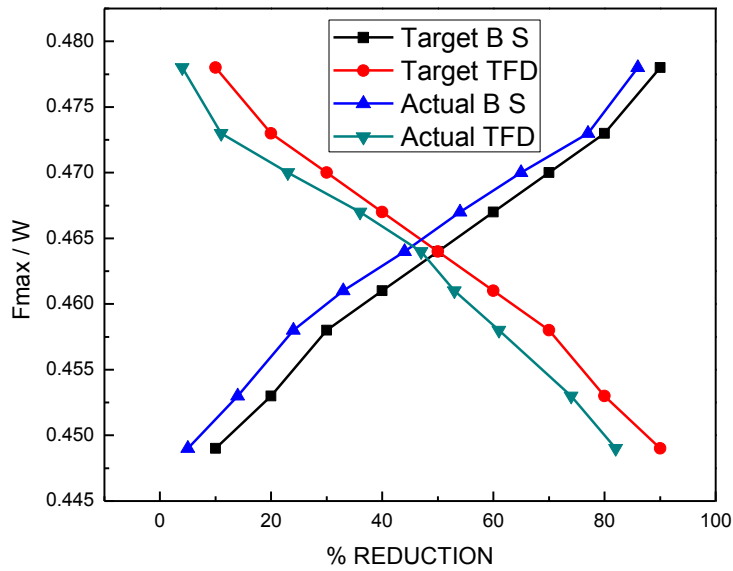


Figure 4.8 Comparisons between target and actual percentage reduction in base shear and top storey displacement for Kobe earthquake (Network-3).

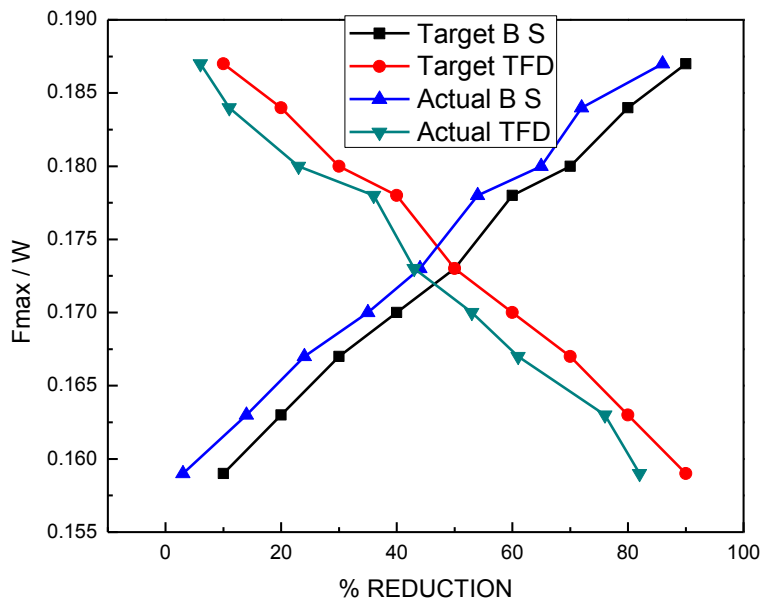


Figure 4.9 Comparisons between target and actual percentage reduction in base shear and top storey displacement for Spitak earthquake (Network 3).

The same comparison is shown for base shear in Figures 4.6 and 4.7. When both percentage reductions in peak top floor displacement and maximum base shear (Network-3), the

comparisons are shown in Figures 4.8 and 4.9. Note that in the figures, TFD means top floor displacement and BS means base shear. It is seen from the figures that the difference between the target and the actual percentage reduction is very small, nearly of the order of 5% for both earthquakes. This shows that the ANNs are well trained.

### 4.3.2 Testing for unknown problems

For testing neural network for unknown problems, the earthquakes considered are listed in Table 4.2.

Table 4.2 Summary of Earthquake Time Histories

<b>YEAR</b>	<b>EARTHQUAKE</b>	<b>RECORDING STATION</b>	<b>PGA (m/s<sup>2</sup>)</b>
1940	El cento (California)	Imperial valley	3.1276
1940	EL Alamo (Spain)	EL Centro array	0.5072
1980	Victoria (Mexico)	Cucapah	0.6611
1994	Northridge (Los Angeles)	LA – University Hospital	1.1694
2001	Bhuj	Ahmedabad	1.0382

To the unknown problems, the target and actual percentage of reductions are compared as they were done for known problems for three cases, namely, percentage reductions for peak top floor displacement only, maximum base shear only and both responses together. The variations of peak control forces with percentage reductions are shown in Figures 4.10 to 4.27 for different earthquakes listed in Table 4.2.



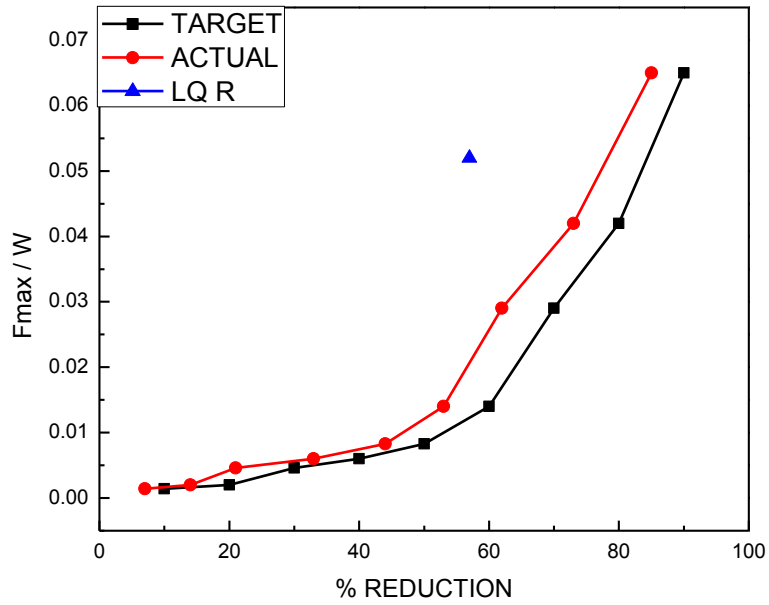


Figure 4.10 Comparison between target and actual percentage reduction in top floor displacement for Bhuj earthquake (Network1).

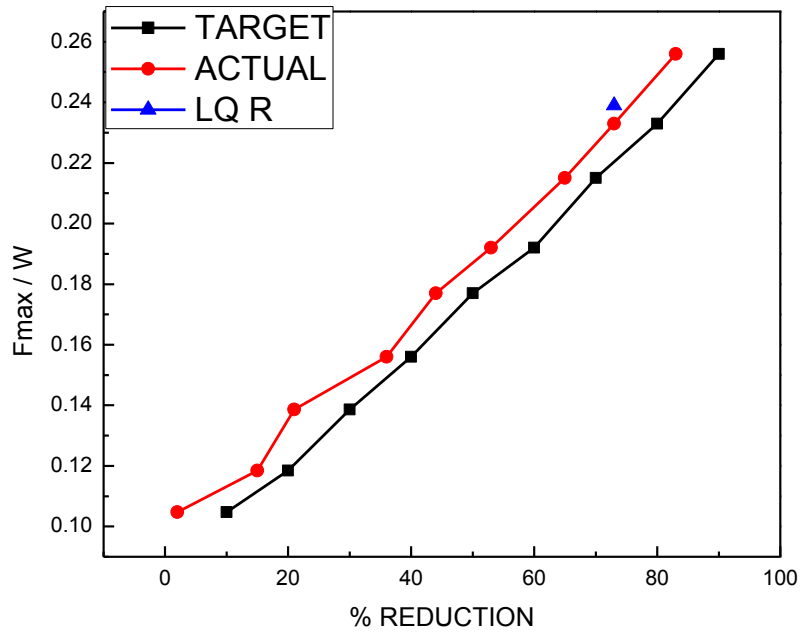


Figure 4.11: Comparison between target and actual percentage reduction in top floor displacement for Elcentro earthquake (Network1).

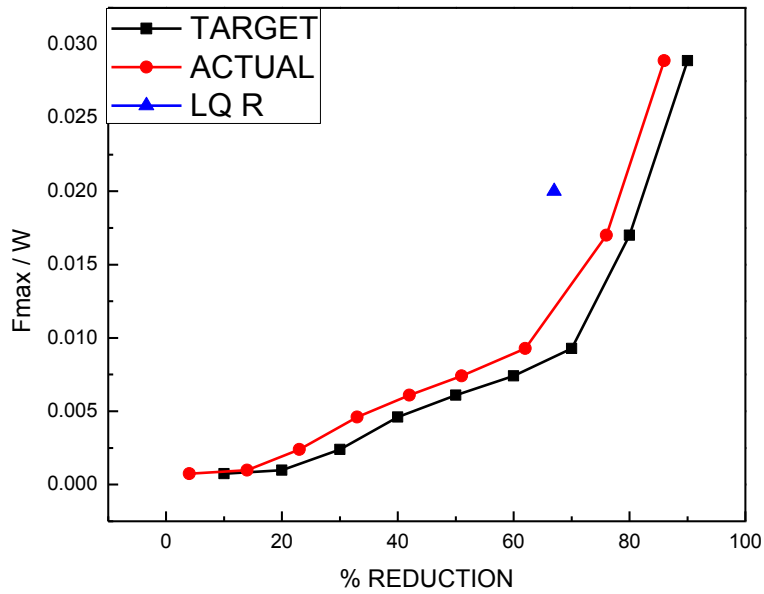


Figure 4.12 Comparison between target and actual percentage reduction in top floor displacement for Eliamo earthquake (Network 1).

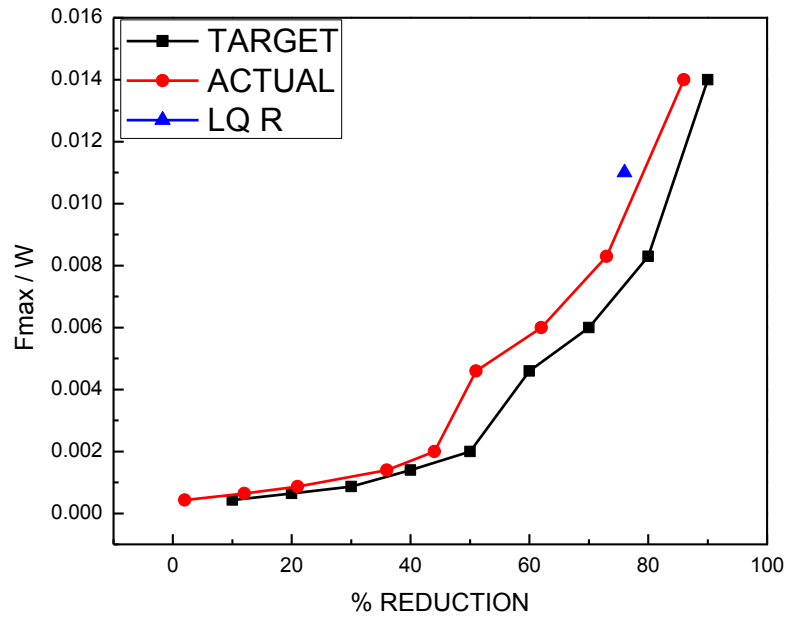


Figure 4.13 Comparison between target and actual percentage reduction in top floor displacement for Lomapieta earthquake (Network 1).

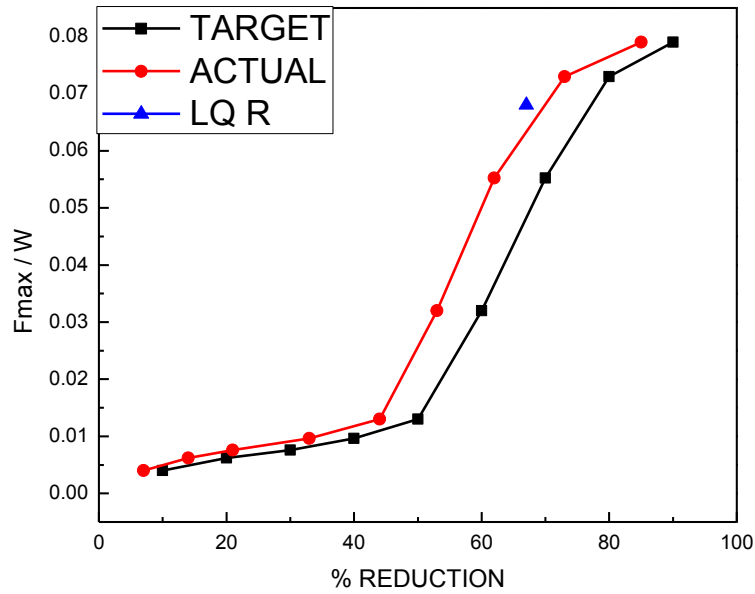


Figure 4.14 Comparison between target and actual percentage reduction in top floor displacement for Northridge earthquake (Network 1).

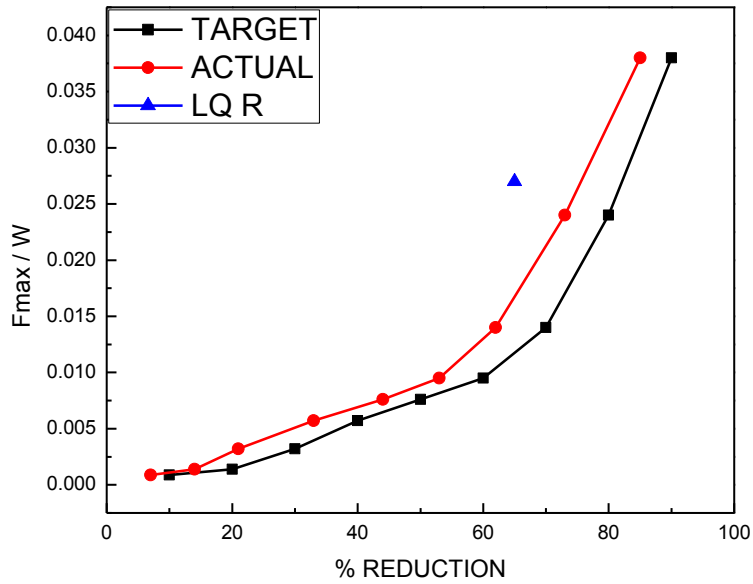


Figure 4.15 Comparison between target and actual percentage reduction in top floor displacement for Victoria earthquake (Network 1).

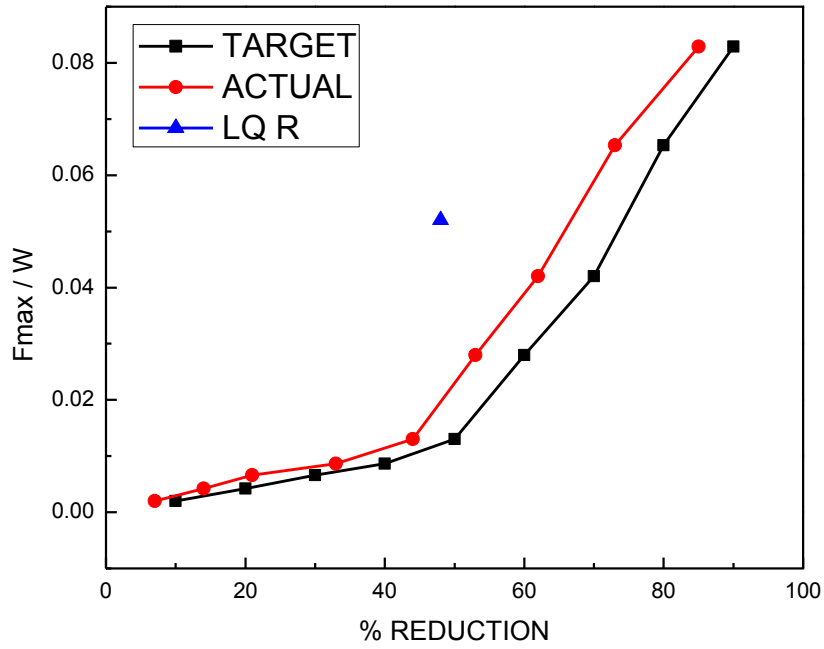


Figure 4.16 Comparison between target and actual percentage reduction in base shear for Bhuj earthquake (Network 2).

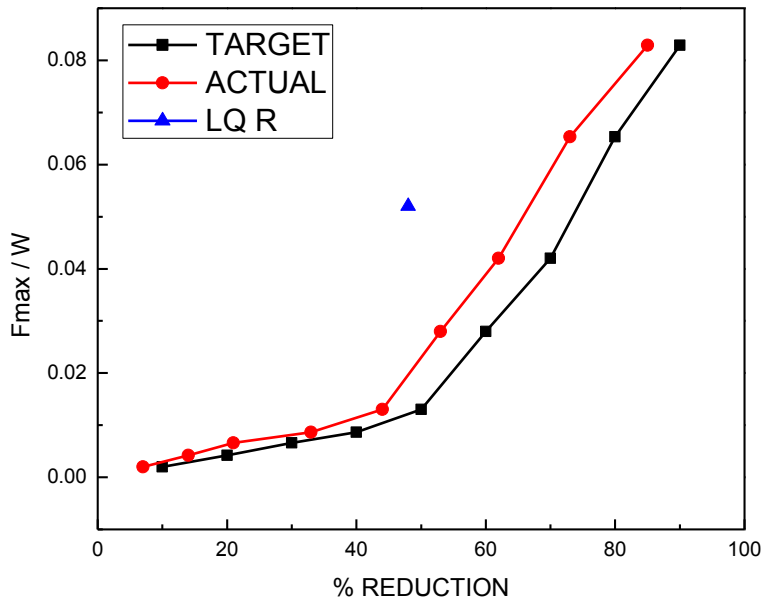


Figure 4.17 Comparison between target and actual percentage reduction in base shear for Elcentro earthquake (Network 2).

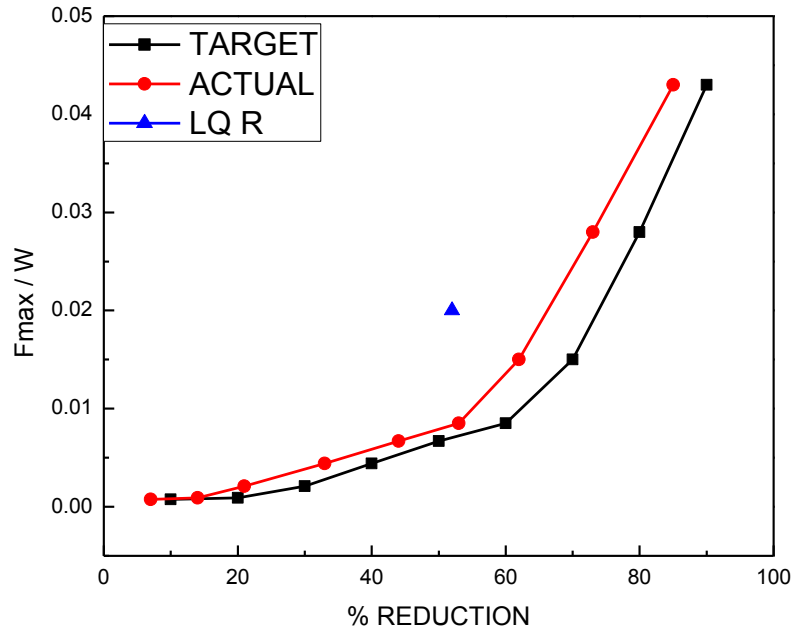


Figure 4.18 Comparison between target and actual percentage reduction in base shear for Eliamo earthquake (Network 2).

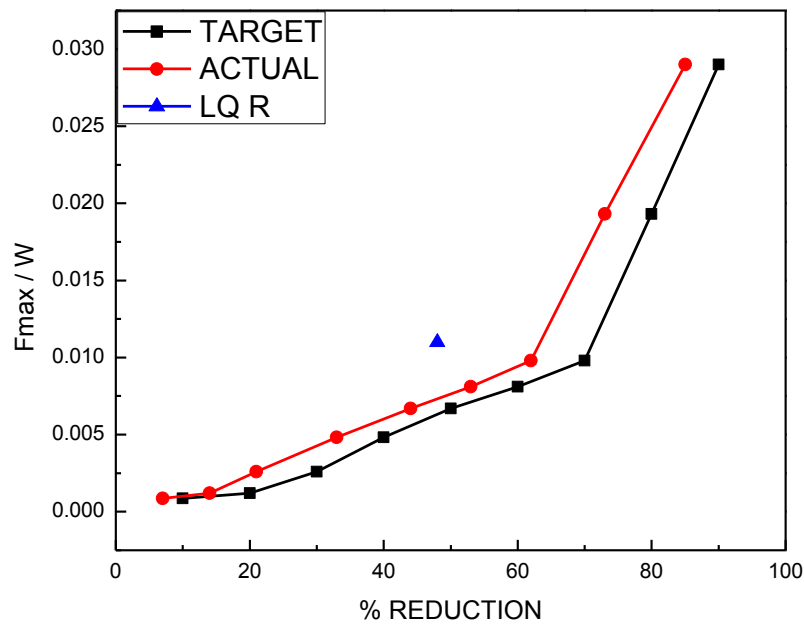


Figure 4.19 Comparison between target and actual percentage reduction in base shear for Lomapieta earthquake (Network 2).

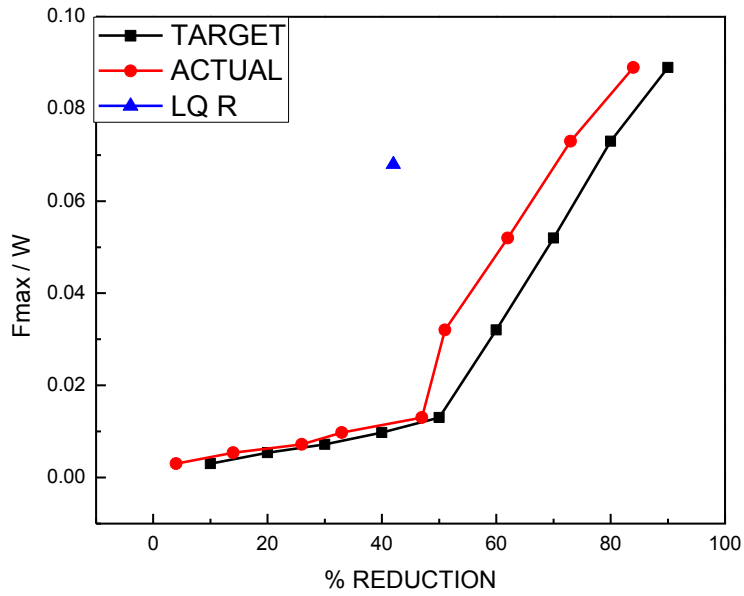


Figure 4.20 Comparison between target and actual percentage reduction in base shear for Northridge earthquake (Network 2).

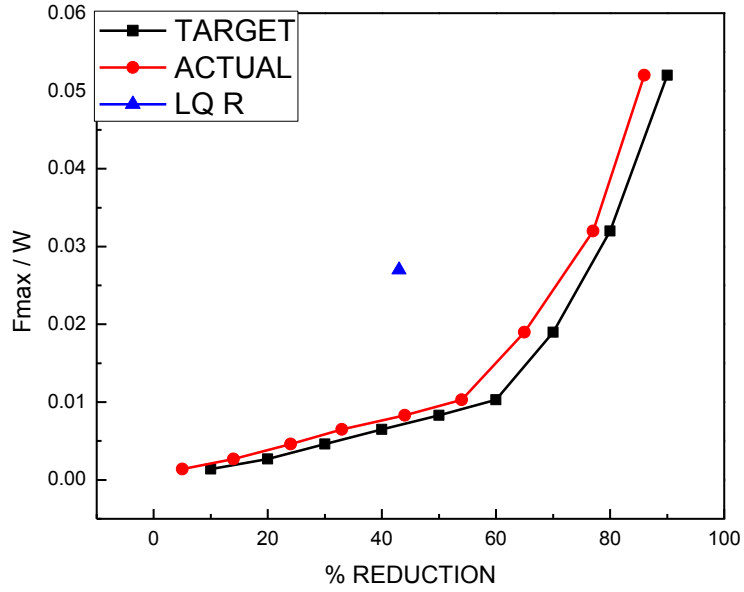


Figure 4.21 Comparison between target and actual percentage reduction in base shear for Victoria earthquake (Network 2).

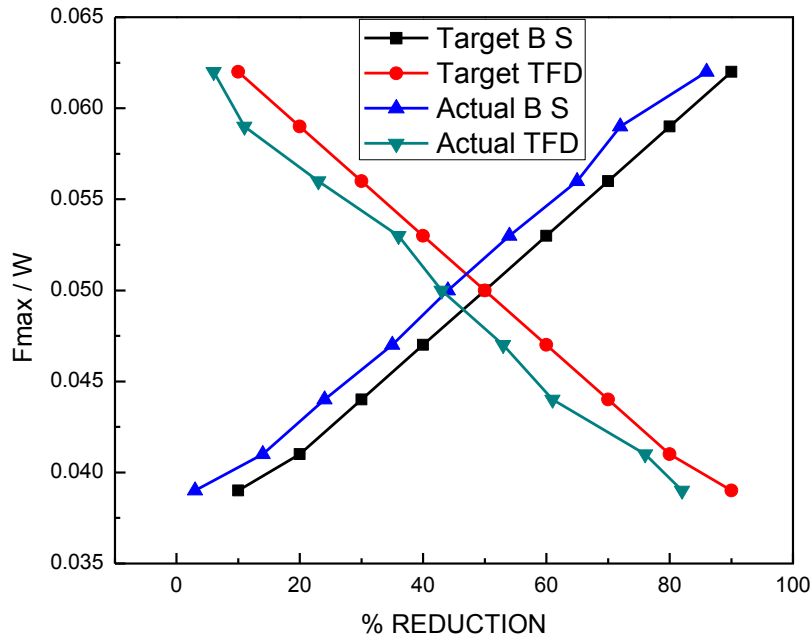


Figure 4.22 Comparisons between target and actual percentage reduction in base shear and top storey displacement for Victoria earthquake (Network 3).

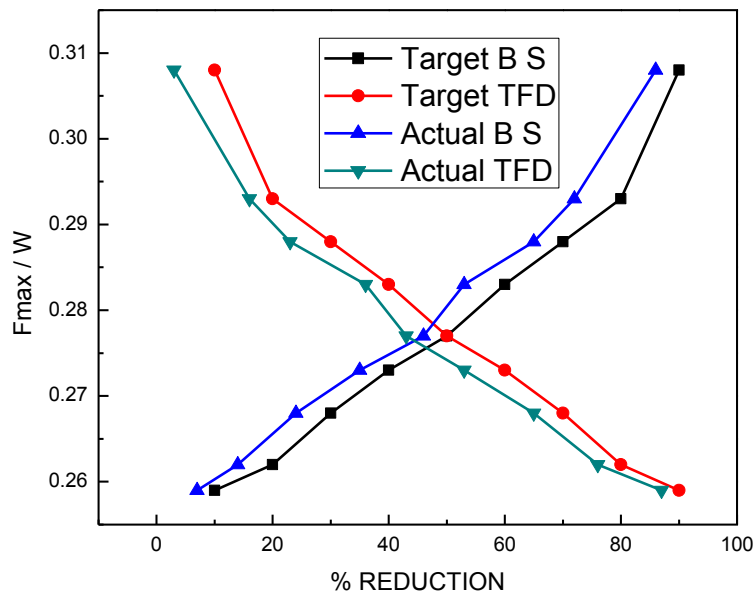


Figure 4.23 Comparisons between target and actual percentage reduction in base shear and top storey displacement for Elcentro earthquake (Network 3).

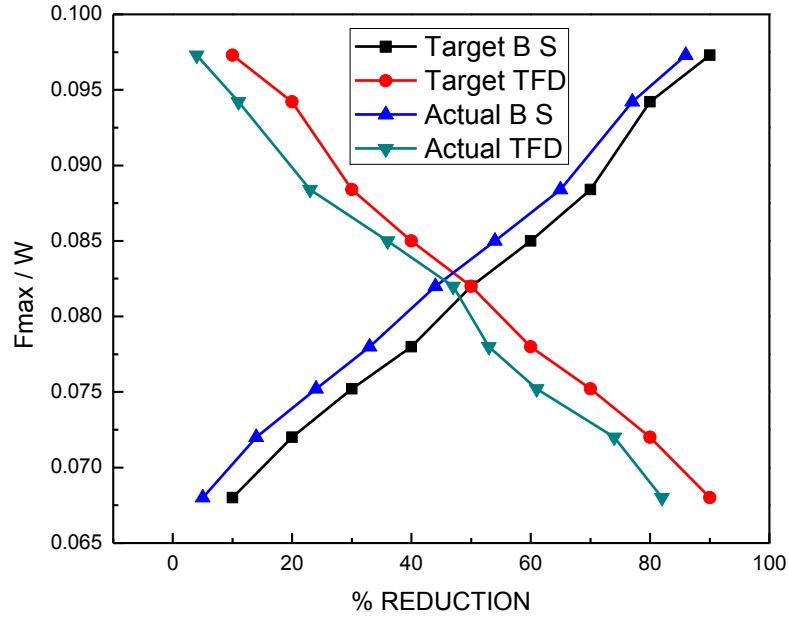


Figure 4.24 Comparisons between target and actual percentage reduction in base shear and top storey displacement for Bhuj earthquake (Network 3).

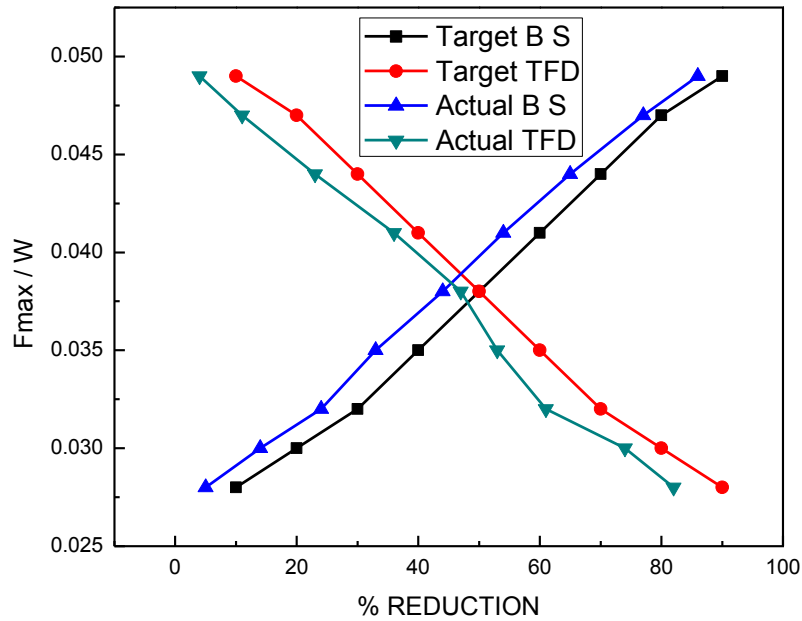


Figure 4.25 Comparisons between target and actual percentage reduction in base shear and top storey displacement for Eliamo earthquake (Network 3).



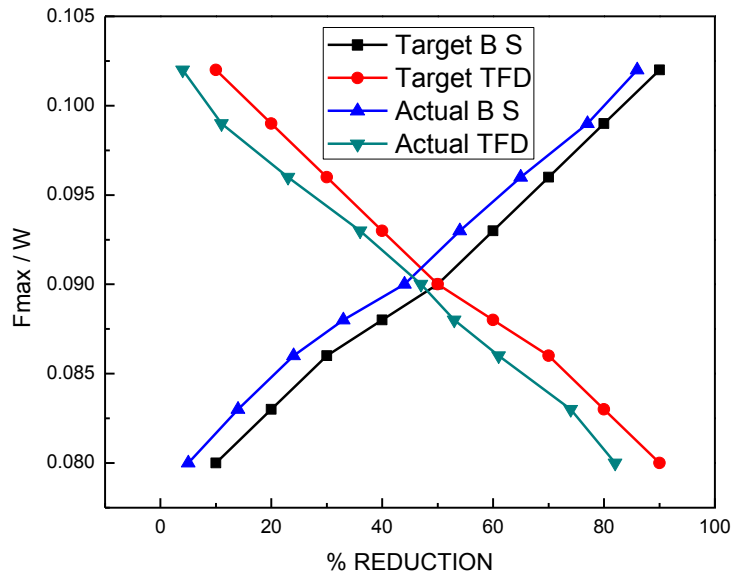


Figure 4.26 Comparisons between target and actual percentage reduction in base shear and top storey displacement for Northridge earthquake (Network 3).

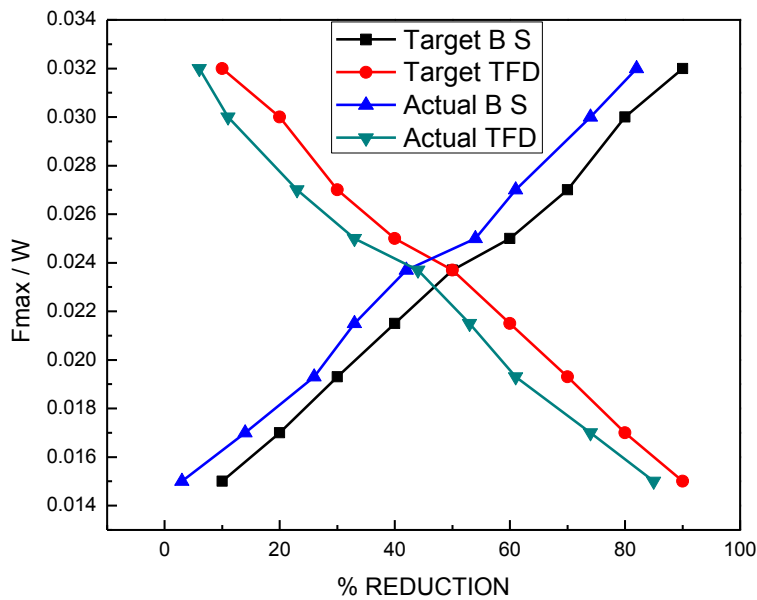


Figure 4.27 Comparisons between target and actual percentage reduction in base shear and top storey displacement for Lomapieta earthquake (Network 3).

It can be seen from the figures that for all the three neural networks, the difference between the target and actual percentage reductions vary within 5 to 10% for all the earthquakes

considered in the study. It is generally seen that near the lower ends of percentage reduction, the difference between the two is small, less than 5 % for most of the cases. Thus, the ANNs are well trained for predicting control forces for target percentage reductions of responses.

In order to compare the performances of ANN control and LQR control, the same building frame is controlled by LQR algorithm. For the ANN control, actual percentage reductions in maximum base shear and peak top storey displacement are considered. It is seen from Figures 4.10 to 4.27 that percentage reductions in peak top storey displacement and the corresponding peak values of control force are nearly the same for two algorithms'. LQR provides about 7-8% less reduction in peak top storey displacement for the same peak control forces in ANN and LQR control. The percentage reduction in maximum base shear, obtained by LQR, is highly underestimated. Thus, it is seen that the ANN control presented in the study is more efficient as compared to LQR control.

Note that for real time application of the ANN control algorithm, only the ground motion needs to be inputted in the ANN. Feedback responses from the structure are not required. In that sense, the control algorithm may be viewed as a feed forward algorithm. Both the known and unknown problems used for testing the ANN, belong to the class of earthquakes for which neural networks were trained. Further, the peak ground acceleration levels of the known and unknown problems were within the maximum peak ground acceleration level, considered in the training.

### **4.3.3 Testing of neural network for problems outside the range of training**

In order to test the efficiency of the trained ANN for solving unknown problems having much different characteristics than those for which it was trained, two types of ground motions are considered (i) simulated narrow band earthquakes from a given power spectral density function (PSDF) of ground motion and (ii) near field earthquake with fling step effect. The PSDF of ground motion and the time history of near field earthquake are shown in Figures 4.28 and 4.29. The PSDF of a narrow band earthquake is the Clough and Penzin double filter PSDF with  $w_s = 2\pi$ ,  $w_g = 0.1 w_s$  and  $\zeta_g = \zeta_s = 0.4$ . Peak ground accelerations, two within the range of training, 0.15g and 0.3g and two outside the range of training, 0.45g and 0.6g are considered. The results of the study are summarized in the Tables 4.2 to 4.7.

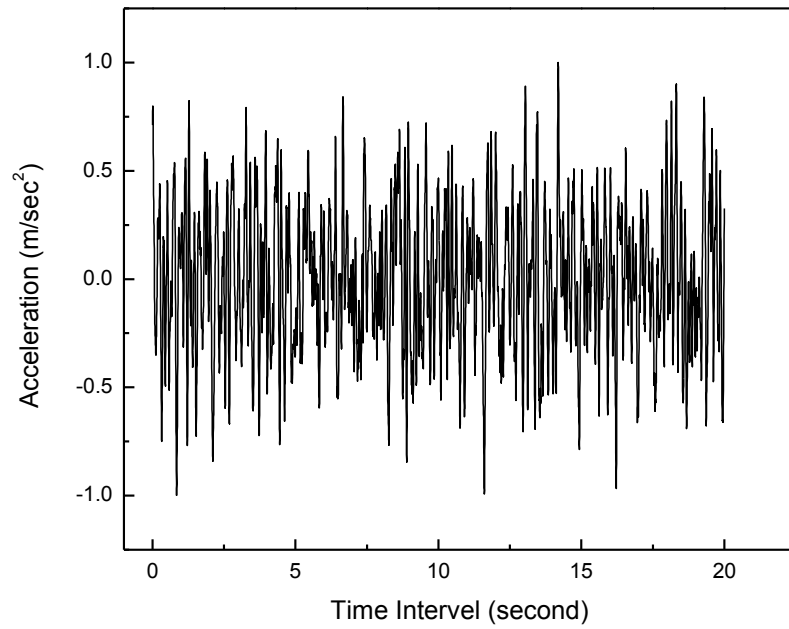


Figure 4.28 Normalized time history of the simulated narrowband earthquake (PSDF as Clough and Penzien double filter PSDF).

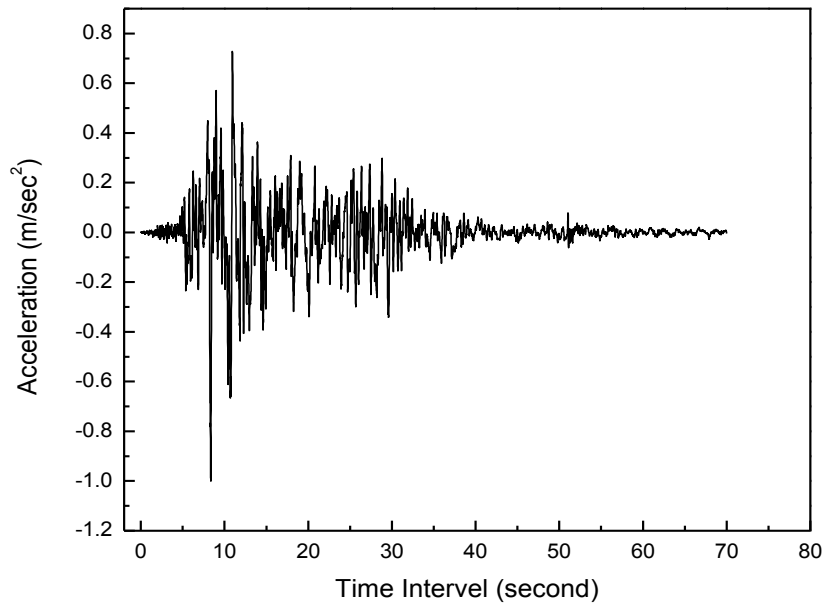


Figure 4.29 Normalized near field time history of earthquake with fling step effect (Chi- Chi earthquake, 1999).

Table 4.2 Results for Narrowband Earthquake

Peak ground acceleration	Target percentage reduction		$F_{max} / W$	Actual percentage reduction		Results from LQR	
	Base shear	Top storey displacement		Base shear	Top storey displacement	Base shear	Top storey displacement
0.15g	50	50	0.11	46	47	28	48
0.3g	50	50	0.28	45	46	34	53
0.45g	50	50	0.39	43	44	41	62
0.6g	50	50	0.52	41	42	47	71

Table 4.3 Results for Near field time history with Fling step effect

Peak ground acceleration	Target percentage reduction		$F_{max} / W$	Actual percentage reduction		Results from LQR	
	Base shear	Top storey displacement		Base shear	Top storey displacement	Base shear	Top storey displacement
0.15g	50	50	0.14	45	46	20	44
0.3g	50	50	0.3	44	45	32	48
0.45g	50	50	0.42	43	44	38	54
0.6g	50	50	0.56	41	42	43	65

Table 4.4 Results for Narrowband Earthquake

Peak ground acceleration	Target percentage reduction		$F_{max} / W$	Actual percentage reduction		Results from LQR	
	Base shear	Top storey displacement		Base shear	Top storey displacement	Base shear	Top storey displacement
0.15g	75	40	0.15	73	38	28	48
0.3g	75	40	0.32	71	35	34	53
0.45g	75	40	0.44	67	33	41	62
0.6g	75	40	0.57	66	32	47	71

Table 4.5 Results for Near field time history with Fling step effect

Peak ground acceleration	Target percentage reduction		$F_{max} / W$	Actual percentage reduction		Results from LQR	
	Base shear	Top storey displacement		Base shear	Top storey displacement	Base shear	Top storey displacement
0.15g	75	40	0.19	73	37	20	44
0.3g	75	40	0.36	70	35	32	48
0.45g	75	40	0.47	68	33	38	54
0.6g	75	40	0.62	64	32	43	65

Table 4.6 Results for Narrowband Earthquake

Peak ground acceleration	Target percentage reduction		$F_{max} / W$	Actual percentage reduction		Results from LQR	
	Base shear	Top storey displacement		Base shear	Top storey displacement	Base shear	Top storey displacement
0.15g	40	75	0.13	37	73	28	48
0.3g	40	75	0.31	36	71	34	53
0.45g	40	75	0.41	34	68	41	62
0.6g	40	75	0.54	32	66	47	71

Table 4.7 Results for Near field time history with Fling step effect

Peak ground acceleration	Target percentage reduction		$F_{max} / W$	Actual percentage reduction		Results from LQR	
	Base shear	Top storey displacement		Base shear	Top storey displacement	Base shear	Top storey displacement
0.15g	40	75	0.16	38	73	20	44
0.3g	40	75	0.32	36	71	32	48
0.45g	40	75	0.43	34	67	38	54
0.6g	40	75	0.60	31	65	43	65

Two cases are solved (i) equal percentage of reductions in responses and (ii) different percentage of reductions in responses. It is seen from the table that the target and actual percentage reductions in base shear and top storey displacement are nearly the same. In both cases (i) and (ii) for the lower range of PGA values, the difference is within 5-10%. Actual percentage reduction is slightly less than the target percentage reduction. For higher range of PGA values, the difference between the target and actual percentage reduction increases.

#### 4.4 Conclusion

An ANN control scheme is presented for target reduction in responses. Two responses are considered, namely, the maximum base shear and peak top storey displacement. For the trained neural network, the percentage reductions in response quantities of interest and the time history of ground motion enter as inputs. From the output node, the required time history of control force is derived. Three architectures of ANN are considered, as below

- i. Percentage reduction in top storey displacement and time history of ground motion as inputs.

- ii. Percentage reduction in maximum base shear and time history of ground motion as inputs.
- iii. Percentage reduction in maximum base shear, top storey displacement and time history of ground motion as inputs.

For all three ANNs, output node provides the time history of control force. The neural networks are trained and tested offline. The training is accomplished with ten time histories of far field earthquake records. The data set is augmented by scaling peak ground acceleration of each ground motion in the range of 0.05g to 0.4g at an interval of 0.05g. The testing is accomplished with the help of known and unknown problems. For testing the ANN, control force is obtained from neural network for a target percentage reduction of response and the time history of ground motion. The time history of control force obtained from the neural network is then used to find the reduction of the response quantity of interest analytically, which is termed as the actual and compared to the target one. Apart from testing the ANN for the known and unknown problems, it was tested for time history of earthquakes belonging to a different class from the ones used for training. Further, peak ground acceleration values are considered outside the range of values for which ANN was trained. The different class of earthquakes includes near field earthquake with fling step effect and simulated narrowband earthquake. The results of the numerical study lead to the following conclusions:

1. All three neural networks were well trained. The time history of control force obtained from the neural network provides the reduction in response very close to the target one.
2. The error between the actual and the target percentage reduction is of the order of 5 – 10%. When both percentage reduction in maximum base shear and peak top storey displacement are considered, it is found that the difference between the target and actual percentage reduction in peak top storey displacement is better than that of maximum base shear.
3. The difference between the actual and target percentage reduction in responses are not very large for peak ground acceleration levels for which neural network was not trained.
4. The trained neural network is effective in predicting the required control force for the target percentage reduction in responses, even for narrow band earthquake and near field earthquake with fling step effect, for which they were not trained.

5. In the above cases, the difference between the target and actual percentage reduction of responses are of the same order, as those observed for the far field earthquake.
6. Although data sets for training the ANN were prepared using LQR, the trained ANN in general predicts better time history of control force as compared to LQR for unknown problems providing more reductions in responses to the same level of peak control force. In some cases, the difference is small while in other cases it is significant.

## CHAPTER-5

# PREDICTIVE ACTIVE CONTROL FOR SITE SPECIFIC GROUND MOTION

### 5.1 Introduction

Prediction of the reduction of response for building frames with the help of active control, by way of placing a single actuator at the top of the frame is a problem of practical interest. The control strategy may be employed for both damaged and undamaged structures. Damaged building frames are retrofitted using active structural control to meet the future earthquake demands. The undamaged structure may be an old building or a new building whose performance may have to be enhanced for meeting the future earthquake demands.

As mentioned in the previous chapter, the prediction of the reduction in response to a pre decided target level constitutes an inverse problem for which artificial neural network (ANN) is widely used in structural control. Although the considerable literature exists on the ANN control of building frames, not much literature is reported for predictive active control of building frames for site specific random ground motion. In this chapter, an ANN based active control of the ten storey building frame is presented for a pre decided target reduction in the response of the building frames for site specific random ground motion represented by its PSDF. Two types of sites are considered in the study, namely the hard soil and the soft soil. The results of the study are verified by obtaining the same reduction using LQR algorithm.

### 5.2 Theory

As described in the previous chapter, finding the time history of control force for a pre-decided percentage reduction of responses, called target percentage reduction, constitutes an inverse problem. Since ANN is widely used for solving the inverse problem, the method of finding the desired time history of control force for the target percentage reduction in response adopts ANN.

Problems of ANN consist of two parts, namely, training and testing of the neural network. There are two types of training and testing of the neural network, namely, offline and online as mentioned in the previous chapter. Since the prediction of the control force for the future



earthquake is the objective of the study here, offline training is adopted. The trained neural network is then utilized for online application of the structural control problem.

### 5.1.1 Training of the neural network

The ANN is trained using simulated data set. For simulation, the time history of both control force and excitation are simulated from their respective PSDFs. For this purpose, it is assumed that the PSDF of control force has the same shape as that of the ground motion. As a result, the PSDF of ground motion is normalized by assuming  $s_o$  to be unity in Equation 5.1.

The Clough and Penzin double filter PSDF given by Equation 5.1 and shown in Figure 5.1 is used to model the future earthquake process at the site.

$$S_{\ddot{x}_g} = s_o \frac{[1+(2\zeta_s\rho_s)^2]}{[(1-\rho_s^2)^2+(2\zeta_s\rho_s)^2][(1-\rho_g^2)^2+(2\zeta_s\rho_s)^2]} \rho_g^4 \quad (5.1)$$

In which,  $\zeta_g$ ,  $w_g$  and  $\zeta_s$ ,  $w_s$  are the filter coefficients for the first and second filter respectively.

By setting  $s_o=1$ , Equation 5.1 takes the form

$$S_{\ddot{x}_g} = \frac{[1+(2\zeta_s\rho_s)^2]}{[(1-\rho_s^2)^2+(2\zeta_s\rho_s)^2][(1-\rho_g^2)^2+(2\zeta_s\rho_s)^2]} \rho_g^4 \quad (5.2)$$

Monte Carlo simulation is used to simulate the ensemble of time histories of  $\ddot{x}_g$  from Equation 5.1. Each time history is divided by its peak value, thus obtaining an ensemble of normalized time history records corresponding to Equation 5.1.

For a set of values of PGA and peak control forces, ensemble of the time history records of the ground acceleration and the control force is generated. By making permutation and combinations, desired number of the pairs of time history records of the ground acceleration and the control force are obtained. Using these pairs, percentage reductions in the response quantities of interest are determined by time history analysis of the building frame using SIMULINK tool box. Dataset, thus generated is used for training the ANN.

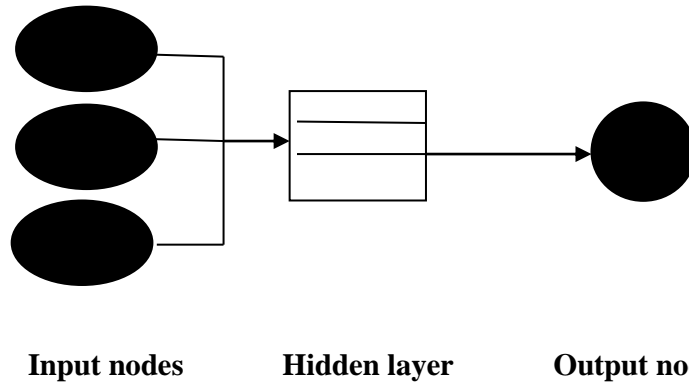


Figure 5.1: A block diagram representation of a three layered ANN

The ANN has three input nodes and one output node having three hidden layers as shown in Figure 5.1. The number of nodes considered in the three hidden layers is obtained using the trial and search to achieve the best possible reduction for a given set of the time histories of the ground acceleration and the control force. The transfer function for the nodes consists of Tansig. Classical feed forward, back propagation algorithm is used for training. ANN tool box of MATLAB is utilized for this purpose. The number of data sets for training is selected based on the mean square error excepted as tolerance limit. For each data set, numbers of epoch for achieving the required tolerance limit are fixed from different trials. Training function is Trainlm, adaption learning function is Learnngdm and performance function is MSE.

### 5.1.2 Testing neural network

The trained neural network is tested for both known and unknown data set. The testing for the neural network consists of the following steps (known problem)

- i. Consider a pair of data set consisting of time histories of the ground motion and the control force from the data sets prepared for training the neural network.
- ii. The target percentage reductions are taken as those obtained from the solution of the control problem using Simulink.
- iii. In the input node, the time history of ground acceleration and target percentage reduction of maximum top storey displacement and base shear are provided. The time history of control force obtained from the output node of the ANN is recorded.
- iv. With the time history of control force obtained from the neural network, the control problem is solved in Simulink using the time history of the ground motion provided in the input node.

- v. The percentage reduction of maximum top storey displacement and base shear are recorded and compared with those of target values.
- vi. For the unknown problems, the time history of ground motion is generated for a PGA which is not included in the data set. The testing procedure consists of following steps
  - a) The simulated time history of ground motion is provided in the input nodes along with the target percentage reduction in maximum top storey displacement and base shear as desired.
  - b) The corresponding time history of the control force is obtained from the output node of the neural network.
  - c) The time history of the control force, thus obtained is used for controlling the response of the system under the ground motion provided in the input nodes of the ANN.
  - d) The control responses are obtained using SIMULINK tool box of MATLAB.
  - e) The percentage reductions in the peak top storey displacement and the maximum base shear obtained from the analysis are compared with the desired target percentage reductions.

### 5.3 Numerical examples

For each earthquake record, a ten storey building frame is analyzed with its properties same as mentioned in the Chapter 3. An actuator controller is placed on the top floor of the building in the form of active tendon.

Two types of soil conditions are considered in the study, namely, the hard soil and the soft soil. The filter coefficients for two types of soil are taken as,  $w_g=0.1 w_s$ ,  $w_s = 2\pi$  and  $\zeta_g = \zeta_s = 0.4$  for soft soil and  $w_g=0.1 w_s$ ,  $w_s = 10\pi$  and  $\zeta_g = \zeta_s = 0.8$  for hard soil.

The plots of the two PSDF's are shown in the Figure 5.2.

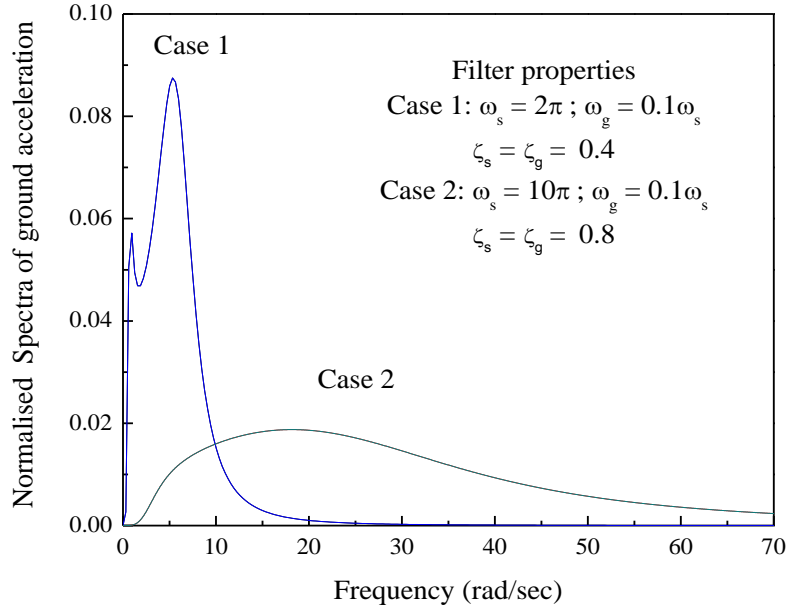
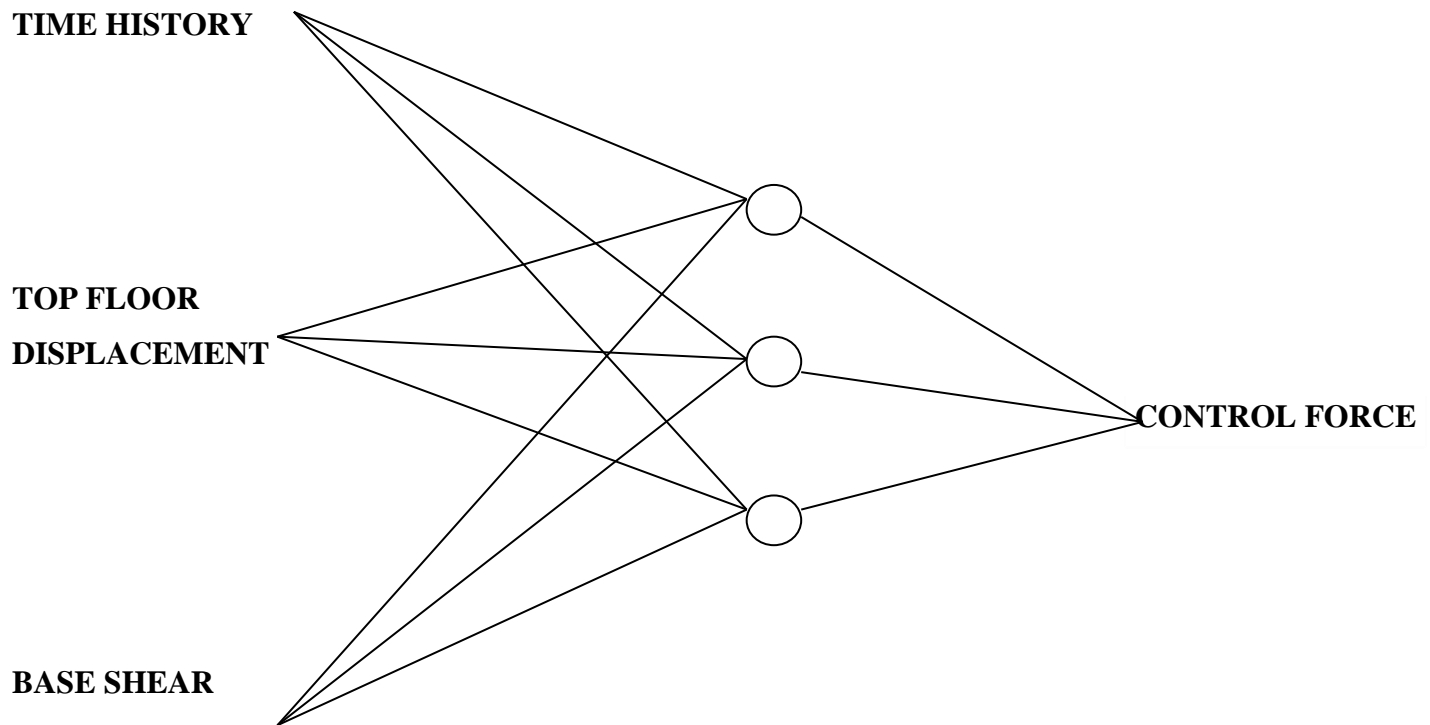


Figure 5.2 Normalized PSDF of Ground Acceleration

Eight records of ground motions for different PGA values are generated for each type of soil. Similarly, twenty records of control forces for different values of peak control force are generated. The combinations of PGA and control forces used for performing the training data are shown in the Table 5.1. Typical time histories of simulated ground motions and the control force are shown in Figure 5.4 to 5.11. The architecture of the ANN used for training and testing is shown in Figure 5.3.

Table 5.1 Combinations of PGA and peak control force used in the training data.

PGA of excitation	Peak control force per unit weight of building frame
0.05g	0.05, 0.2
0.1g	0.1, 0.3, 0.4
0.15g	0.25, 0.35, 0.45
0.2g	0.1, 0.4
0.25g	0.15, 0.3
0.3g	0.1, 0.4, 0.5
0.35g	0.15, 0.35, 0.45
0.4g	0.2, 0.5



**INPUT NODES**

**HIDDEN LAYER**

**OUTPUT NODE**

Figure5.3: Architecture of ANN used for training and testing.

While training the neural network, mean square error tolerance is obtained as 0.0035 for 1000 numbers of epochs. Analytically obtained percentage reduction for peak top storey displacement and base shear varies between 2% and 8% for the hard soil and 4% and 9% for the soft soil. According to the method of training, data sets as described above are used for training.

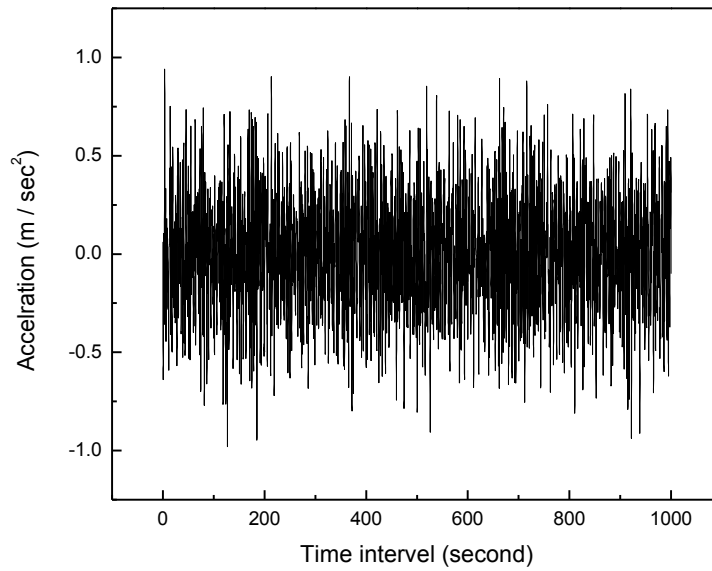


Figure 5.4 Typical simulated time history of ground acceleration (PGA=0.1g) for hard soil condition.

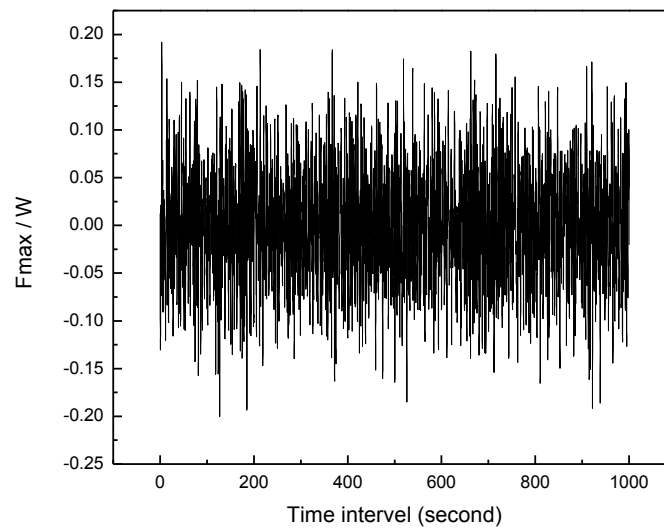


Figure 5.5 Typical time histories of simulated control force (peak= 0.2W) for hard soil.

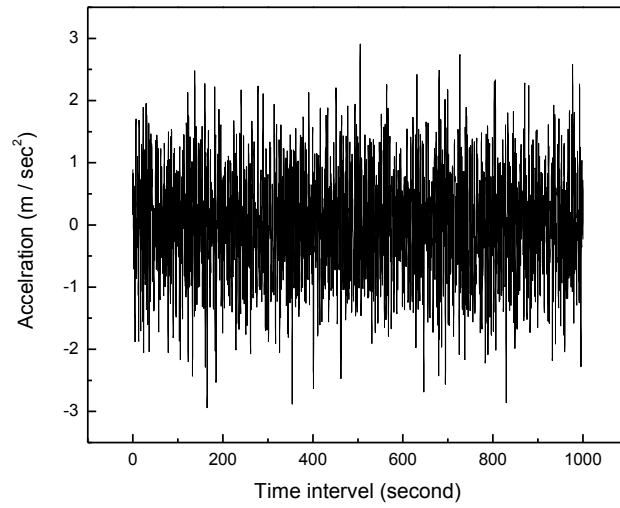


Figure 5.6 Typical simulated time history of ground acceleration (PGA=0.3g) for hard soil condition.

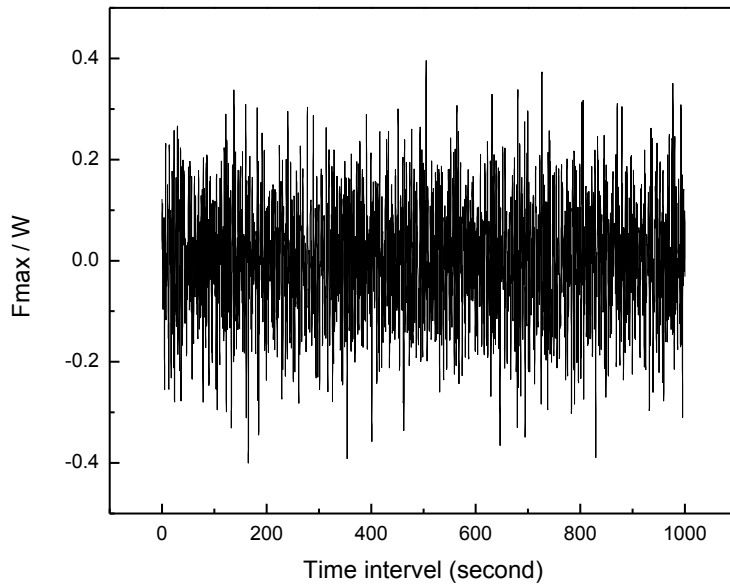


Figure 5.7 Typical time histories of simulated control force (peak= 0.4W) for hard soil.

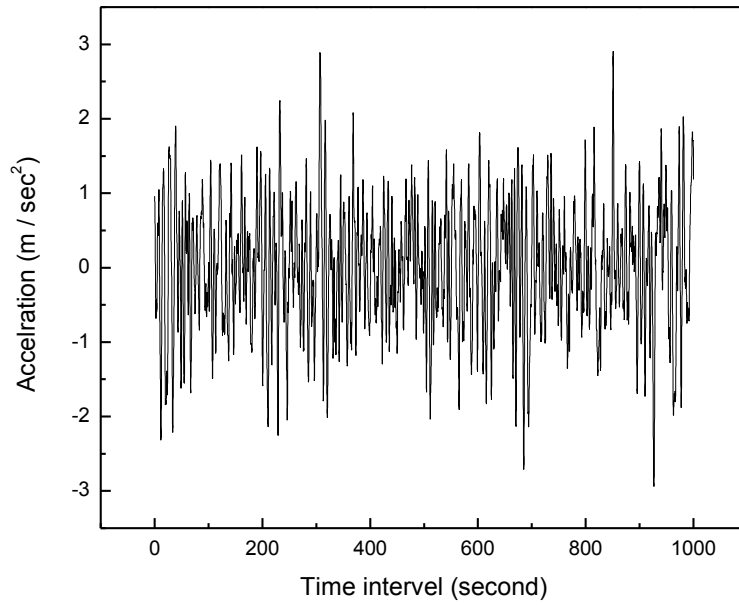


Figure 5.8 Typical simulated time history of ground acceleration (PGA=0.3g) for soft soil condition.

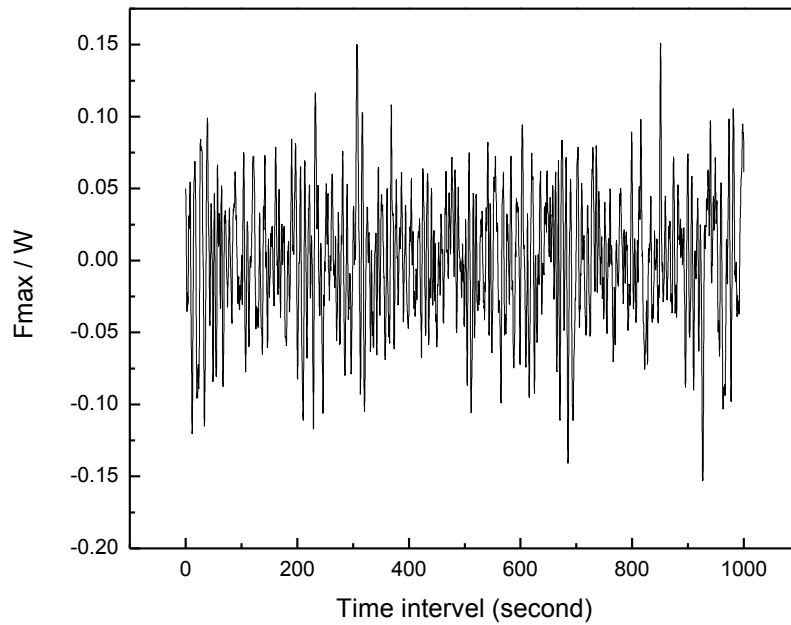


Figure 5.9 Typical time histories of simulated control force (peak= 0.15W) for soft soil



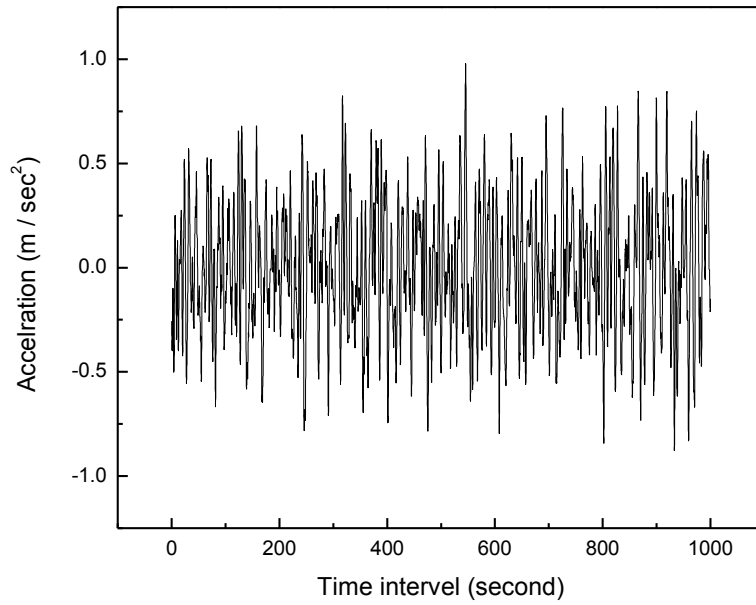


Figure 5.10 Typical simulated time history of ground acceleration (PGA=0.1g) for soft soil condition.

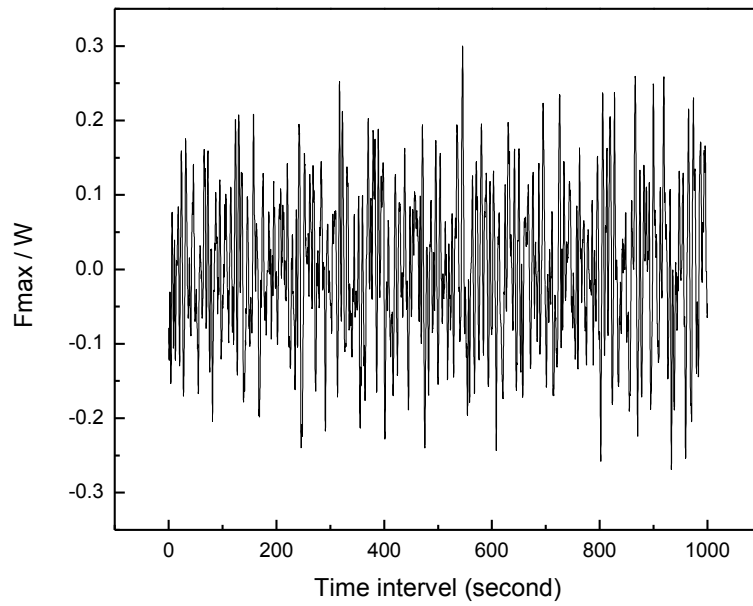


Figure 5.11 Typical time histories of simulated control force (peak=0.3W) for soft soil.

## 5.4 Discussions of results

### 5.4.1 Results of the hard soil.

Testing of the neural network is done for both known and unknown data set combinations. In the figures below, the plot between the normalized peak value of the control force, the percentage reduction in peak top storey displacement and the maximum base shear are depicted. The target values indicate the values of the percentage reductions in the maximum base shear and the peak top storey displacement given as input to the neural network. The corresponding output from the neural network is the time history of the control force for the specified ground motion. Thus, percentage reductions in responses obtained by SIMULINK toolbox using the time history of control force obtained from the ANN output nodes are termed as actual percentage reductions.

For the known problem, results in two cases are depicted in Figure 5.12 namely, different percentage reductions in the maximum base shear and the maximum peak storey displacement and the same percentage reductions in both response quantities. In Figures.5.12 and 5.13, it is seen that in both cases the target and actual curves are quite close to each other for the known problem. This shows that the training of neural network is satisfactory for predicting the time history of the control force of the known problems.

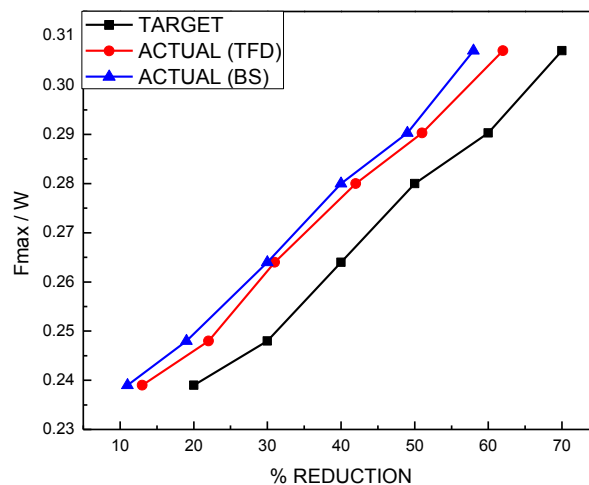


Figure 5.12 Comparison between target and actual percentage of reductions in base shear and top floor displacement (target value remains the same for both) for PGA 0.35g (known problem)

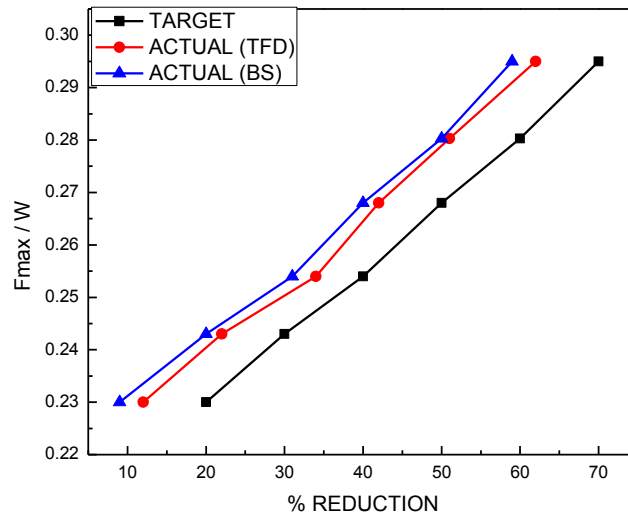


Figure 5.13 Comparison between target and actual percentage reductions in base shear and top floor displacement for (20% fixed target reduction in Base shear) for  $PGA=0.35g$  (known problem)

For unknown problems, different time histories of the ground accelerations other than the training sets are obtained corresponding to  $PGA$  levels of  $0.05g$  to  $0.4g$  at an interval of  $0.05g$ . Thus, eight problems are considered for the hard soil as shown in Figures 5.14 to 5.40. The difference between the target and the actual percentage reductions in responses is not very significant. The maximum difference is of the order of 5-8%. Further, the pattern of variation of curves does not remain the same for all ground accelerations considered. The actual percentage reduction is always less than the target one. The figures show that the maximum control force increases with the increase in the percentage reduction of response, as expected. Also, the maximum control force increases with the increase in the value of the  $PGA$ . As mentioned before, two cases are considered, namely, the same percentage reductions in both response quantities (Figure 5.14 to 5.21) and different percentage reductions in the maximum base shear and the peak top storey displacement (Figure 5.22 to 5.39).

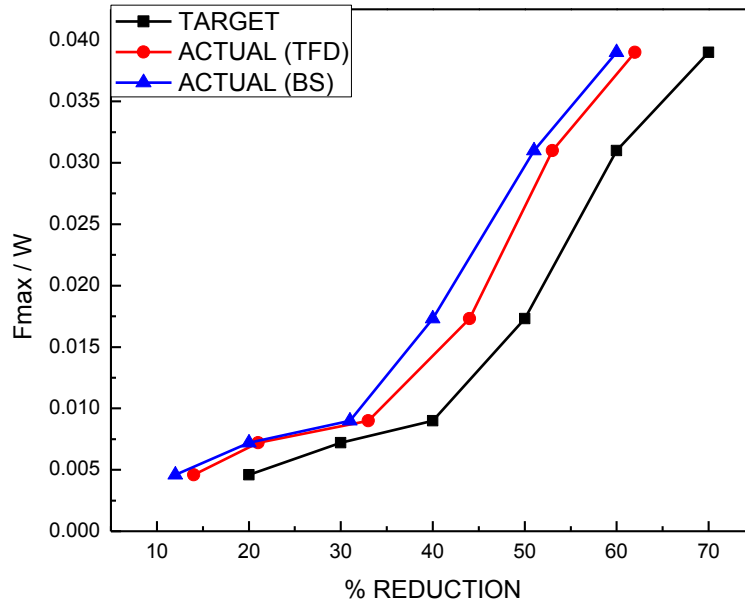


Figure 5.14 Comparison between target and actual percentage reductions in base shear and top floor displacement for PGA 0.05g.

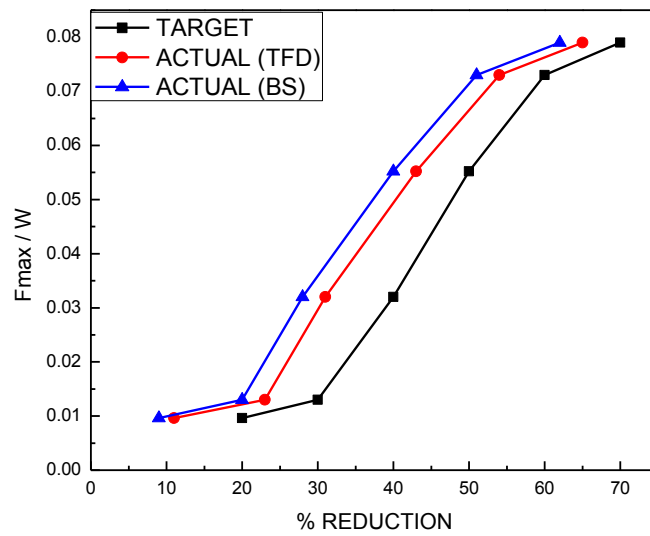


Figure 5.15 Comparison between target and actual percentage reductions in base shear and top floor displacement for PGA 0.10g

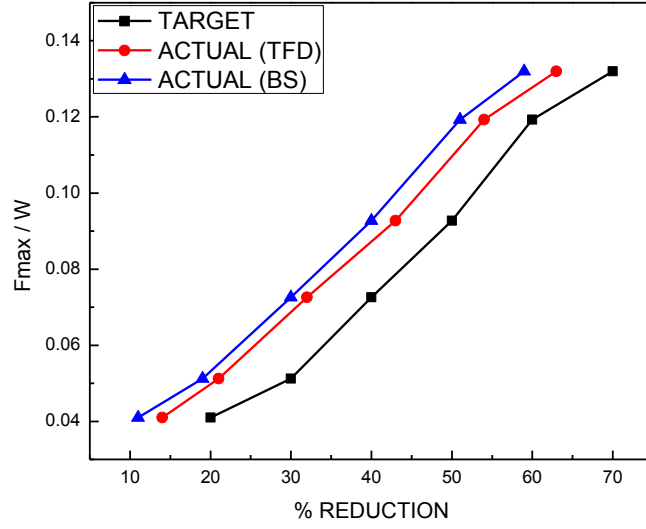


Figure 5.16 Comparison between target and actual percentage reductions in base shear and top floor displacement for PGA 0.15g

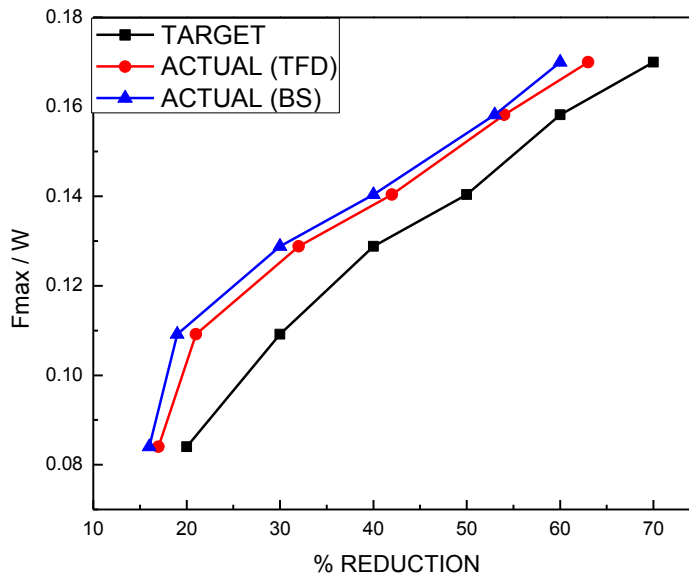


Figure 5.17 Comparison between target and actual percentage reductions in base shear and top floor displacement for PGA 0.2g

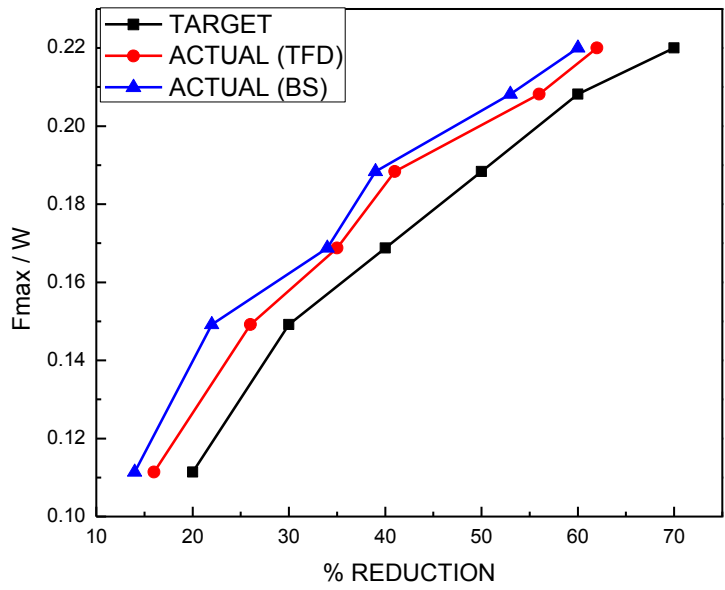


Figure 5.18 Comparison between target and actual percentage reductions in base shear and top floor displacement for PGA 0.25g

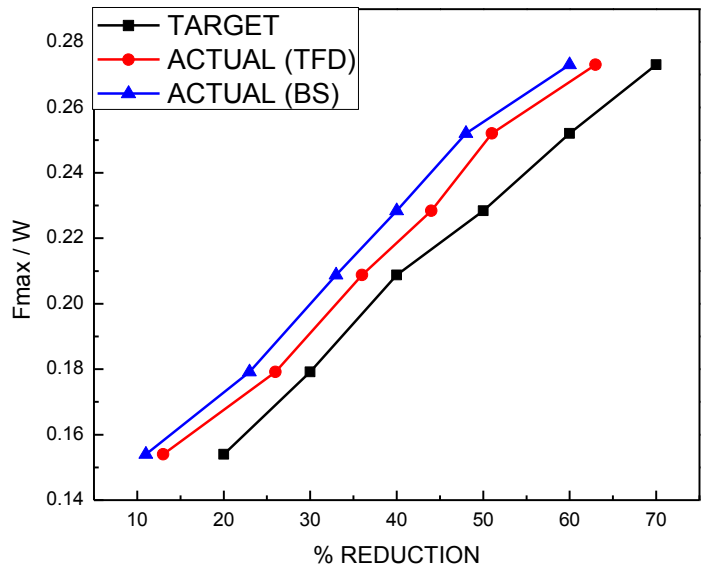


Figure 5.19 Comparison between target and actual percentage reductions in base shear and top floor displacement for PGA 0.30g

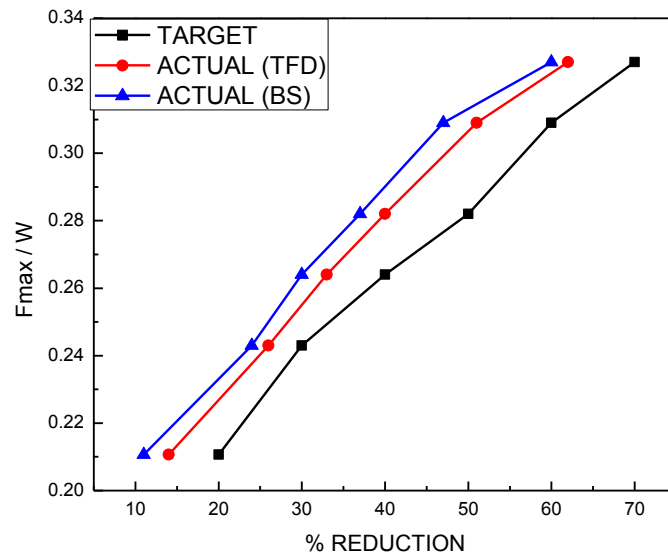


Figure 5.20 Comparison between target and actual percentage reductions in base shear and top floor displacement for PGA 0.35g

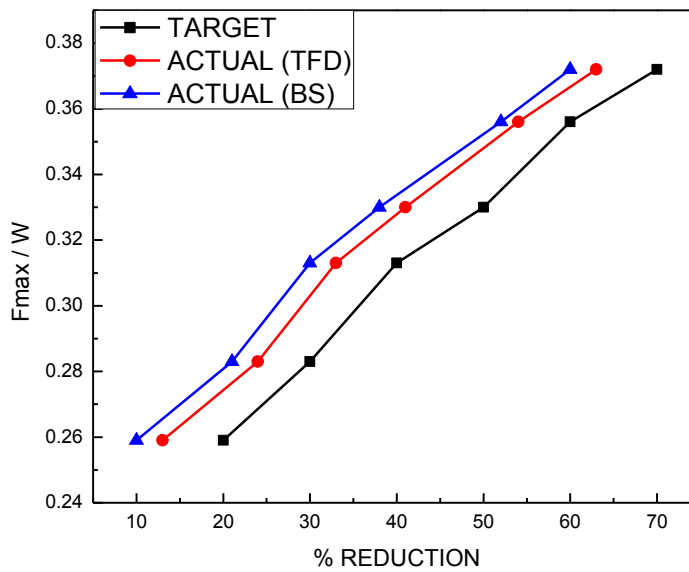


Figure 5.21 Comparison between target and actual percentage reductions in base shear and top floor displacement for PGA 0.40g

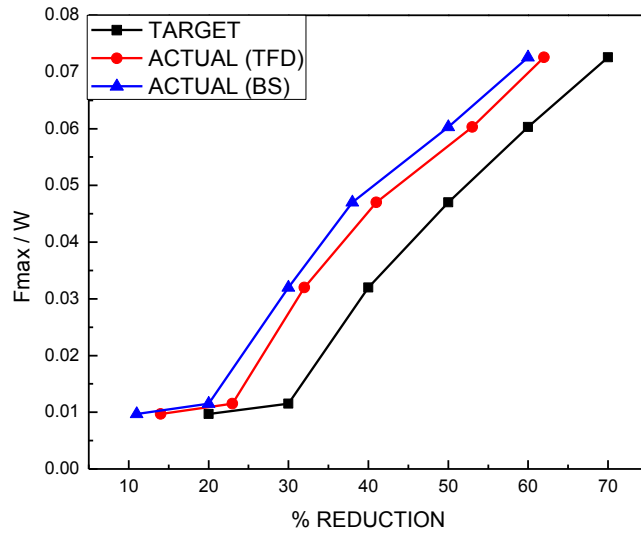


Figure 5.22 Comparison between target and actual percentage reductions in base shear and top floor displacement (for fixed 20% target reduction in base shear) for PGA=0.1g

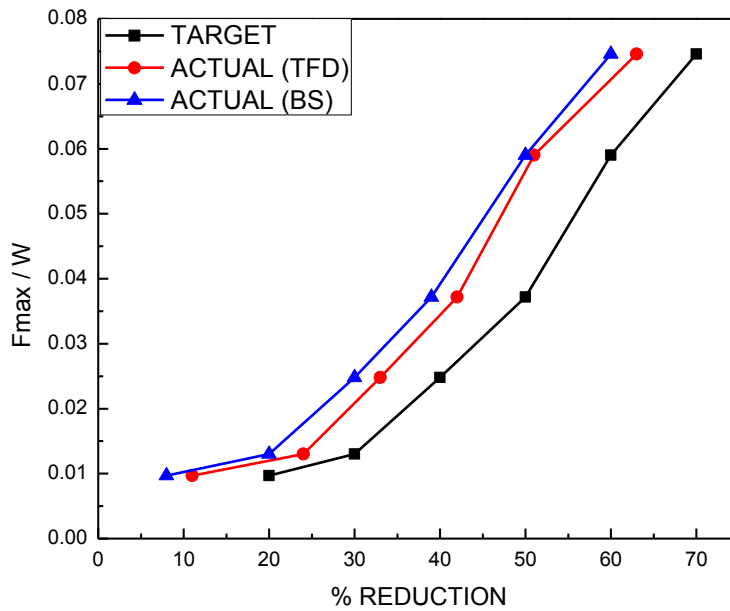


Figure 5.23 Comparison between target and actual percentage reductions in base shear and top floor displacement (for fixed 30% target reduction in base shear) for PGA=0.1g



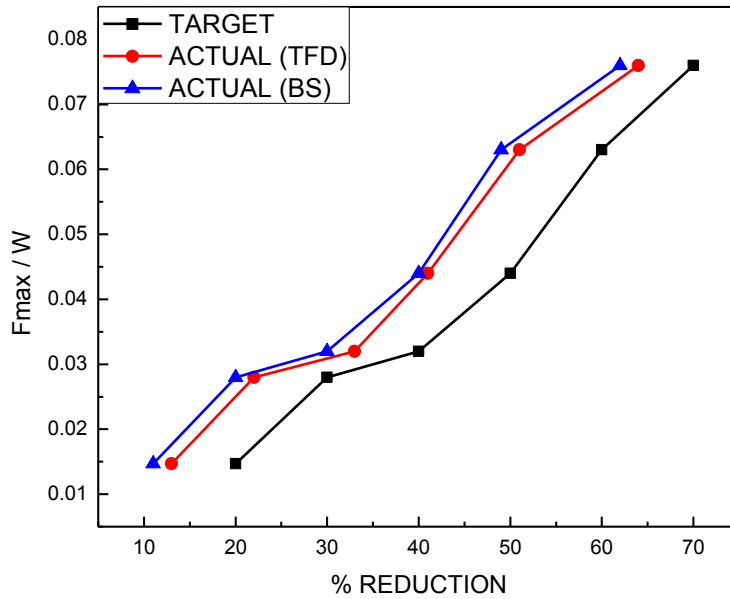


Figure 5.24 Comparison between target and actual percentage reductions in base shear and top floor displacement (for fixed 40% target reduction in base shear) for PGA=0.1g

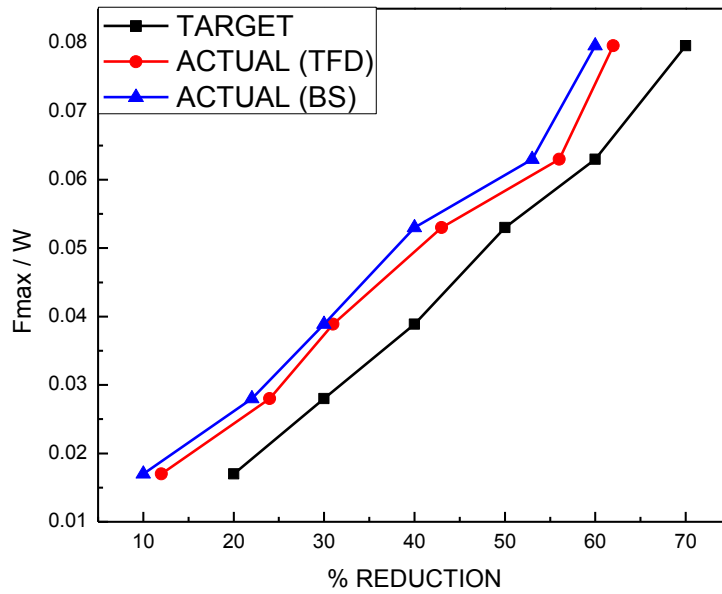


Figure 5.25 Comparison between target and actual percentage reductions in base shear and top floor displacement (for fixed 50% target reduction in base shear) for PGA=0.1g

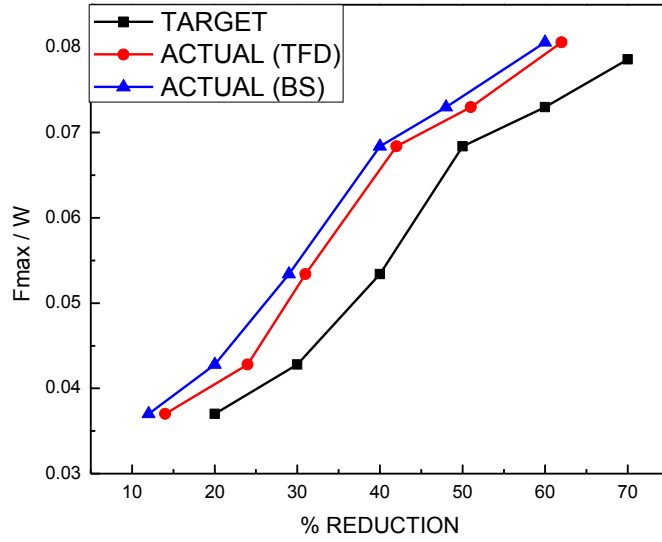


Figure 5.26 Comparison between target and actual percentage reductions in base shear and top floor displacement (for fixed 60% target reduction in base shear) for PGA=0.1g

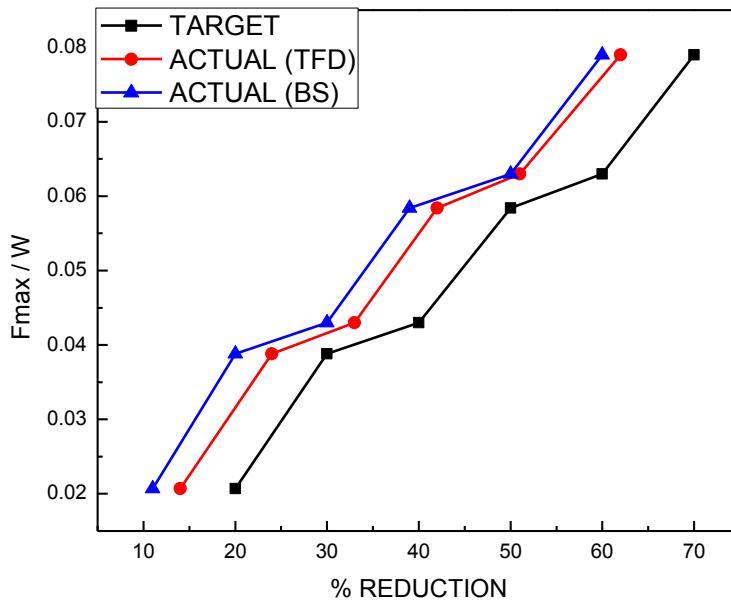


Figure 5.27 Comparison between target and actual percentage reductions in base shear and top floor displacement (for fixed 70% target reduction in base shear) for PGA=0.1g

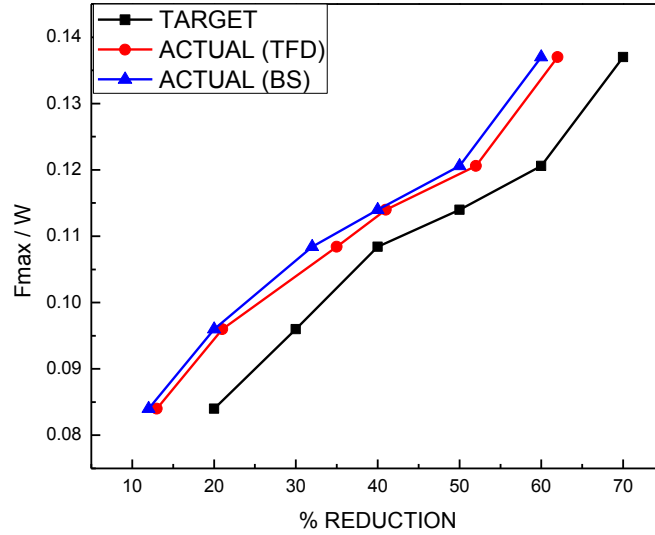


Figure 5.28 Comparison between target and actual percentage reductions in base shear and top floor displacement (for fixed 20% target reduction in base shear) for  $PGA=0.2g$

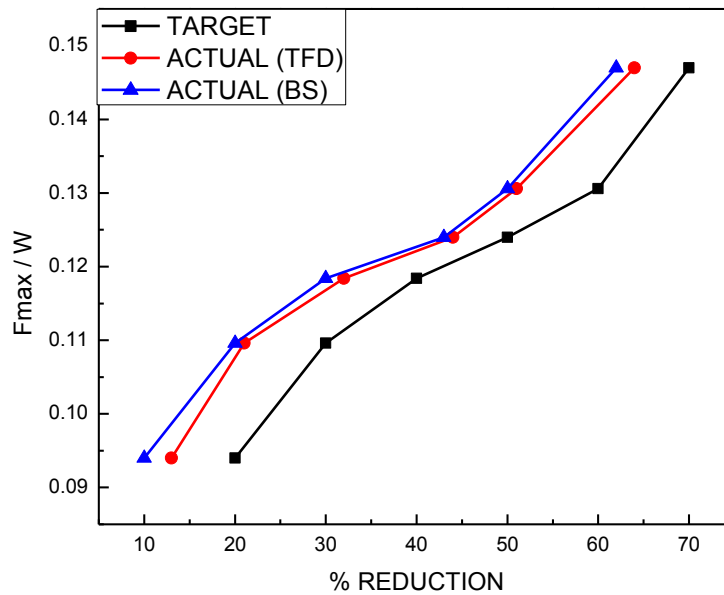


Figure 5.29 Comparison between target and actual percentage reductions in base shear and top floor displacement (for fixed 30% target reduction in base shear) for  $PGA=0.2g$

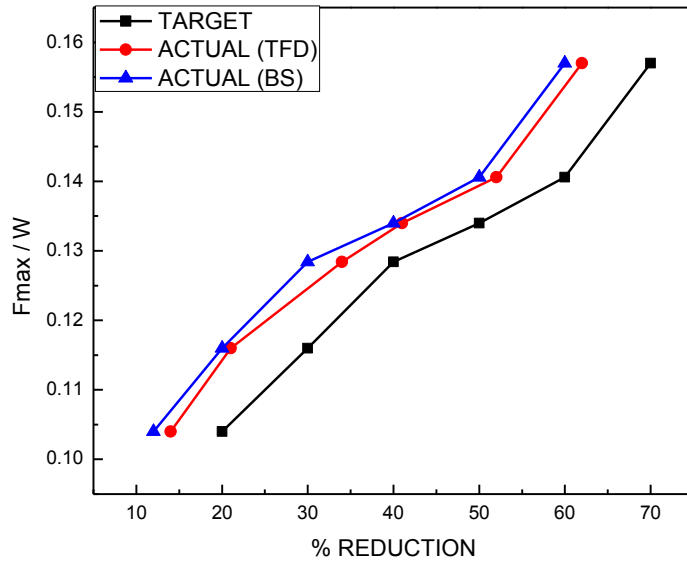


Figure 5.30 Comparison between target and actual percentage reductions in base shear and top floor displacement (for fixed 40% target reduction in base shear) for PGA=0.2g

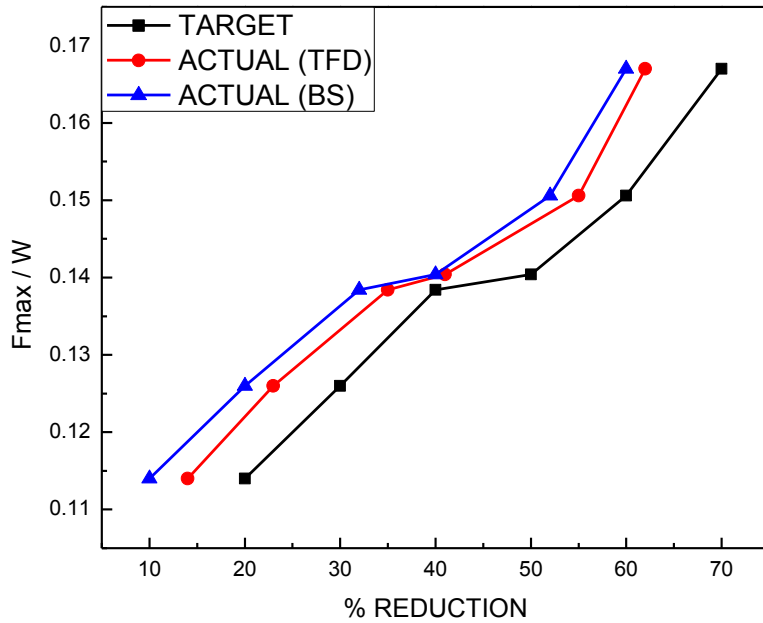


Figure 5.31 Comparison between target and actual percentage reductions in base shear and top floor displacement (for fixed 50% target reduction in base shear) for PGA=0.2g

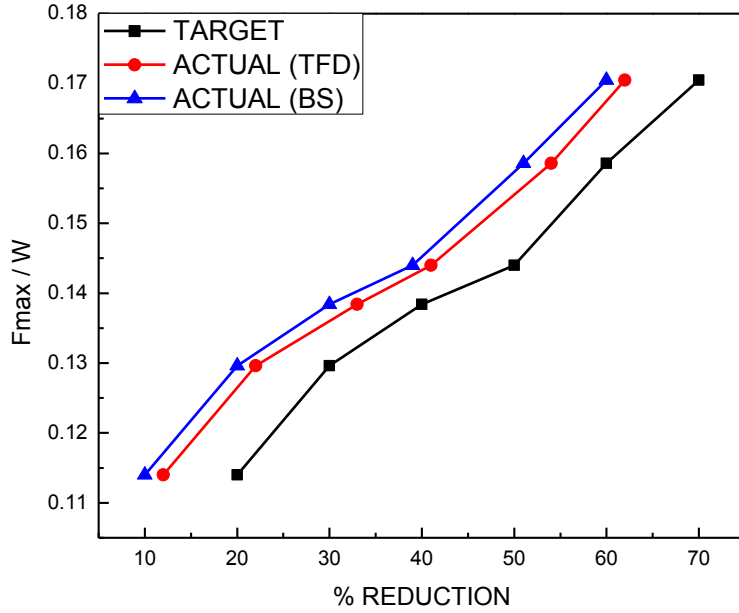


Figure 5.32 Comparison between target and actual percentage reductions in base shear and top floor displacement (for fixed 60% target reduction in base shear) for PGA=0.2g

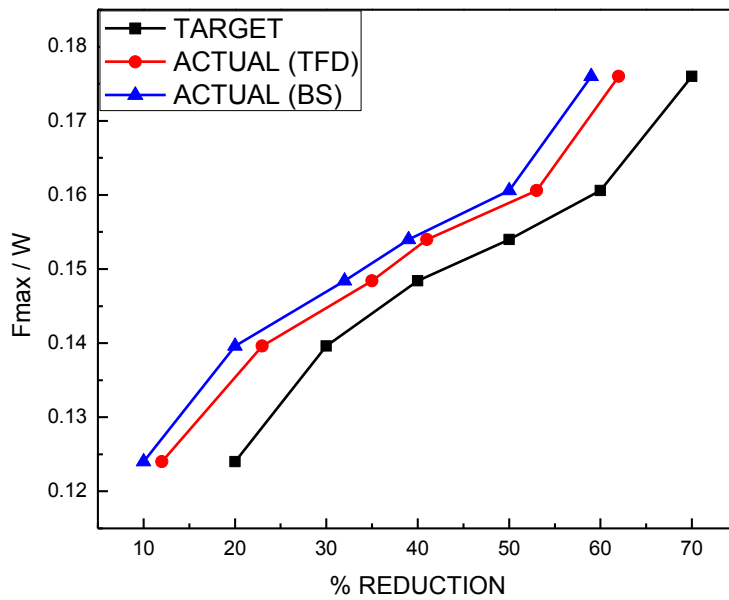


Figure 5.33 Comparison between target and actual percentage reductions in base shear and top floor displacement (for fixed 70% target reduction in base shear) for PGA=0.2g

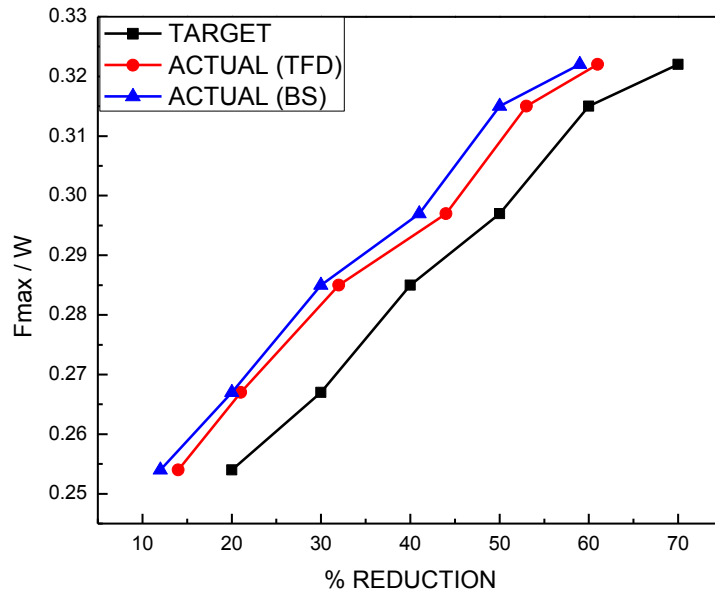


Figure 5.34 Comparison between target and actual percentage reductions in base shear and top floor displacement (for fixed 20% target reduction in base shear) for PGA=0.4g

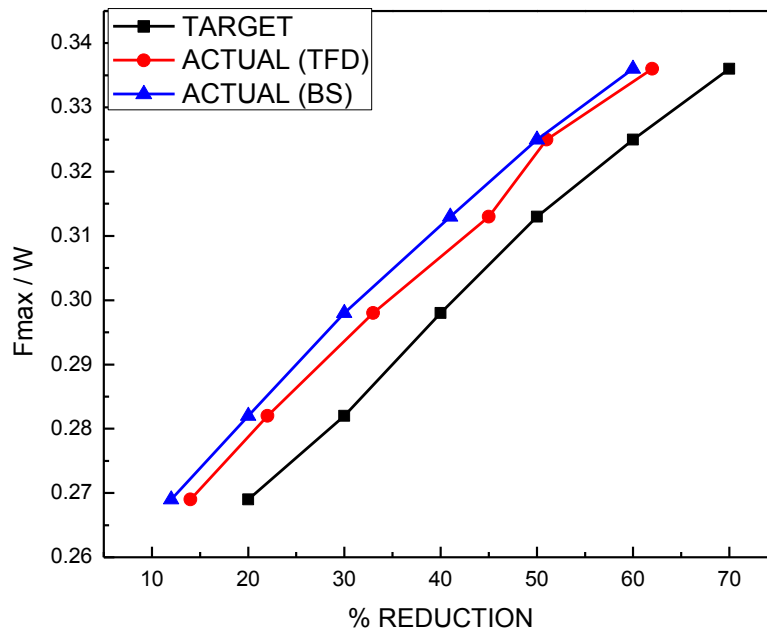


Figure 5.35 Comparison between target and actual percentage reductions in base shear and top floor displacement (for fixed 30% target reduction in base shear) for PGA=0.4g

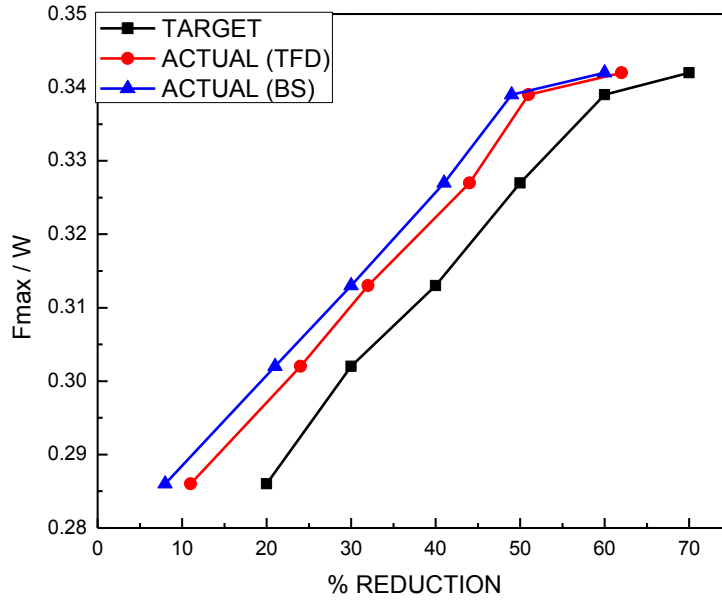


Figure 5.36 Comparison between target and actual percentage reductions in base shear and top floor displacement (for fixed 40% target reduction in base shear) for PGA=0.4g

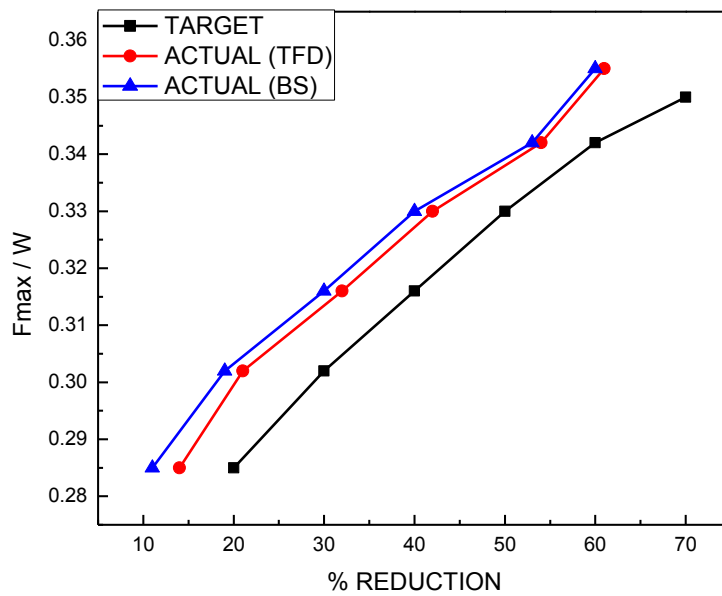


Figure 5.37 Comparison between target and actual percentage reductions in base shear and top floor displacement (for fixed 50% target reduction in base shear) for PGA=0.4g

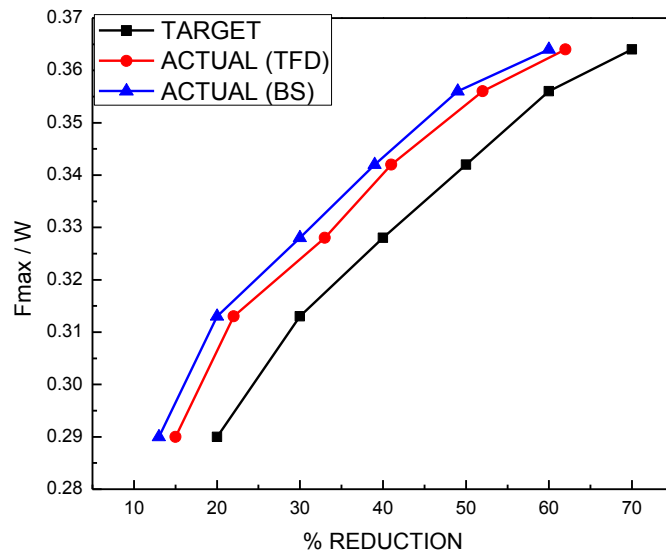


Figure 5.38 Comparison between target and actual percentage reductions in base shear and top floor displacement (for fixed 60% target reduction in base shear) for PGA=0.4g

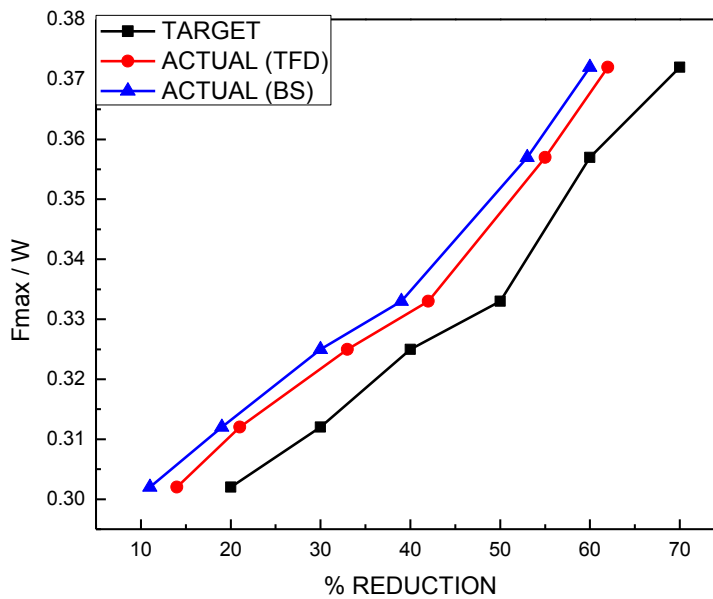


Figure 5.39 Comparison between target and actual percentage reductions in base shear and top floor displacement (for fixed 70% target reduction in base shear) for PGA=0.4g



In the case of different percentage of reductions in base shear and top storey displacement, three values of the PGA are considered for the study namely, 0.1g, 0.2g and 0.4g. In this case (Figure 5.22 to 5.39), the patterns of variation of the target and the actual percentage reduction remain nearly the same as those for the same target percentage of reductions in the two responses (Figure 5.14 to 5.21). Further, it is seen from the figures that the peak control force requirement is essentially governed by the percentage reduction in top floor displacement. For example, referring to Figure 5.39, it is seen that for a PGA level of 0.4g and the percentage reduction in the top floor displacement of 70%, the peak control force varies from 0.3 to 0.37 when the percentage reduction in base shear increases from 20% to 70%.

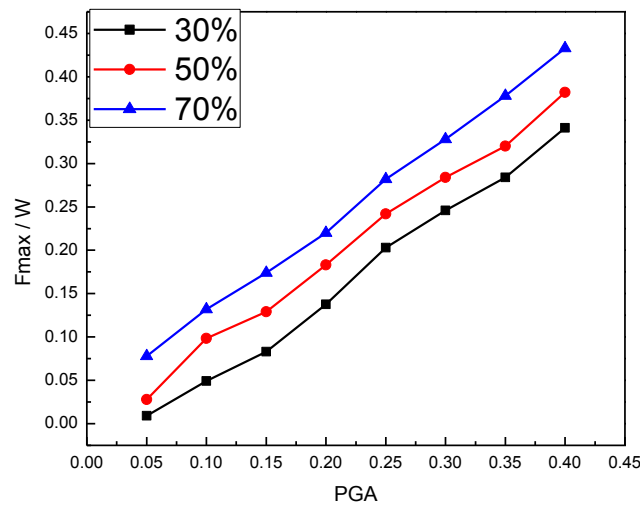


Figure 5.40 Variation of peak control force with PGA for the same percentage reduction of both responses (hard soil).

Figure 5.40 shows the variation of peak control force with the PGA for the same percentage reduction in the base shear and the peak storey displacement. For lower values of the peak ground acceleration ( $\leq 0.2g$ ), the maximum control force remains within 20-25% of the building weight for a percentage reduction in responses of the order of 70%. Further, an increase in the peak ground acceleration leads to a higher value of the peak control force and at double the value of the peak ground acceleration, i.e.,  $PGA = 0.4g$ , maximum control force is of the order of 40% of building weight for a percentage reduction of responses of about 70%. Thus, the control force requirement could be significantly high at a peak ground acceleration level of

ground motion, nearly equal to 0.4g, which is considered as the size of an extreme earthquake in India.

#### 5.4.2 Testing the neural network for the soft soil condition

Testing of the neural network for ground motions in the soft soil condition is carried out similar to what is done in the case of the hard soil for the same percentage reduction in responses. The comparisons between the variation of peak control force with the target and the actual percentage reductions of responses for the same target reduction in both response quantities are shown in Figures 5.41 to 5.48.

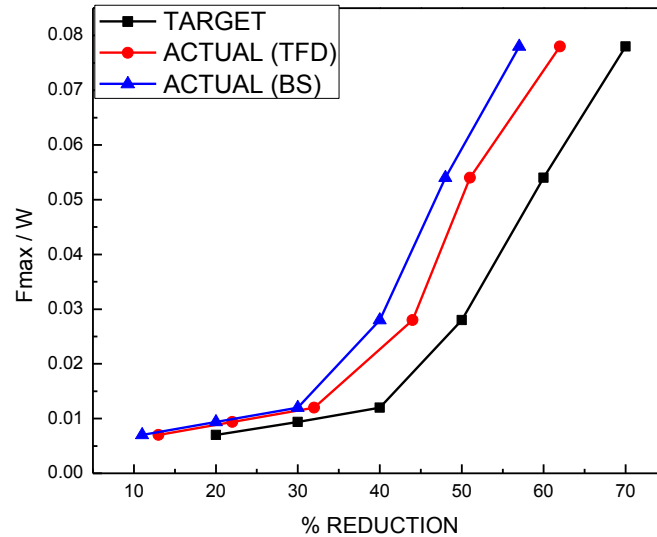


Figure 5.41 Comparison between the target and actual percentage of reduction in base shear and top floor displacement (target value remains same for both) for PGA 0.05g

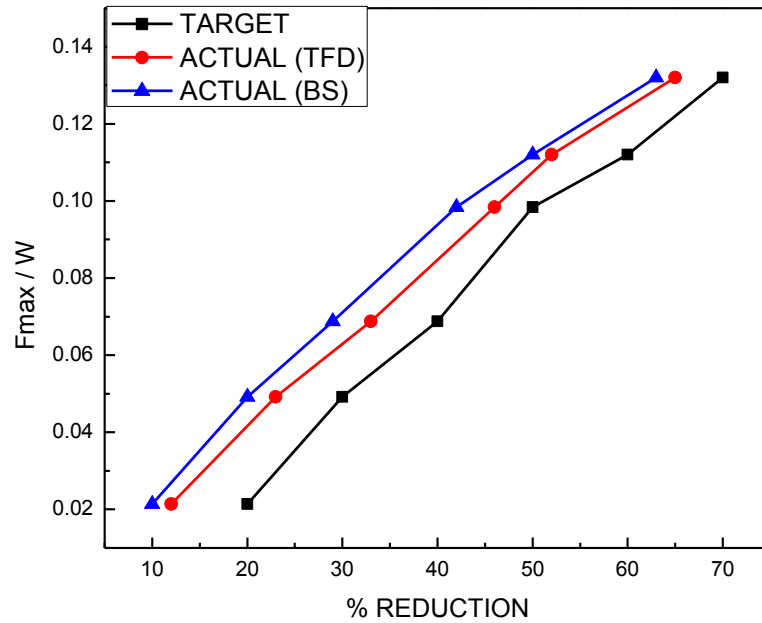


Figure 5.42 Comparison between the target and actual percentage of reduction in base shear and top floor displacement (target value remains same for both) for PGA 0.10g

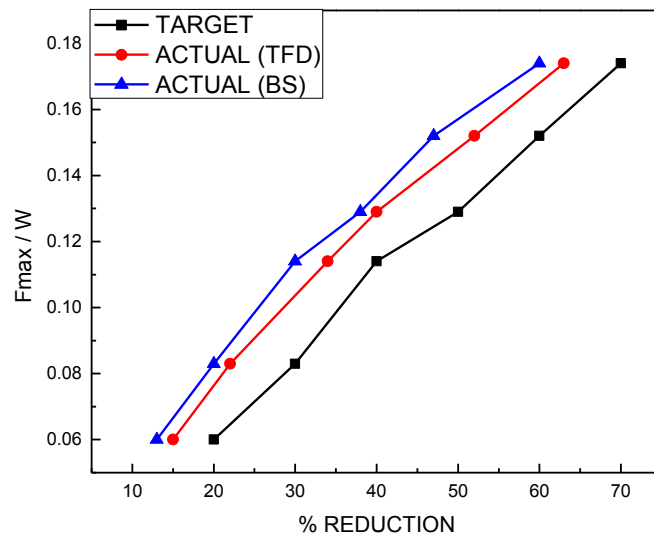


Figure 5.43 Comparison between the target and actual percentage of reduction in base shear and top floor displacement (target value remains same for both) for PGA 0.15g

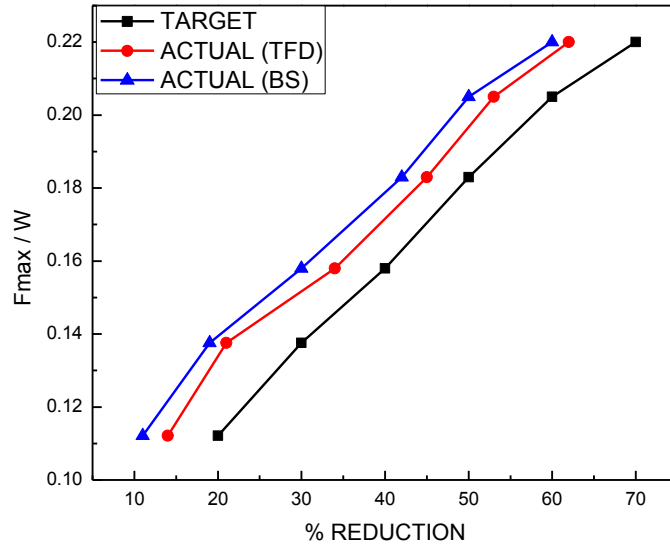


Figure 5.44 Comparison between the target and actual percentage of reduction in base shear and top floor displacement (target value remains same for both) for PGA 0.20g

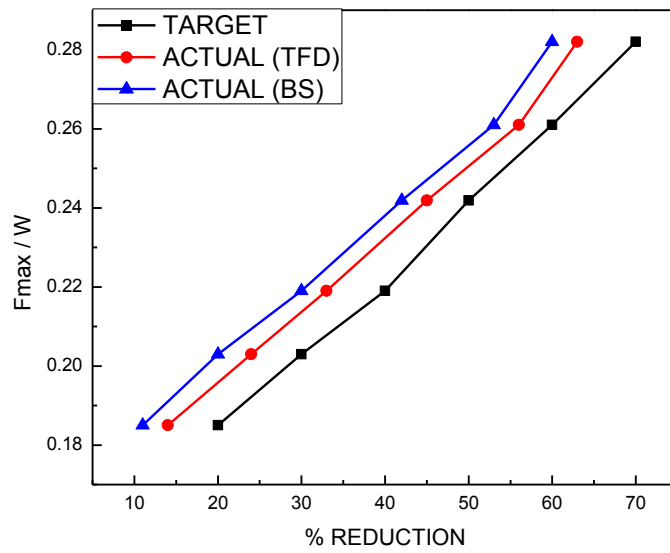


Figure 5.45 Comparison between the target and actual percentage of reduction in base shear and top floor displacement (target value remains same for both) for PGA 0.25g

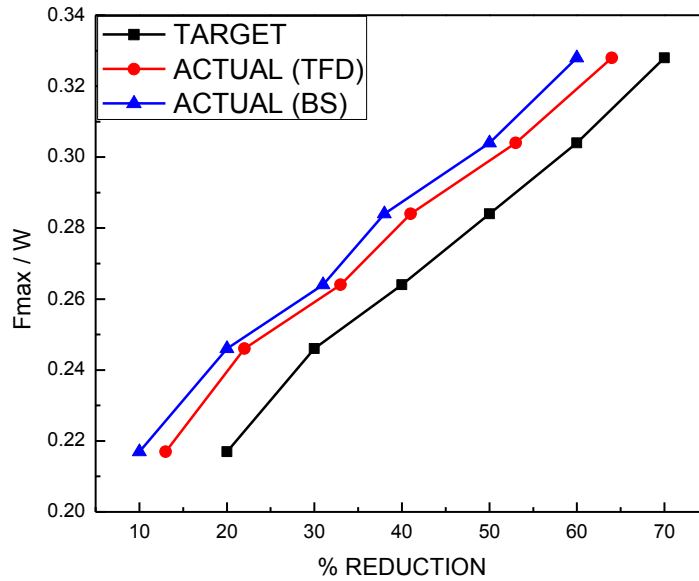


Figure 5.46 Comparison between the target and actual percentage of reduction in base shear and top floor displacement (target value remains same for both) for PGA 0.30g

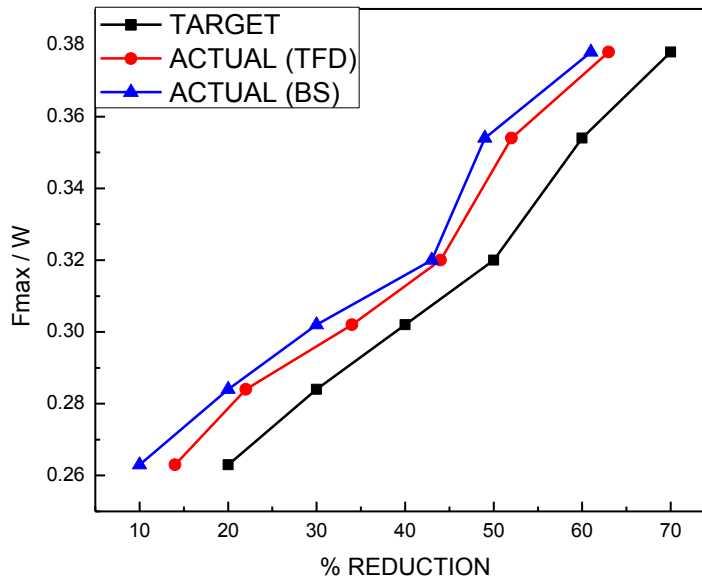


Figure 5.47 Comparison between the target and actual percentage of reduction in base shear and top floor displacement (target value remains same for both) for PGA 0.35g

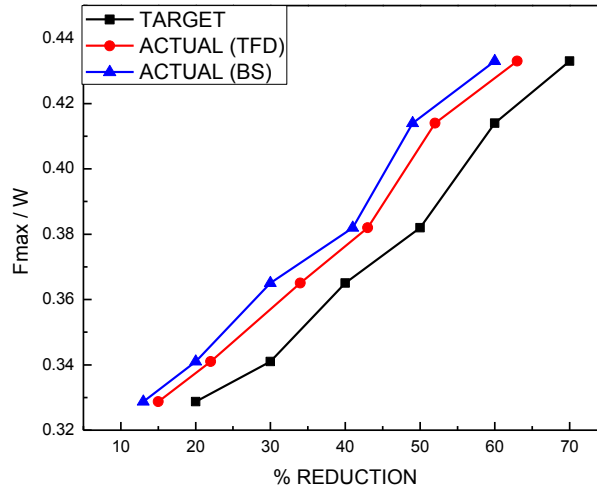


Figure 5.48 Comparison between the target and actual percentage of reduction in base shear and top floor displacement (target value remains same for both) for PGA 0.4g

The trends of results remain the same as those in the hard soil condition. The maximum difference in the percentage reduction between the target and the actual responses is about 5% to 9%. The actual percentage reduction is less than the target.

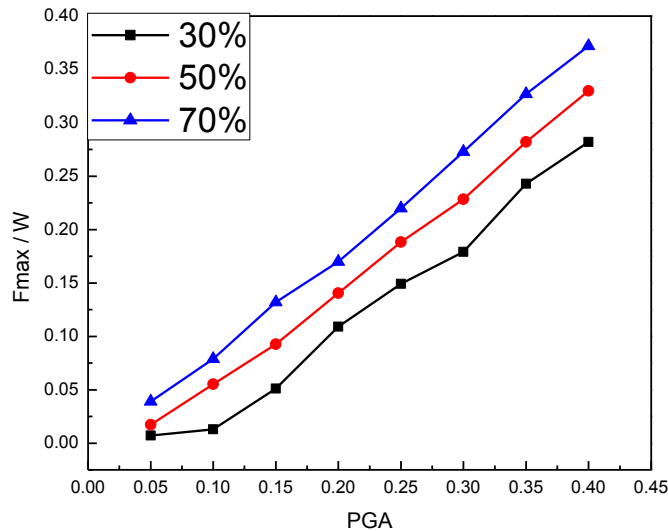


Figure 5.49 Variation of peak control force with PGA for the same percentage reductions of both responses (soft soil).

The pattern of variation is nearly the same as that observed for the hard soil condition. The maximum value of control force is of the order of 35% of the building weight for 0.4g peak ground acceleration.

### 5.4.3 Testing of the neural network for the unknown problems outside the range of PGA used in training

The neural network was tested for the unknown problems outside the range of peak ground acceleration values of ground motion used in the training of the neural network. For this purpose, the simulated time histories of ground motion corresponding to the hard soil condition are obtained for the peak ground acceleration levels of 0.5g and 0.6g. In the input nodes, the same percentage reductions in the maximum base shear and the peak top storey displacement are provided. The plots of the variations of peak control force with the percentage reduction of responses are shown in Figures 5.50 and 5.51.

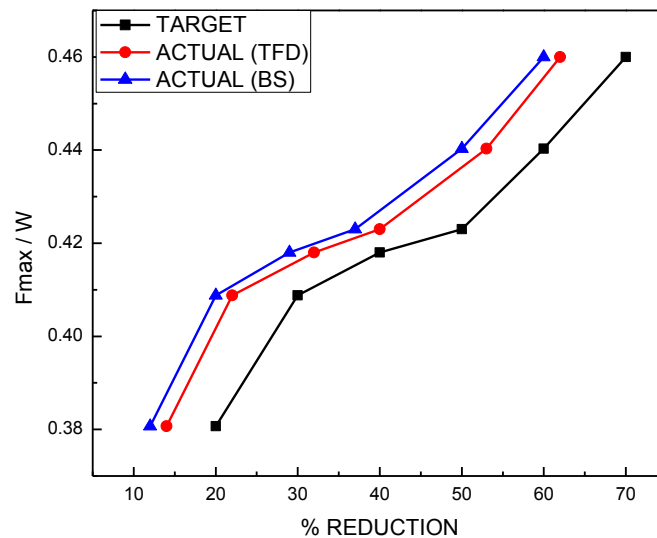


Figure 5.50 Comparison between target and actual percentage reductions in base shear and top floor displacement for PGA 0.5g.

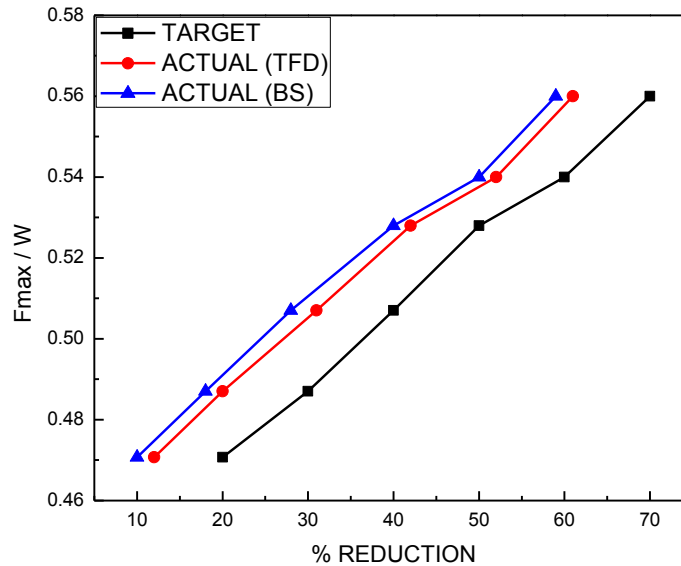


Figure 5.51 Comparison between target and actual percentage reductions in base shear and top floor displacement for PGA 0.6g.

It is seen from the figures that the trends of variation are similar to those of lower values of peak ground acceleration for which the neural network is trained. The maximum difference between the reductions in response to the target and the actual is about 5 to 8%. For higher peak ground acceleration, the maximum control force is found to be very high. For example, for the peak ground acceleration of 0.6g, there is a 50% reduction in response and the peak control force is about 54% of the building weight.

#### 5.4.4 Comparison between the linear quadratic regulator (LQR) and ANN control

In order to compare between the performances of ANN control and LQR control, the same building frame is controlled by LQR algorithm for three time history records corresponding to the hard soil condition having peak ground acceleration values as 0.1g, 0.2g and 0.4g. For the ANN control, percentage reductions in the maximum base shear and the peak top storey displacement are retained at the same. The results are shown in Figures 5.52 to 5.54.



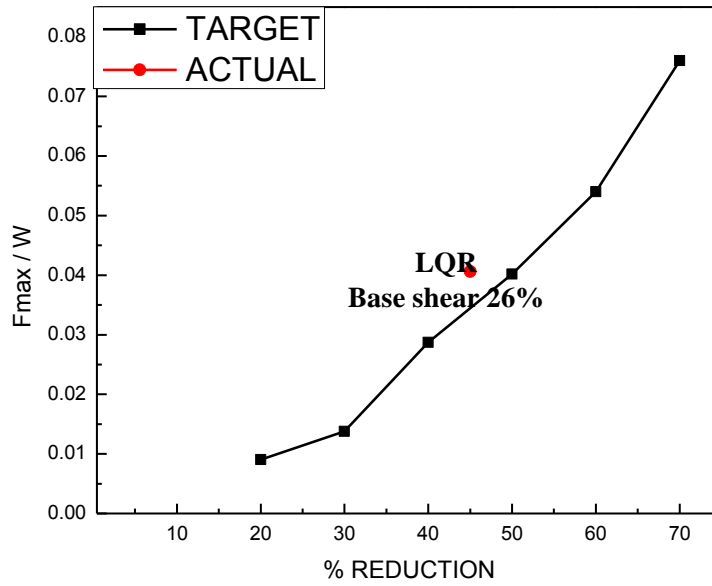


Figure 5.52 Comparison between target and LQR percentage reductions in base shear and top floor displacement for PGA= 0.1g

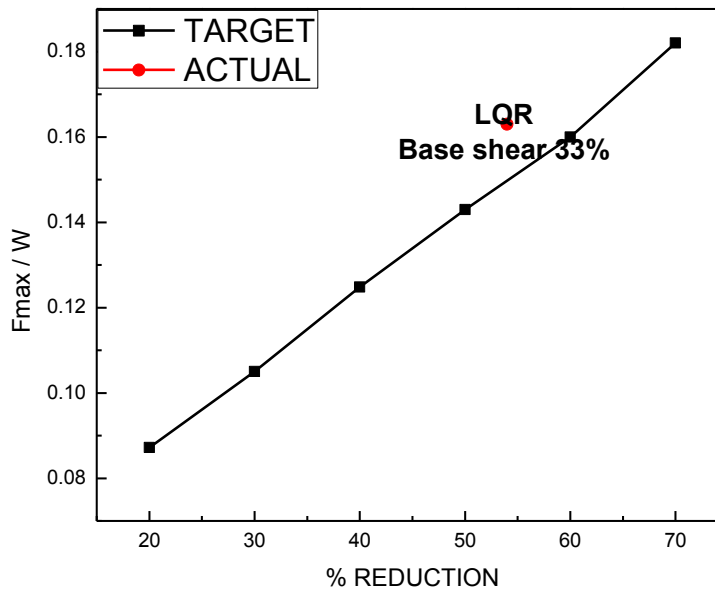


Figure 5.53 Comparison between target and LQR percentage reductions in base shear and top floor displacement for PGA= 0.2g

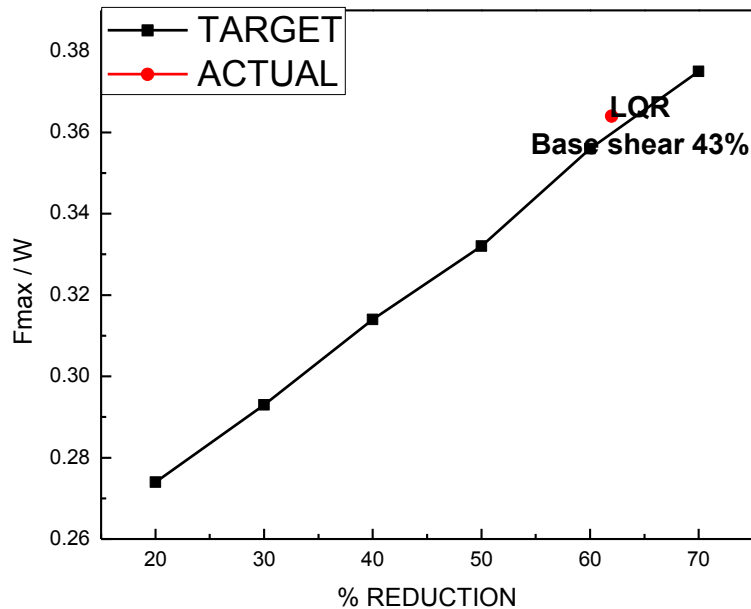


Figure 5.54 Comparison between target and LQR percentage reductions in base shear and top floor displacement for PGA= 0.4g

It is seen from the figures that percentage reduction in peak top storey displacement and corresponding peak values of the control force are close to the two cases; LQR provides about 5% less reduction in the peak top storey displacement for the same peak control force in ANN and LQR control. The percentage reduction in the maximum base shear, obtained by LQR is highly underestimated. Thus, it is seen that the ANN control presented in the study is more efficient, as compared to LQR control.

## 5.5 Conclusions

An ANN based control strategy is developed for obtaining a target percentage reduction in responses for future earthquakes, modeled as a stationary random process, which is specified by the PSDF of ground motion. The control strategy is much practical importance in places where the soil condition is well known and therefore, the nature of the PSDF can be well specified. Two cases are considered in the study, namely, the hard soil and the soft soil. The Clough and Penzin double filter PSDF is used to model the future earthquake process at the site. ANN is trained and tested offline. The architecture of the neural network is shown in Figure 5.1

having three input nodes and one output node. In real life application, the measured ground excitation is fed into one of the input nodes, while the other two nodes contain target percentage reduction of the maximum base shear and the peak top storey displacement of the building frame for which the ANN is trained. The output node provides the desired control force, which is utilized in the actuation of the actuator (placed at the top) for controlling the response of the building. The training of the neural network is accomplished using synthetically generated earthquake records from the assumed PSDF of ground acceleration. From the numerical results of the ten storey building frame considered in study, the following conclusions can be drawn:

1. With the help of twenty simulated earthquake records, the ANN was trained in providing the necessary time histories of control force to achieve the target percentage reductions in responses.
2. The testing was done for both known and unknown problems, for a varied range of PGA values (0.1g to 0.6g) and for the maximum target percentage reduction in responses of 70%.
3. For both known and unknown problems, it was found that the difference between the target and the actual percentage reductions, obtained analytically using the time history of control force predicted by the ANN varied between 5 to 9%.
4. The peak value of control force increases with the increase in peak ground acceleration value as it would be expected. For a peak ground acceleration level of 0.4g, the peak control force of the order of 35% of the building weight is required. However, for the lower range of the peak ground acceleration value, i.e. 0.25g the peak control force remains within 15% of the building weight.
5. The above conclusion shows that the proposed ANN control scheme is able to provide percentage reductions in responses of the order of 50%-70% with one actuator using a reasonable order of control force under ordinary earthquake level (up to a PGA of 0.25g).
6. The performance of the neural network for a level of peak ground acceleration, greater than the range of peak ground acceleration for which it was trained is found to be satisfactory.
7. The peak control force requirement is primarily driven by the required percentage reduction in the top storey displacement, i.e. for fixed percentage reduction of peak top

storey displacement. The peak control force does not significantly vary with the variation of the target percentage reduction in the base shear.

8. Comparison between the proposed control scheme with the standard LQR algorithm shows that the latter provides the same peak control force to obtain the percentage reduction in the peak top storey displacement same as that obtained by the ANN, but the percentage reduction in the maximum base shear is significantly underestimated by LQR.

## CHAPTER-6

# CONCLUSIONS AND RECOMMENDATIONS FOR FUTURE WORK

### 6.1 Conclusion

The thesis deals with three topics of research, namely, optimal placement of actuators in active control of building frames, predictive ANN control, and predictive ANN control for site specific random ground motion. Not much work is reported in literature on last two topics, while considerable research has been carried out in the first topic. However, the first topic addresses a practical problem, in which the control of response quantities is achieved with a limited number of actuators which could be placed, with selected combinations of actuators, in certain floors for some particular reasons.

From the point of application, in online control of responses, the predictive ANN control schemes presented in the study are meaningful. Most of the control schemes provide the reduction of responses within an expected range of values. These problems are formulated and solved as direct problem. The ANN control schemes presented in the study provide the desired control force for target percentage in reduction of responses. For training the ANN control scheme, developed for non-specific ground motions, the data sets are prepared by scaling each earthquake record at different PGA levels. For the ANN control for site specific ground motions, two types of ground motions are considered, namely broadband excitation and narrowband excitations. Data sets are prepared using simulation technique. Both ANN control schemes are tested for known and unknown data sets and also outside the domain of the data sets for which they were trained.

A 10 storey shear frame building is taken as an illustrative example for the study. The conclusions drawn from the study are limited to the nature of example and cannot be generalized. However, the trend of the results obtained from the study offers a good understanding of control problems being attended in the thesis. The important results from the study are summarized as below

- 1) For a single actuator, peak top floor displacement and maximum inter storey drift increases, as the actuator is placed at higher floor. The maximum reductions are achieved when the actuator is placed on the 10th floor.
- 2) For the base shear, the pattern of variation is opposite to that of maximum top floor displacement and maximum inter storey drift.
- 3) The variation of the R factor (percentage reduction/unit C.F.) is of the same nature as that of percentage reduction in responses for peak top floor displacement and maximum base shear. However, this variation of base shear is different from the percentage reduction of response, as in the case of Bhuj earthquake.
- 4) Higher percentage reduction in responses can be achieved by increasing no. of actuators to control, as it would be expected. However, considerable reduction in response can be achieved with single actuator also.
- 5) The maximum control force required to control the responses increases with increase in PGA level of the earthquake. The maximum control force does not change significantly with the no. of actuators used. However, percentage reduction in responses changes significantly with the number of actuators used.
- 6) The time history of the control force obtained from the neural network provides a reduction in response very close to the target value. Therefore, all the three neural networks were well trained in the case of predictive control of building frames.
- 7) The error between the actual and the target percentage reduction is of the order of 5–10%. When both percentage reduction in the maximum base shear and the peak top storey displacement are considered, it is found that the difference between the target and the actual percentage reduction in the peak top storey displacement is better than that of the maximum base shear.
- 8) The difference between the actual and the target percentage reduction in responses is not very large for peak ground acceleration levels for which the neural network was not trained.
- 9) The trained neural network is effective in predicting the required control force for the target percentage reduction in responses, even for narrow band earthquake and near field earthquake with fling step effect, for which they were not trained.

- 10) The difference between the target and the actual percentage reduction in responses is of the same order, as observed for far field earthquakes.
- 11) Data sets for training the ANN are prepared using LQR predicts better time history of control force as compared to LQR for unknown problems, providing more reductions in responses for the same level of peak control force. In some cases, the difference is small while in other cases it is significant.
- 12) With the help of twenty simulated earthquake records, the ANN is trained in providing the necessary time histories of the control force to achieve the target percentage reduction of responses.
- 13) The performance of the neural network for the level of peak ground acceleration, greater than the range of peak ground acceleration for which it was trained is found to be satisfactory.
- 14) The peak control force requirement is primarily driven by the required percentage reduction in top storey displacement, i.e. for the fixed percentage reduction of the peak top storey displacement. The variation of the peak control force with the variation in the target percentage reduction for the base shear is not found to be very significant.
- 15) Comparison between the proposed control schemes with the standard LQR algorithm shows that the latter provides the same peak control force to obtain the percentage reduction in the peak top storey displacement same as that obtained by the ANN, but the percentage reduction in the maximum base shear is significantly underestimated by LQR.

## **6.2 Recommendation for future work**

The following studies may be carried out as an extension of the present study

- 1) Optimal placement of actuators for achieving the best control using controllability index.
- 2) Optimal placement of actuators for uniform percentage reduction of response for more than one response parameter.
- 3) Development of the ANN control scheme for target percentage reduction by considering more numbers of response parameters using two actuators.
- 4) Extending the ANN control by considering both feedback and feed forward information.
- 5) To develop a stochastic ANN control scheme for random ground motion represented by their PSDFs.

## REFERENCES

1. Adeli H and Panakkat A.(2009). “A probabilistic neural network for earthquake magnitude prediction.” *Computer aided civil and infrastructure engineering*, **24(4)**, pp 280-292.
2. Abdel-Rohman, M. and Leipholz, H. H. (1983). “Active control of tall buildings.” *Journal of Structural Engineering*, **109(3)**, pp. 628-645.
3. Mohammed Aldawod, Bijan Samali, Fazel Naghdy, Kenny C.S. Kwok (2003), “Active control of along wind response of tall building using a fuzzy controller”, *Engineering Structures*, **23**, 1512–1522.
4. A. S. Ahlawat and A. Ramaswamy (2002), “Multiobjective Optimal Fuzzy Logic Control System for Response Control of Wind-Excited Tall Buildings”, *Journal of Engineering Mechanics*, **130(4)**, pp 524.
5. A.K. Chopra, “Dynamics of Structures: Theory and application to Earthquake engineering”, 4th edition. (Prentice Hall, 2001)
6. Aksakalli, V. and Ursu, D (2006), "Control of nonlinear stochastic systems: model-free controllers versus linear quadratic regulators. in Decision and Control.", *45th IEEE Conference*
7. Alavinasab, A., Moharrami. H, and Khajepour. A (2006), "Active Control of Structures Using Energy Based LQR Method.", *Computer Aided Civil and Infrastructure Engineering*, 2006. **21(8)**: pp. 605-611.
8. Amir, S., and Xuan, W. (2014). “Vibration Control of Two Adjacent Structures Using a Non-Linear Damping System.” *World Academy of Science, Engineering and Technology, International Journal of Civil, Environmental, Structural, Construction and Architectural Engineering*, **8(2)**, pp.188-191.
9. Ankireddi, S. and Yang, T.Y. (1996). “Simple ATMD control methodology for tall buildings subject to wind loads”. *Journal of Structural Engineering* **122**:1, 83-91
10. Bani-Hani, K. and Ghaboussi, J. (1998). “Nonlinear structural control using neural network.” *Journal of Engineering Mechanics*, **124(3)**, pp 319-327.



11. Battaini, M., Casciati, F., and Faravelli, L. (1998). "Fuzzy control of structural vibration. An active mass system driven by fuzzy controller." *Earthquake Engineering. and Structural Dynamics.*, **27(11)**, pp1267–1276.
12. Boujari, M., Ghorbani-Tanha, A. K., Rahimian, M., and Rahami, H. (2012). "Two degrees of freedom PID control for active vibration control of structures." *Proceedings of the 15th World Conference on Earthquake Engineering*, pp. 24-28.
13. Beliakov, G. and A. Abraham, (2002) "Global optimisation of neural networks using a deterministic hybrid approach in Hybrid Information Systems.", *Springer*, pp. 79-92.
14. Bhardwaj, M. and T. Datta (2006), "Semiactive fuzzy control of the seismic response of building frames." *Journal of Structural Engineering*, **132(5)**, pp. 791-799.
15. Cai, G., and Huang, J. (2002). "Discrete-time variable structure control method for seismic-excited building structures with time delay in control." *Earthquake engineering & structural dynamics*, **31(7)**, pp. 1347-1359.
16. C. R. Arjun and A. Kumar (2011) "Neural network estimation of duration of strong ground motion using Japanese earthquake records," *Soil Dynamics and Earthquake Engineering*, **31(7)**, pp. 866–872.
17. Chang, J.C.H and Soong, T.T (1980)"Structural control using active tuned mass damper" *Journal of Engineering Mechanics Division*, **106**, 1091-1098
18. Chen, H.M., Tsai, K.H., Qi, G. Z., Yang, J. C.S. and Amini, F. (1995). "Neural networks for structural control." *Journal of Computing in Civil Engineering*, ASCE, **9(2)**, PP. 168-176.
19. Chen-Wu Chen, Po-Chen Chen, Wei-Ling Chiang, (2013) "Modified intelligent genetic algorithm-based adaptive neural network control for uncertain structural systems".*Journal of vibration and control*, **19(9)**.
20. Chhabra, D., G. Bhushan, and P. Chandna (2016) "Optimal placement of piezoelectric actuators on plate structures for active vibration control via modified control matrix and singular value decomposition approach using modified heuristic genetic algorithm". *Mechanics of Advanced Materials and Structures.*, **23(3)**, pp. 272-280.
21. Chung, L. L., Reinhorn, A. M., and Soong, T. T. (1988). "Experiments on active control of seismic structures". *Journal of Engineering Mechanics*, **114(2)**, pp.241-256.

22. Clough, R. and Penzin, J. (1993). "Dynamics of Structures". 2<sup>nd</sup> edition McGraw-Hill, New York, NY.
23. Datta, T. K (2003)., "A state-of-the-art review on active control of structures". *ISET Journal of earthquake technology*, **40(1)**, pp. 1-17.
24. Deepak Kumar Gupta and Rajendra K. Pandey (2016) "Knowledge domain states mapping concept for controller tuning in an interconnected power network" *International Journal Electrical Power & Energy Systems*, **80**, pp. 160-170.
25. Doyle, J. C., Glover, K., Khargonekar, P. P., and Francis, B. A. (1989). "State-space solutions to standard H/sub 2/ and H/sub infinity/ control problems.", *IEEE Transactions on Automatic control*, **34(8)**, pp. 831-847.
26. Djedoui, N., Ounis, A., and Abdeddaim, M. (2016). "Active Vibration Control for Base-Isolated Structures Using a PID Controller against Earthquakes." *International Journal of Engineering Research in Africa*, **26**, pp. 99-110.
27. Etedali, S., Sohrabi, M. R., and Tavakoli, S. (2013). "Optimal PD/PID control of smart base isolated buildings equipped with piezoelectric friction dampers." *Earthquake Engineering and Engineering Vibration*, **12(1)**, pp. 39-54.
28. Fan, Y.-Y., X.-H. Shen, and Y.-J. Sang (2011). "No reference image sharpness assessment based on contrast sensitivity." *Guangxue Jingmi Gongcheng (Optics and Precision Engineering)*, **19(10)**, pp. 2485-2493.
29. Fisco N. R., and Adeli H (2011) "Smart structures: Part I—Active and semi-active control." *Scientia Iranica, Transactions A: Civil Engineering*, **18(3)**, pp. 275–284.
30. Gang Mei, Ahsan Kareem., and Jeffrey C. Kantor. (2001) "Real-time model predictive control of structures under earthquakes" *Earthquake Engineering Structural Dynamics*; **30**:995–1019
31. Ghaboussi, J. and Joghataei, A. (1995). "Active control of structures using neural networks." *Journal of Engineering Mechanics, ASCE*, **121(4)**, pp. 555-567.
32. Ghaffarzadeh, H., and Younespour, A. (2014). "Active tendons control of structures using block pulse functions." *Structural Control and Health Monitoring*, **21(12)**, pp. 1453-1464.

33. S Gholizadeh, E Salajegheh (2009). "Optimal design of structures subjected to time history loading by swarm intelligence and an advanced metamodel", *Computer Methods in Applied Mechanics and Engineering*, **198 (40)**, 2936-2949
34. Gleb Beliakov and Ajith Abraham, (2002) "Global Optimization of Neural Networks Using Deterministic Hybrid Approach, Hybrid Information Systems, Advances in Soft Computing", *Physica Verlag, Germany*, **379**, pp. 79-92
35. Guclu, R. (2006). "Sliding mode and PID control of a structural system against earthquake." *Mathematical and Computer Modelling*, **44(1)**, pp. 210-217.
36. Gunaydm, M, H., and Dogan, Z. S. (2004). "A neural network approach for early cost estimation of structural systems of buildings." *International Journal of Project Management*. **22(7)**, 595-602.
37. Hassani, K. and W.-S. Lee.(2014). "Optimal tuning of linear quadratic regulators using quantum particle swarm optimization." *Proceedings of the International Conference of Control, Dynamics and Robotics*.
38. Housner, GW., et al (1997), "Structural Control: Past, Present and Future", *Journal of Structural Engineering, ASCE*, 123(9), pp897-971
39. Housner, G., Bergman, L. A., Caughey, T. K., Chassiakos, A. G., Claus, R. O., Masri, S. F., Skelton, R..E., Soong, T.T., Spencer, B.F. and Yao, J. T. (1997). "Structural control: past, present, and future." *Journal of engineering mechanics*, **123(9)**, pp. 897-971.
40. Jangid, R. and T. Datta (1994) "Nonlinear response of torsionally coupled base isolated structure." *Journal of structural engineering*, **120(1)**, pp. 1-22.
41. Jin Cheng, Q.S. Li, Ru-cheng Xiao (2008), "A new artificial neural network-based response surface method for structural reliability analysis" *Probabilistic Engineering Mechanics*,**23(1)** ,pp51-63.
42. A. Karamodin , H.H. Kazemi and M.R. Akbarzadeh-T. (2008). "Semi-active Control of Structures Using Neuro-Predictive Algorithm for MR Dampers" *The 14th World Conference on Earthquake Engineering*, Beijing, China.
43. Kaveh Hassani and Won-Sook Lee.(2014) "Optimal Tuning of Linear Quadratic Regulators using Quantum Particle Swarm Optimization" *International Conference on Control, Dynamic Systems and Robotics*, **1(1)**, pp 59.

44. Ju-Tae Kim, Hyung-Jo Jung, and In-Won Lee (200), "Optimal structural control using neural networks". *Journal of Engineering Mechanics*, ASCE, **126(2)**, pp 2001-2019.
45. Kobori, T., Koshika, N., Yamada, N., and Ikeda, Y. (1991). "Seismic response controlled structure with an active mass driver system. Part1: Design." *Earthquake Eng. Structural Dynamics*, **20**, 133-139
46. Q.SLi, D.KLiuJ, QFang, A.PJeary and C.KWong (2000), "Damping in buildings: its neural network model and AR model", *Engineering Structures*, **22( 9)**, pp 1216-1223.
47. Li, Y.(2004). "Simulation of structural seismic responses based on neural networks." *Proceedings of the 13th World Conference on Earthquake Engineering*.
48. Madan, A. (2006). "General approach for training back propagation neural networks in vibration control of multidegree-of-freedom structures." *Journal of Computing in Civil Engineering*, ASCE, **20(4)**, pp.247-260.
49. Maind, S.B. and P. Wankar.(2014) "Research paper on basic of Artificial Neural Network." *International Journal on Recent and Innovation Trends in Computing and Communication*,. **2(1)**, pp. 96-100.
50. Mei, G., A. Kareem, and J.C. Kantor. (2001) "Real time model predictive control of structures under earthquakes." *Earthquake engineering & structural dynamics*, **30(7)**, pp. 995-1019.
51. Naimimohasses, R..(1995). "Sensor optimization using neural network sensitivity measures." *Measurement Science and Technology*, **6(9)**, pp. 1291.
52. Narendra, K. S., and Parthasarathy, K., "Identification and control of dynamical systems using neural networks", *IEEE Trans. Neural Networks* **1(1)**, 4-27, 1990.
53. Nerves, A. C.and Krishnan, R. (1995). "Active control strategies for tall civil structures." *Industrial Electronics, Control, and Instrumentation, Proceedings IEEE*, **2**, pp. 962-967.
54. Pantelides, C.P. (1990) "Optimum Design of Activily Controlled Structures", *Earthquake Engrg. Structural Dynamics*, Vol. 19, 583-596
55. Rahmat, M.F., H. Wahid, and N.A. Wahab. (2010) "Application of intelligent controller in a ball and beam control system." *International Journal on Smart Sensing and Intelligent Systems*, **3(1)**, pp. 45-60.
56. Rahim Guclu, Hakan Yazici (2008) "Vibration control of a structure with ATMD against earthquake using fuzzy logic controllers"; *Journal of sound and vibration*, **318**, pp 36-49.

57. Rao, M.M. and Datta, T.K. (1998). "Use of ANN of linear active control of structures." *Proceedings of 11<sup>th</sup> Symposium on Earthquake Engineering*, **II**, pp. 705-712.
58. Roy, A., D. Dutta, and K. Choudhury.(2013) "Training artificial neural network using particle swarm optimization algorithm." *International Journal of Advanced Research in Computer Science and Software Engineering*, **3(3)**.
59. Rumelhart.D.E.,and McClelland,J.L.(1986) "Parallel Distributed Processing: Explorations in the Microstructure of Cognition" Volume 1,*Foundations*. Cambridge, MA MIT Press.
60. S.Pourzeynali, H.H. Lavasani, A.H.Modarayi (2007) "Active control of high rise building structures using fuzzy logic and genetic algorithms"; *Engineering Structure*; **29**, pp346-357.
61. Sarbjeet, S. and T. Datta. (1998) "Open-closed-loop linear control of building frames under seismic excitation." *Journal of Structural Engineering*, **124(1)**, pp. 43-51.
62. Salajegheh E., S Gholizadeh "Optimum design of structures by an improved genetic algorithm using neural networks", *Advances in Engineering Software*, **36 (11)**, 757-767
63. Soong, T. and Spencer, B. (2000). "Active, semi-active and hybrid control of structures." *Bulletin of the New Zealand National Society for Earthquake Engineering*, **33(3)**, pp. 387-402.
64. Shooshtari, M., and Saatcioglu, M. (2004). "Active structural control of concrete structures for earthquake effects." *Proceedings of the 13th Word Conference on Earthquake Eng*, pp. 2721.
65. Shafieezadeh, A., Ryan, K., and Chen, Y. (2008). "Fractional order filter enhanced LQR for seismic protection of civil structures." *Journal of Computational and Nonlinear Dynamics*, **3(2)**, pp.21-44.
66. Sinan Korkmaz. (2011) "A review of active structural control: challenges for engineering informatics" *Computers and Structures*, **89**, pp 2113–2132.
67. Singh, M.P. and Moreschi, L.M. (2002). "Optimal placement of dampers for passive response control." *Earthquake engineering & structural dynamics*, **31(4)**, pp. 955-976.
68. Sivanandam SN, Sumathi S and Deepa SN (2007) "Introduction to fuzzy logic using MatLab." *Heidelberg: Springer*.

69. Soong, T. T. (1987). "Active structural control in civil engineering." *National Centre for Earthquake Engineering Research*.
70. Soong, T. T., Masri, S. F., and Housner, G. W. (1991). "An overview of active structural control under seismic loads." *Earthquake Spectra*, **7(3)**, pp.483-505.
71. Spencer Jr, B. F., Suhardjo, J., and Sain, M. K. (1994). "Frequency domain optimal control strategies for a seismic protection." *Journal of Engineering Mechanics*, **120(1)**, pp. 135-158.
72. Spencer, B.F., and Nagarajaiah, S.(2003). "State of the art of structural control." *Journal of Structural Engineering*, ASCE, 129(7), pp.845-856.
73. Scott, R.C.(2000). "Active control of wind-tunnel model aeroelastic response using neural networks." *SPIE's 7th Annual International Symposium on Smart Structures and Materials*.
74. Seung-yung Ok, Dong-Seok Kim, Kwan-Soon Park and Hyun-MooKoh (2007) "Semi-active fuzzy control of cable-stayed bridges using magneto-rheological dampers" *Engineering Structures*, **29(5)**, pp 776-788.
75. Symans , M.D., Constantinou, M. C.(1999) "Semi-active control systems for seismic protection of structures: a state-of-the-art review." *Engineering Structures*, **21**, pp.469–487
76. Tagliarini, G.A., J.F. Christ, and E.W. Page. (1991) "*Optimization using neural networks*". IEEE transactions on computers, **40(12)**, pp. 1347-1358.
77. Thenozhi, S., and Yu, W. (2014). "Stability analysis of active vibration control of building structures using PD/PID control." *Engineering Structures*, **81**, pp. 208-218.
78. Tongpadungrod, P., T. Rhys, and P. Brett. (2003). "An approach to optimise the critical sensor locations in one-dimensional novel distributive tactile surface to maximise performance." *Sensors and Actuators : Physical*, **105(1)**, pp. 47-54.
79. B.Widrowand, M.A.Lehr and Adaline.(1990) "An Engineering Model for Neurocomputing" *Proceedings of the International Conference on Fuzzy Logic and Neural Networks*, Japan.

80. Swaroop K. Yalla, Ahsan Kareem , Jeffrey C. Kantor (2001), “Semi-active tuned liquid column dampers for vibration control of structures”. *Engineering Structures* ,**23**, pp1469–1479
81. Yang, J.N., Akbarpour, A. & Ghaemmaghami, (1987). “New optimal control algorithms for structural control”. *Journal. of Engineering. Mechanics. ASCE*, **113**, pp.1369-1387
82. Yao, JTP. (1972), “Concept of Structural Control”, *Journal of the Structural Division, ASCE*, 98(ST7), pp1567- 1574
83. Sae-Ung, S., and Yao, J.T.P., "Active Control of Building Structures”, *Journal of the Engineering Mechanics Division, ASCE*, v. 104, n. EM2, April 1978, pp. 335-350
84. Yingmin Li, David Brooks, Zhigang Hu, Kevin Skadron, and Pradip Bose,(2004) "Understanding the Energy Efficiency of Simultaneous Multithreading," *International Symposium on Low-Power Electronics and Design*, pp44-49.
85. L.A.Zadeh (1965), “Fuzzy sets”. *Information and Control*, **8(3)**, pp 338-353.
86. Zadeh L. A., (1965), “Fuzzy Sets And Systems”, *System Theory*, **15**, pp. 29-37.
87. Zhi Q. Gu, S. Olutunde Oyadiji (2008) "Application of MR damper in structural control using ANFIS method",*Computers and structures*, **86**, pp 427- 436.

# Rajshree Charan

Email: [rhcharan-appmech@msubaroda.ac.in](mailto:rhcharan-appmech@msubaroda.ac.in), [charan.rajshree@gmail.com](mailto:charan.rajshree@gmail.com)

M: +91-9409236669, 91-8849947925

Date of birth: 22/08/1988

## ACADEMIC QUALIFICATIONS

Year	Degree	Institute	CGPA / Percentage
2019	Ph.D	Malaviya National Institute of Technology (MNIT), Jaipur(Rajasthan)	8.0
2011	M.Tech	Malaviya National Institute of Technology (MNIT), Jaipur(Rajasthan)	8.35
2009	B.Tech	Government Engineering college, Kota(Rajasthan)	72%
2005	XII	D.A.V school (CBSE)	62%
2003	X	St.Paul School (CBSE)	72%

## TEACHNING/PROFESSIONAL SUMMARY

Position Held	Name of Organization	Joining Year	Experience
Assistant Professor	The Maharaja Sayajirao University of Baroda, Vadodara(Gujarat Government)	October 2013 onwards	5 Years
Junior Engineer (J.En)	Jaipur Development Authority, Urban Development and Housing Department,(Rajasthan Government)	Nov.'2010	1 year
Assistant Professor	Kautilya Institute of Engineering and Technology, Jaipur	June'2010	5 months



Publication Details

Rajshree Charan, S. D. Bharti, M. K. Shrimali (2014) “Prediction of behavior of a building under earthquake using artificial neural network” 9 th Structural Engineering Convention, IIT, Delhi.

Rajshree Charan, S. D. Bharti, M. K. Shrimali (2013) “Control and optimization of dynamic system using artificial neural network” Young Researchers and Graduate Symposium, NIT, Jaipur.

Rajashree Charan, P V Ramana(2013), "Damage Assessment for Houses Subjected to Multi-Hazards Using Fuzzy Logic" NuiCONE 2013 by Nirma University at Ahmedabad

Rajshree Charan, S. D. Bharti, M. K. Shrimali (2012) "Repair and rehabilitation of Cable stayed bridge: case study” at Fourth International Conference on Structural Stability and Dynamics (ICSSD 2012), 4–6 January, 2012, Malviya National Institute of Technology, Jaipur.

Rajshree Charan, S. D. Bharti, M. K. Shrimali (2012) “ Wind Huzard assessment of a multistory building using Fuzzy logic” 8th Biennial Conference on Structural Engineering Convention (SEC– 2012),NIT, Surat.

Research Project

Sr.No.	Title	Total outlay in lacs	Duration	Funding agency
1	Finite Element modeling and experimental study of steel-concrete long composite columns	2	2018-2020	MSU, Baroda